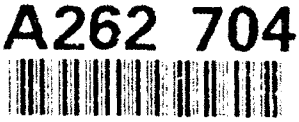

CRL COLUMBIA UNIVERSITY

JOINT SERVICES ELECTRONICS PROGRAM
ANNUAL PROGRESS REPORT NO. 42

RESEARCH INVESTIGATION DIRECTED TOWARD EXTENDING THE USEFUL RANGE OF THE ELECTROMAGNETIC SPECTRUM

Contract DAAL03-91-C-0016
For the Period October 1, 1991 - September 30, 1992

Presented to:
THE JOINT SERVICES TECHNICAL ADVISORY COMMITTEE
Representing: THE U.S. ARMY RESEARCH OFFICE,
THE OFFICE OF NAVAL RESEARCH,
and THE AIR FORCE OFFICE OF SCIENTIFIC RESEARCH

Submitted by:
COLUMBIA RADIATION LABORATORY
DEPARTMENTS OF CHEMISTRY, APPLIED PHYSICS,
AND ELECTRICAL ENGINEERING
COLUMBIA UNIVERSITY in the City of New York
NEW YORK, NEW YORK 10027

December 31, 1992

SECURITY CLASSIFICATION OF THIS PAGE

REPORT DOCUMENTATION PAGE

Form Approved OMB No. 0704-0188

1a. REPORT SECURITY CLASSIFICATION Unclassified	1b. RESTRICTIVE MARKINGS
2a. SECURITY CLASSIFICATION AUTHORITY	3. DISTRIBUTION/AVAILABILITY OF REPORT Approved for public release; distribution unlimited.
2b. DECLASSIFICATION/DOWNGRADING SCHEDULE	
4. PERFORMING ORGANIZATION REPORT NUMBER(S) ANNUAL PROGRESS REPORT NO. 42	5. MONITORING ORGANIZATION REPORT NUMBER(S)
6a. NAME OF PERFORMING ORGANIZATION COLUMBIA UNIVERSITY COLUMBIA RADIATION LABORATORY 6b. OFFICE SYMBOL (If applicable)	7a. NAME OF MONITORING ORGANIZATION Department of the Army
6c. ADDRESS (City, State, and ZIP Code) Columbia Radiation Laboratory Columbia University, Rm1001 Schapiro CEPSR 530 W. 120th St., New York, NY 10027	7b. ADDRESS (City, State, and ZIP Code) U.S. Army Research Office, P.O. Box 12211 Research Triangle Park, NC 27709-2211
8a. NAME OF FUNDING/SPONSORING ORGANIZATION Department of the Army 8b. OFFICE SYMBOL (If applicable)	9. PROCUREMENT INSTRUMENT IDENTIFICATION NUMBER DAAL03-91-C-0016
8c. ADDRESS (City, State, and ZIP Code) P.O. Box 12211 Research Triangle Park, NC 27709-2211	10. SOURCE OF FUNDING NUMBERS PROGRAM ELEMENT NO. / PROJECT NO. / TASK NO. / WORK UNIT ACCESSION NO.

11. TITLE (Include Security Classification)
RESEARCH INVESTIGATION DIRECTED TOWARD EXTENDING THE USEFUL RANGE OF THE ELECTROMAGNETIC SPECTRUM

12. PERSONAL AUTHOR(S) M.Teich, I.Herman, R. Osgood,Jr., G. Flynn, E.Yang, B.Bent and R.White
Columbia Radiation Laboratory, Columbia University

13a. TYPE OF REPORT	13b. TIME COVERED	14. DATE OF REPORT (Year, Month, Day)	15. PAGE COUNT
Annual Progress Report	FROM 10/1/91 TO 9/30/92	December 31, 1992	111 pages

16. SUPPLEMENTARY NOTATION The views, opinions and/or findings contained in this report are those of the author(s) and should not be construed as an official Department of the Army position, policy, or decision, unless so designated by other documentation.

17. COSATI CODES			18. SUBJECT TERMS (Continue on reverse if necessary and identify by block number)
FIELD	GROUP	SUB-GROUP	See attached "KEYWORDS"

19. ABSTRACT (Continue on reverse if necessary and identify by block number)

See attached "ABSTRACT"

20. DISTRIBUTION/AVAILABILITY OF ABSTRACT ☒ UNCLASSIFIED/UNLIMITED ☐ SAME AS RPT. ☐ DTIC USERS	21. ABSTRACT SECURITY CLASSIFICATION Unclassified
22a. NAME OF RESPONSIBLE INDIVIDUAL George W. Flynn and/or Richard M. Osgood	22b. TELEPHONE (Include Area Code) (212) 854-3265 22c. OFFICE SYMBOL

DD Form 1473, JUN 86 Previous editions are obsolete. SECURITY CLASSIFICATION OF THIS PAGE

Joint Services Electronics Program

DAAL03-91-C-0016

ANNUAL PROGRESS REPORT NO. 42
RESEARCH INVESTIGATION DIRECTED TOWARD EXTENDING THE USEFUL RANGE OF THE ELECTROMAGNETIC SPECTRUM

covering the period

October 1, 1991 - September 30, 1992

Object of the Research: Basic research in the fields of quantum electronics; electromagnetic propagation, detection and sensing; and solid state electronics.

The research reported in this document was made possible through support extended to the Columbia Radiation Laboratory, Columbia University, by the Joint Services Electronics Program (U.S. Army Research Office, Office of Naval Research, and the Air Force Office of Scientific Research) under Contract DAAL03-91-C-0016.

Submitted by: G. Flynn, Director, Columbia Radiation Laboratory
M. Teich, I. Herman, R. Osgood, G. Flynn, E. Yang, B. Bent and R. White, Principal Investigators

Coordinated by: L. Meizler, Departmental Administrator
B. Blegen, E. Ragland and C. Kim, Coordinators

Columbia Radiation Laboratory
COLUMBIA UNIVERSITY in the City of New York
Rm 1001 Schapiro CEPSR, 530 W. 120th St.
New York, New York 10027

RESEARCH SUPPORT

The research reported in this document was made possible through support extended to the Columbia Radiation Laboratory, Columbia University, by the Joint Services Electronics Program (U.S. Army Research Office, Office of Naval Research, and the Air Force Office of Scientific Research) under Contract DAAL03-91-C-0016.

Portions of this work were also supported by:

DEFENSE ADVANCED RESEARCH PROJECTS AGENCY/
AIR FORCE OFFICE OF SCIENTIFIC RESEARCH
Grant No. F49620-89-C-0088
Grant No. F49620-92-J-0414

ARMY RESEARCH OFFICE
Contract DAAL03-89-K-0028

NATIONAL SCIENCE FOUNDATION
Grant CHE-88-16581
Grant PHY-88-20540

DEPARTMENT OF ENERGY
Grant DE-FG02-90-ER-14104
Grant DE-FG02-88-ER-13937

OFFICE OF NAVAL RESEARCH
Contract N00014-86-K-0694
Contract N00014-88-K-0299

SEMICONDUCTOR RESEARCH CORPORATION
Contract SRC-88-SJ-055

IBM CORPORATION
IBM Materials Research Program

The support of these agencies and corporations is acknowledged in the text.

ANNUAL PROGRESS REPORT NO. 42

CONTENTS

KEYWORDS (Block 18 of Report Documentation Page)

1/f noise
adhesion
AES
AlGaSb
AlInAs/GaInAs
aluminum
amorphous semiconductor
angular momentum
Auger recombination
Auston switch
bit-error rate
CaF_2/Si
carrier lifetime
channel capacity
charge transfer
charge transfer salts
charge transport
chemical reactions
chlorine abstraction reaction
chlorine atoms
Cl, D_2S, DCl, C_6D_{12}, S_2Cl_2, NO_2, CS_2, H_2O
cold rotations
collision dynamics
copper
Cu(111), Cu(100), Cu(110)
dielectric loss
diode lasers
Doppler profile
electron collisions
electron cyclotron resonance
electron excitation
electron scattering
electron-cyclotron-resonance source
electrons
energy transfer
engineering
erbium-doped fiber amplifier
excimer lasers
exciton absorption
fractal noise
GaAs/AlGaAs
gas-surface interactions
GaSb
Ge
GeSi
heterojunction bipolar transistor
HgCdTe
high pressure
high resolution electron energy loss spectroscopy (HREELS)
hot vibrations
information transmission
InGaAs/InP
InGaSb/AlGaSb
interfaces
interphase engineering
lightwave communication
metal/polymer
negative differential resistance
noncentral-negative-binomial distribution
optical postamplifier
optical preamplifier
optical receiver
oxide removal
p-i-n
photoluminescence
phonons
photo-reflectivity
photocathode
photodiode
photoemission
photon counting
plasma etching
PMDA-ODA
point process
polyimides
polymers
probability of error
quantum confinement
quantum-box lasers
quantum-wire lasers
Raman scattering
recoil velocity
reflection absorption infrared spectroscopy (RAIRS)
renewal process
resonances
scanning tunneling microscopy (STM)
scanning tunneling spectroscopy (STS)
Schottky barrier
Si
SiGe oxide
silicon
space-charge-limited emission
squeezed light
strained layers
strained quantum well
superlattices
surfaces
surface passivation
tensile strain
thin film
tunneling
vibrational energy
vibrational spectroscopy
x-ray photoelectron spectroscopy (XPS)
XPS
ZnSe/ZnMnSe
ZnTe/ZnCdTe

ABSTRACT (Block 19 of Report Documentation Page)

We have made two important discoveries regarding the photon statistics in telecommunications devices. In the first, we have shown that the channel capacity of optical receivers in which photon arrival times are observed cannot be improved by modifying an initially Poisson photon stream and making it sub-Poisson. For photon-counting receivers, however, channel capacity enhancement is possible. In the second, we have evaluated system performance in the case of a cascade of fiber amplifers. We have found that the photon-number distribution at the output of a cascade of erbium-doped fiber amplifiers, with coherent light at the input, turns out to be the noncentral-negative-binomial distribution, even in the presence of intervening loss.

We have made significant advances in the investigation of the fundamental optical properties of semiconductors. For example, two relatively simple fractal renewal processes provide a framework for understanding charge transport in amorphous semiconductors; they give rise to spectral power densities with 1/f-like behavior. A new approach for enhancing exciton absorption and increasing the saturation limit in quantum wells, using tensile strain, is suggested; the method relies on valence-band mixing in a strained quantum well. The Auger recombination lifetime in a HgCdTe quantum wire is calculated to be shorter than that in a quantum well, but far shorter than that in a quantum box. Consequently, it seems that improved temperature performance can be expected from long-wavelength quantum-box lasers but not from quantum-wire lasers.

Electronic properties of strained ZnSe-based II-VI semiconductor heterostructures were investigated at elevated pressure by photoluminescence This study confirmed that ZnSe/ZnMnSe superlattices have Type I alignment and demonstrated the tuning of biaxial strains in ZnSe epilayers on GaAs by the splitting of the heavy and light hole peaks. Optical properties of other light emitting II-VI materials were investigated, including ZnTe/ZnCdTe superlattices grown by MBE, and ZnSe and ZnS films grown on GaAs by

pulsed laser ablation. A modified Keating model was developed to predict phonon frequencies in strained Si and Ge, including strained layers of these semiconductors at ambient and elevated pressure. Refinements in this model began by including extra terms found in the valence bond model and terms that are explicitly due to anharmonicity. The temperature dependence of phonons in GeSi alloys was studied, and was found to show behavior of the Si-Si modes in c-Si, and the Ge-Ge modes in c-Ge.

Recently in a series of experiments, we have shown that atoms generated in a remote, low pressure plasma can be used to remove the native oxide and other atmospheric-induced impurities from the surface of III-V semiconductor wafers. This is an extremely important finding for future and present GaAs-based device technology because the process is low-temperature and it acts only on the top monolayer of the wafer surface. In one particularly successful example of this technique, we have used H atoms from a microwave electron-cyclotron-resonance H_2 plasma to effect low-temperature oxide removal and surface passivation techniques for preparing single-crystal GaSb surfaces.

One of our major recent accomplishments in the area of two-photon-photoemission (2PPE) spectroscopy was the application of this technique for observation of very short lived excited electronic states. We utilized a nanosecond light source to observe states with lifetimes on the order of a femtosecond, thus enhancing the utility of 2PPE spectroscopy as a surface probe. Since image resonances arise from the quenching of image states by coupling to the bulk continuum, their observation indicates that the surface electrons in these states are not immediately lost to the bulk but rather reflect several times from potential energy discontinuities at the surface of the metal. Thus, we might hope to use the shape of these resonances to act as probes of the magnitude and form of the surface potential-energy barrier.

We have also made significant progress in theoretical studies of surface plasmons, derived from the results of our previous experimental work on the dependence of image-potential states with the variation of surface temperature.

Finally, we have further improved our two-photon photoemission experimental setup, making it suitable for performance of bichromatic 2PPE (Bi2PPE) studies. The advantage of a Bi2PPE spectroscopy technique is its improved signal to noise ratio as compared to conventional 2PPE.

A series of experiments have been performed to investigate the STM images of molecules which are adsorbed onto well characterized surfaces. These studies include investigations of structurally related, terminally substituted n-alkanes adsorbed on highly ordered pyrolytic graphite surfaces; investigations of a series of synthetic polymer adsorbates; and studies of adsorbates which constitute different generations of carboxylate-terminated starburst dendrimers. The application of the STM to the investigation of these surface adsorbates reveals details of molecule-surface interactions and molecule-molecule interactions, as well as the role of these forces in molecular epitaxy and long range surface adsorbate ordering. In addition these studies provide a better understanding of the mechanisms and limitations of STM techniques for imaging molecules adsorbed on surfaces.

Time domain tunable diode laser absorption spectroscopy has been used to measure rotationally resolved transient absorption line shapes and nascent rotational populations for CO_2 molecules excited into the (00^02) vibrational state by collisions with translationally hot hydrogen atoms. The 00^02 rotational population distribution and rotationally resolved linewidths are remarkably similar to those previously obtained for 00^01. Within the context of the "breathing ellipsoid" model used to interpret the data, the similar rotational distributions and translational recoils for 00^01 and 00^02 suggest that these two states are excited by similar collision trajectories, wherein asymmetric stretching excitation is optimized when H strikes near the end of the O-C-O molecule. The magnitude of population scattered into 00^02 is ~21 times smaller than that scattered into 00^01.

The effects of electron cyclotron resonance (ECR) hydrogen, nitrogen, and ammonia plasmas on AlGaAs/GaAs heterojunction transistors have been studied by x-ray

photoelectron spectroscopy. Experimental evidence shows that the ECR hydrogen plasma removes the native oxide on the GaAs surface and recovers the surface order. A mixed nitride-oxide surface layer is formed after nitrogen and ammonia plasma treatments. The appearance of the nitride layer correlates with the passivation of the GaAs surface and the much improved I-V characteristics of AlGaAs/GaAs heterojunction bipolar transistors. The base current at low current level, which is caused mostly by surface leakage, is reduced by a factor of more than 200 after passivation.

Electron cyclotron resonance (ECR) plasma oxidation of SiGe alloys was investigated at temperatures from room temperature to 500°C. Both Si and Ge are shown to be fully oxidized, forming SiO_2 and GeO_2. Auger depth profiling reveals that there is no Ge-rich SiGe layer after oxidation. With increasing temperature up to 500°C, the oxide is stoichiometric and it does not lose its GeO_2 component. Oxidation has also been carried out at both positive and negative sample bias in order to identify the role of ions, electrons, and neutrals. From biasing experiments negative oxygen ions and atomic neutrals appear to be the major reaction species.

New methods for depositing polymer thin films for microelectronics packaging applications and characterizing the molecular structure and electronic properties of those films are under development. Ultra-thin (30 - 200 Å) films of the polyimide insulator (PMDA-ODA) have been deposited on metal and semiconductor substrates by vapor deposition and spin coating. Model systems of oriented hydrocarbon chains have also been prepared on copper surfaces by a new H atom addition procedure. The elemental composition of the films has been determined by x-ray photo-emission and the molecular structure has been characterized by vibrational spectroscopy. Scanning tunneling spectroscopy studies show that the electronic structure of these films is inhomogeneous over a length scale of nanometers. More importantly, there are local regions where electronic states are observed in the "quasi-gap" of these nominally insulating polymer thin films. These states may explain the unexpected conductivity that has been observed for

ultra-thin polyimide films. Studies are in progress to determine if these gap states are the result of local crystallinity or a particular molecular orientation within the polymer film. Bulk properties such as dielectric losses can manifest themselves as increased conductivity in a material and optical absorption. The correlation of molecular level structure with bulk properties will allow for new thin film fabrication methods.

PUBLICATIONS

B. E. A. Saleh and M. C. Teich, "Information Transmission with Photon-Number-Squeezed Light," Proc. IEEE **80**, 451 (1992) [Special issue on quantum electronics edited by J. Whinnery].

T. Li and M. C. Teich, "Performance of a Lightwave System Incorporating a Cascade of Erbium-Doped Fiber Amplifiers," Opt. Commun. **91**, 41 (1992).

S. B. Lowen and M. C. Teich, "Fractal Renewal Processes as a Model of Charge Transport in Amorphous Semiconductors," Phys. Rev. B **46**, 1816 (1992).

Y. Jiang, M. C. Teich, and W. I. Wang, "Enhanced Exciton Absorption and Saturation Limit in Strained InGaAs/InP Quantum Wells," J. Appl. Phys. **71**, 769 (1992).

Y. Jiang M. C. Teich, W. I. Wang, and J. R. Meyer, "Auger Recombination in HgCdTe Quantum Wires and Quantum Boxes," J. Appl. Phys. **71**, 3394 (1992).

Z. Lu, Y. Jiang, W. I. Wang, M. C. Teich, and R. M. Osgood, Jr., "GaSb-Oxide Removal and Surface Passivation Using an Electron Cyclotron Resonance Hydrogen Source," J. Vac. Sci. Tech. B **10**, 1856 (1992).

Z. Sui, P. P. Leong, I. P. Herman, G. S. Higashi, and H. Temkin, "Raman Analysis of Light-Emitting Porous Silicon," Appl. Phys. Lett. **60**, 2086 (1992).

J. A. Tuchman and I. P. Herman, "General Trends in Changing Epilayer Strains through the Application of Hydrostatic Pressure," Phys. Rev. B **45**, 11 929 (1992).

J. A. Tuchman and I. P. Herman, "General Trend in the Effect of Hydrostatic Pressure on Mismatch Strains in Semiconductor Heterostructures," Bull. Am. Phys. Soc. **37**, 688 (1992).

Z. Sui, P. P. Leong, I. P. Herman, G. S. Higashi, and H. Temkin, "Raman Analysis of Light-emitting Porous Silicon," Bull. Am. Phys. Soc. **37**, 564 (1992).

Z. Sui, P. P. Leong, I. P. Herman, G. S. Higashi, and H. Temkin, "Analysis of the Structure of Porous Silicon by Raman Scattering,". Mat. Res. Soc. Symp. Proc. **256**, 13 (1992).

J. A. Tuchman, S. Kim, Z. Sui and I. P. Herman, "Exciton Photoluminescence of Bulk ZnSe and ZnSe Epilayers under Hydrostatic Pressure," Phys. Rev. B **46**, 13 371 (1992).

J. A. Tuchman, Z. Sui, S. Kim and I. P. Herman, "Photoluminescence of ZnSe/ZnMnSe Superlattices under Hydrostatic Pressure." J. Appl. Phys. (1992), accepted.

H. K. Liou, P. Mei, U. Gennser, and E. S. Yang, "Effects of Ge Concentration on SiGe Oxidation Behavior," Appl. Phys. Lett. **59**, 1200 (1991).

H. K. Liou, X. Wu, U. Gennser, E. S. Yang, V. P. Kesan, S. S. Iyer and K. N. Tu, "Interfacial Reactions and Schottky Barriers of Pt and Pd on Epitaxial $Si_{1-x}G_x$ Alloys," Appl. Phys. Lett. **60**, 577 (1992).

P. W. Li, Q. Wang, E. S. Yang, "Chemical and Electrical Characterization of AlGaAs / GaAs Heterojunction Bipolar Transistors Treated by Electron Cyclotron Resonance Plasmas," Appl. Phys. Lett. **60**, 1996 (1992).

P. W. Li, H. K. Liou, E. S. Yang, S. S. Iyer, T. P. Smith, III, and Z. Lu, "Formation of Stoichiometric SiGe Oxide by Electron Cyclotron Resonance Plasma," Appl. Phys. Lett. **60**, 3265 (1992).

B. Quiniou, W. Schwarz, Z. Wu and R. M. Osgood, Jr., "Photoemission from Thick Overlying Epitaxial Layers of CaF_2 on Si(111)," Appl. Phys. Lett. **60**, 183 (1992).

Z. Wu, B. Quiniou, J. Wang and R. M. Osgood, Jr., "Temperature and Adsorbate Dependence of the Image-Potential States on Cu(100)," Phys. Rev. B**45**, 9406 (1992).

B. Quiniou and R. M. Osgood, Jr., "Image-Potential States and Surface Plasmons: Temperature Dependence," submitted for publication in Phys. Rev. B (August 4, 1992).

B. Quiniou, V. Bulovic and R. M. Osgood, Jr., "Observation of Image-Potential-Induced Resonances on Cu(110) Using the Two-Photon Photoemission Technique," submitted for publication in Phys. Rev. B (November 2, 1992).

B. MacDonald, C. Guest, M. Freiler, R. Scarmozzino, A. Smith, R. Hunter, Jr., and R. M. Osgood, Jr., "Efficient Multiple via Etching of Polyimide Films using Fresnel Phase Zone Plate Arrays," submitted for publication in Appl. Opt. (November 18, 1992).

J. Park, Y. Lee, J. F. Hershberger, J. M. Hossenlopp, and G. W. Flynn, "Chemical Dynamics of the Reaction between Chlorine Atoms and Deuterated Cyclohexane," J. Am. Chem. Soc. **114**, 58 (1992).

J. J. Breen and G. W. Flynn, "STM Studies of the Synthetic Polypeptide: Poly-γ-benzyl-L-glutamate," J. Phys. Chem. **96**, 6825 (1992).

R. E. Weston, Jr. and G. W. Flynn, "Relaxation of Molecules with Chemically Significant Amounts of Energy: The Dawn of the Quantum State Resolved Era," Ann. Rev. Phys. Chem., **43**, 559-589 (1992).

C. K. Ni and G. W. Flynn, "Correlation between Molecular Recoil and Molecular Orientation in Collisions of Symmetric Top Molecules with Hot Hydrogen Atoms," Chem. Phys. Lett. **193**, 69 (1992).

S. A. Hewitt, L. Zhu, and G. W. Flynn, "Diode Laser Probing of CO_2 and CO Vibrational Excitation Produced by Collisions with High Energy Electrons from 193 nm Excimer Laser Photolysis of Iodine," J. Chem. Phys. **97**, 6397 (1992).

J. J. Breen, J. S. Tolman, and G. W. Flynn, "STM Studies of Vapor Deposited Films of TTF and Iodine," accepted for publication.

L. Zhu and G. W. Flynn, Diode Laser Probing of OCS and N_2O Vibrational Excitation Produced by Collisions with High Energy Electrons from 193 nm Excimer Laser Photolysis of Iodine," J. Phys. Chem., accepted for publication.

F. A. Khan, T. G. Kreutz, G. W. Flynn, and R. E. Weston, Jr., "Translationally and Rotationally Resolved Excitation of $CO_2(00^02)$ by Collisions with Hot Hydrogen Atoms," accepted for publication.

Hyo-Soo Jeong and R. C. White, "Low Energy Ion Beam Modification of High Performance Electronic Polymer," Mater. Res. Soc. Symp. Proc. **236**, pp. 324-330 (1992).

J.-L. Lin and B. E. Bent, "Iodomethane Dissociation on Cu(111): Bonding and Chemistry of Adsorbed Methyl Groups," J. Vac. Sci. Technol. A **10**, 2202 (1992).

C.-M. Chiang, T. H. Wentzlaff, C. J. Jenks, and B. E. Bent, "Carbon-Carbon Bond Forming Reactions on Cu(11) Surfaces," J. Vac. Sci. Technol. A **10**, 2185 (1992).

J.-L. Lin and B. E. Bent, "C-H Vibrational Mode Softening in Alkyl Groups Bound to Cu(111)," Chem. Phys. Lett. **194**, 208 (1992).

M. Xi. and B. E. Bent, "Evidence for an Eley-Rideal Mechanism in the Addition of Hydrogen Atoms to Unsaturated Hydrocarbons on Cu(111)," J. Vac. Sci. Technol. B, in press.

H.-S. Jeong and R. C. White, "Low Energy Ion Beam Interactions with Electronic Polymer Surfaces," J. Vac. Sci. Technol. A, in press.

M. Xi and B. E. Bent, "Reaction of Deuterium Atoms with Cyclohexane on Cu(111): Hydrogen Abstraction Reactions by Eley-Rideal Mechanisms," submitted to J. Phys. Chem.

E. N. Schulman and R. C. White, "Observation of Nanometer Ordering in Multilayer Films of PMDA-ODA Using the Scanning Tunneling Microscope and Ultra High Vacuum," submitted to J. Vac. Sci. Technol.

S. Zolgharnain and R. C. White, "In-vacuum Synthesis and Characterization of Thin Aromatic Polyimide Films Prepared by a Chemical Vapor Deposition Process," submitted to J. Vac. Sci. Technol.

PRESENTATIONS

M. C. Teich, "Squeezed Light," CUNY City College Physics Colloquium, New York, New York (October 1991); CUNY Hunter College Physics Colloquium, New York, New York (December 1991).

M. C. Teich, "Effect of Dead Space on Gain and Noise of Double-Carrier-Multiplication Avalanche Photodiodes," Annual Meeting of the Optical Society of America, San Jose, California (November 1991) with M. M. Hayat and B. E. A. Saleh.

M. C. Teich, "Nonclassical Light," Annual Meetings of the Danish Optical Society and Danish Physical Society, Odense, Denmark (November 1991), invited Plenary Lecture; Riso National Laboratory Colloquium, Roskilde, Denmark (November 1991).

M. C. Teich, "Comparison of Frequency Tuning Curves and Spontaneous Cellular Vibrations in the Guinea-Pig Cochlea," Annual Meeting of the Association for Research in Otolaryngology, St. Petersburg Beach, Florida (February 1992), with S. E. Keilson, S. M. Khanna and M. Ulfendahl.

M. C. Teich, "Transient Vibrations of Cellular Structures in the Organ of Corti," Annual Meeting of the Association for Research in Otolaryngology, St. Petersburg Beach, Florida (February 1992), with S. M. Khanna, S. E. Keilson and M. Ulfendahl.

M. C. Teich, "Chaotic Vibrations of Outer Hair Cells and Henson Cells in the Cochlea," Annual Meeting of the Association for Research in Otolaryngology, St. Petersburg Beach, Florida (February 1992), with S. E. Keilson, S. M. Khanna, L. Brundin, M. Ulfendahl, and A. Flock.

M. C. Teich, "1/f-Like Spectra in Cochlear Neural Spike Trains," Annual Meeting of the Association for Research in Otolaryngology, St. Petersburg Beach, Florida (February 1992), with T. W. Woo and M. B. Sachs.

M. C. Teich, "Fractal Random Processes," Invited Lecture, Workshop on Stochastic Resonance, Office of Naval Research and NATO, San Diego, California (March 1992).

M. C. Teich, "Photon Optics, Photons and Atoms, Laser Amplifiers, Laser Resonators, and Lasers," Lecture Series, Coastal Systems Station, Panama City, Florida (April 1992). [These lectures are a portion of an intensive course entitled "Lasers and Optical Engineering."]

M. C. Teich, "The Nature of Noise in Photon Amplification," Invited Lecture, Optical Amplifiers and Their Applications Topical Meeting, Santa Fe, New Mexico (June 1992).

M. C. Teich, "Fractal Point Processes in Auditory Neurophysiology," Invited Colloquium, The Santa Fe Institute, Santa Fe, New Mexico (June 1992).

M. C. Teich, "Fractal Processes in Neurophysiology and Cardiology," Cardiology Seminar, Columbia College of Physicians & Surgeons, New York, New York (July 1992).

M. C. Teich, "Noise in Optical Sources and Amplifiers," Invited Tutorial Presentation, Annual Meeting of the Optical Society of America, Albuquerque, New Mexico (September 1992).

I. P. Herman, "Raman Scattering as an in-situ Optical Diagnostic," SPIE meeting on Process Module, Control, and Clustering (Conference 1594), Sept. 13, 1991.

I. P. Herman, "Raman Microprobe Spectroscopy During Surface Modifications," Interdisciplinary Laser Science Conference (ILS -VII), Sept. 25, 1991.

I. P. Herman, "Analysis of the Structure of Light-emitting Porous Silicon by Raman Scattering," MRS, Boston, December 2-6, 1991.

I. P. Herman, "Temperature Dependence of First-Order Raman Scattering in $Ge_{1-x}Si_x$ Bulk Alloys," APS March Meeting, Indianapolis, March 17, 1992.

I. P. Herman, "Raman Analysis of Light-emitting Porous Silicon," APS March Meeting, Indianapolis, March 19, 1992.

I. P. Herman, "Laser Spectroscopy of ZnSe and Ge/Si-based Heterostrucutres under Hydrostatic Pressure," Hughes Research Laboratory, Malibu, CA, May 13, 1992.

I. P. Herman, "Laser Microprobes of Photon-assisted Surface Modifications," CLEO '92, Anaheim, May 14, 1992.

I. P. Herman, "Optical Diagnostics of Microelectronics Materials During Laser Processing and Under Other Unusual Conditions," California Institute of Technology, May 15, 1992.

Z. Lu, Y. Jiang, W. I. Wang, M. C. Teich, and R. M. Osgood, Jr. (invited), "GaSb-oxide Removal and Surface Passivation Using Electron Cyclotron Resonance Hydrogen Plasma," presented at the 19th PCSI Conference, Death Valley, CA, January 28-30, 1992.

P. Li, Z. Lu, U. Gennser, E. Yang, and R. M. Osgood, Jr., "Electron Cyclotron Resonance Plasma Oxidation of SiGe Alloy," poster presented at the Materials Research Society Symposium, Boston, MA, December 2-6, 1991.

R. M. Osgood, Jr., "Laser Photoelectron Spectroscopy," IBM, Almaden, CA, January, 1992.

Q. Yang, W. Schwarz, and R. M. Osgood, Jr. (invited), "Surface Photochemistry on GaAs(110)," Laser Advanced Materials Processing Conference, LAMP '92, Nagaoka, Niigata, Japan, June 7-12, 1992.

R. M. Osgood, Jr., "Laser Surface Interactions and their Application in Integrated Optics and Electronics," presented at the ARO Annual Program Review, Raleigh, North Carolina, April 29, 1992.

R. M. Osgood, Jr., "Laser Manipulation of Electrons at Surfaces," presented at the Columbia University Physics Colloquia, December 11, 1992.

George W. Flynn, "Vibrational, Rotational, and Translational Energy Probes of Chemical and Collision Dynamics," NIST, Gaithersburg, MD, December 1, 1992; Department of Energy, Gaithersburg, MD, December 1, 1992.

George W. Flynn, "Scanning Tunneling Microscopy of Molecular Adsorbates," American Chemical Society, Symposium on Novel Structural, Mechanical, and Electrical Aspects of Chemical Interfaces, San Francisco, CA, April 6, 1992; Symposium on Infrared

Spectroscopy and Polymers, Columbia University, November 24, 1992; Texaco, Beacon, New York, June 30, 1992.

L. Zheng, "Two Mechanisms for Cooling Molecules with Chemically Significant Amounts of Energy," Physical Chemistry Seminar, Columbia University, December 1991.

A. S. Mullin, "Hot Molecules in a Cool Bath: State and Velocity Resolved Collisional Dynamics of Vibrationally Excited Pyrazine + CO_2," Gordon Conference on Atomic and Molecular Interactions, Colby-Sawyer College, New London, NH, July 1992; Physical Chemistry Research Seminar, Dept. of Chemistry, Columbia University, New York, NY, September 1992; Joint Institute for Laboratory Astrophysics and Dept. of Chemistry, University of Colorado, Boulder, CO, September 1992; Dept. of Chemistry, Colorado State University, Fort Collins, CO, September 1992; Evening Departmental Research Seminar, Dept. of Chemistry, Columbia University, New York, NY, December 1992.

C.-K. Ni, "Pressure Shift and Pressure Broadening of Absorption Lines," Physical Chemistry Research Seminar, Dept. of Chemistry, Columbia University, New York, NY, April 1992.

C.-K. Ni, "Correlation Between Molecular Recoil and Molecular Orientation in the Collisions of Hot Hydrogen Atoms and Symmetric Top Molecules," Gordon Conference on Atomic and Molecular Interactions, Colby-Sawyer College, New London, NH, July 1992.

S. K. Schowen, "Desperately Seeking Supercollisions: Methane Collisions with Hot Pyrazine," Dept. of Chemistry, Columbia University, New York, NY, October 1992.

B. Venkataraman, "Generation of Coherent, Tunable VUV Radiation and Its Application in REMPI Processes," Physical Chemistry Research Seminar, Dept. of Chemistry, Columbia University, New York, NY, March 1991.

B. Venkataraman, "State-to-State Dynamics via VUV-MPI Detection of H_2," American Chemical Society Meeting, New York, NY 10027, August 1991.

B. Venkataraman, "Two-Step Ionization - A Tool for Understanding the Photodissociation of 1,3-Butadiene," Dept. of Chemistry, Barnard College, New York, NY, February 1992.

B. Venkataraman, "STM Studies of Molecular Adsorbates," Industrial Associates Program, Dept. of Chemistry, Columbia University, New York, NY.

C.-K. Ni, "Pure Rotational Scattering of CO_2/CO Due to Hot H Atoms," Columbia University, New York, NY, March 1991; Am. Chem. Soc. Meeting, New York, NY, August 1991.

Y. Lee, "Diode Laser Probing of N_2O Following Collisions with $O(^1D)$," Am. Chem. Soc. Meeting, New York, NY, August 1991.

Y. Lee, "Tunable Diode Laser Probe of Chlorine Atoms Produced from the Photodissociation of S_2Cl_2," Am. Chem. Soc. Meeting, New York, NY, August 1991.

L. Zheng,"Quantum State Resolved N_2O Vibrational, Rotational, and Translational Energy Transfer from Highly Vibrationally Excited NO_2 Donors," Am. Chem. Soc. Meeting, New York, NY, August 1991.

B. E. Bent, "Forming Carbon-Carbon Bonds on Copper Surfaces," Department of Chemistry, Carleton College, Northfield, MN, January 1992.

R. C. White (invited), "Metal-Polymer Adhesion: The Use of Scanning Tunneling and Force Microscopy For Characterization of Polyimide Surfaces, Processing, and Their Interfaces with Metals," Fifteenth Annual Meeting of The Adhesion Society, Hilton Head, South Carolina, February 16-19, 1992.

H.-S. Jeong and R. C. White,"Blister Test for Thin Film Structure Adhesion in Microelectronic Packaging," Fifteenth Annual Meeting of The Adhesion Society, Hilton Head Island, SC, February 17-19, 1992.

P. S. Leang and B. E. Bent, "Surface Reactions Leading to Carbon Incorporation in Copper Films Grown by MOCVD," Gordon Research Conference on the Chemistry of Electronic Materials, Oxnard, CA, March 1992.

H. S. Jeong and R. C. White (invited),"Variational Principle of Adhesion Measurements," Electrochemical Society Metropolitan NY Section, Stevens Tech., Hoboken, NJ, March 25, 1992.

E. N. Schulman and R. C. White, "Spectroscopic Study of Thin Conductive Films of Pyromellitic Dianhydride Oxydianiline," 1992 March Meeting of the American Physical Society, Indianapolis, IN, March 16-20, 1992.

J.-L. Lin, M. Xi, and B. E. Bent, "Carbon-Carbon Bond Formation by Reaction of Alkyl and Aryl Iodides with Copper Surfaces," Am. Chem. Soc. Meeting, San Francisco, CA, April 1992.

B. E. Bent, "Carbon-Carbon Bond Formation on Single Crystal Copper Surfaces," Princeton University, Princeton, NJ, April 1992.

B. E. Bent, "Making and Breaking Bonds at Metal Surfaces," Akzo Chemical Co., Dobbs Ferry, NY, September 1992.

B. E. Bent, "Metal Alkyls and Alkyl Radicals: An Organometallic Chemistry of Surfaces," University of California, Berkeley, CA, November 1992.

M. Xi, B. E. Bent, and P. Stevens, "Spectroscopic Characterization of Phenyl Intermediates in the Ullmann Coupling Reaction," Am. Chem. Soc. Meeting, Washington, DC, August 1992.

R. C. White (invited)"Polymer Interphase Formation And Adhesion Mechanisms" (poster), Gordon Research Conference Science of Adhesion, The New Hampton School, New Hampton, New Hampshire, August 10-14, 1992.

M. Xi and B. E. Bent, "Formation, Bonding, and Chemistry of Phenyl Groups on Cu(111)," AVS Fall Meeting, November 1992.

C. Su, M. Xi, Z.-G. Dai, M. F. Vernon, and B. E. Bent, "Dry Etching of GaAs with Cl_2: Correlation of the Surface Cl Coverage and the Etching Rate at Steady State," AVS Fall Meeting, November 1992.

E. N. Schulman and R. C. White, "Observation of Nanometer Ordering in Multilayer Films of PMDA-ODA Using the Scanning Tunneling Microscope and Ultra High Vacuum," American Vacuum Society Meeting, Chicago, IL, November 9-13, 1992.

H.-S. Jeong and R. C. White, "Variational Principal of Thin Film Adhesion," American Vacuum Society Meeting, Chicago, IL, November 9-13, 1992.

H.-S. Jeong and R. C. White, "Low Energy Ion Beam Interactions with Electronic Polymer Surfaces," American Vacuum Society Meeting, Chicago, IL, November 9-13, 1992.

S. Zolgharnain and R. C. White, "In Vacuum Synthesis and Characterization of Thin Polyimide Films Prepared by Chemical Vapor Deposition Process," American Vacuum Society Meeting, Chicago, IL, November 9-13, 1992.

R. C. White (invited), "The Correlation of Measured Thin Film Fracture Strength to Intrinsic Adhesion at Nanometer Scales," International Symposium on Adhesion Measurement of Films and Coatings, I.B.M. Corporation, Cambridge, MA. December 5-7, 1992.

COLUMBIA RADIATION LABORATORY SEMINARS

Matthew Copel (IBM Research Center), "Manipulating SiGe Heteroepitaxy with Surfaces," October 14, 1991.

Eric Mazur (Harvard University), "'Cold Melting': Ultrafast Electronic Disordering of GaAs During Femtosecond Laser Melting," October 21, 1991.

Bruce Schardt (Brookhaven National Labs), "Probing the Structure of the Electrified Interface with Scanning Tunnelling Microscopy," November 11, 1991.

Raphael Reif (M.I.T.), "New Developments in the Chemical Vapor Deposition of Semiconductor Thin Films: $Si_{1-x}Ge_x$ and In-Situ, Real Time Monitoring," November 25, 1991.

James O'Neill (IBM/East Fishkill), "Optical Diagnostic Techniques for Semiconductor Process Monitoring," December 9, 1991.

Theodore Madey (Rutgers University), "Desorption Induced by Electronic Transitions at Surfaces," February 10, 1992.

Owen Webster (E. I. DuPont), "Hypercrosslinked Rigid Rod Polymers: High Surface Area Reactive Solids," February 17, 1992.

Axel Scherer (Bellcore), "The Resolution Limits of Ion Beam Etching," March 9, 1992.

J. Michael White (University of Texas), "Photochemistry at Adsorbate/Substrate Interfaces," March 23, 1992.

C. Randy Giles (AT&T Bell Labs), "Optical Amplifiers for Lightwave Systems," March 30, 1992.

Ruud Tromp (IBM/T.J. Watson Research Center), "In Situ Studies of Surface Dynamics by Low Energy Electron Microscopy," April 13, 1992.

TECHNICAL REPORTS

1 OPTOELECTRONIC MATERIALS, PHOTON GENERATION, AND DETECTION OF RADIATION

1.1 NONCLASSICAL LIGHT GENERATION AND DETECTION

Malvin C. Teich, Principal Investigator (212) 854-3117
Research Area I, Work Unit 1

Progress has been made on several fronts: light generation, light amplification, light detection, and materials. We have carried out investigations pertaining to: 1) the transmission of information with radiation generated in the form of photon-number-squeezed light; 2) the transmission of information in the presence of light amplified by a cascade of erbium-doped fiber amplifiers; 3) the use of fractal renewal processes for modeling the behavior of charge transport in amorphous semiconductor materials; 4) achieving improvements in the properties of compound semiconductor structures; and 5) the usefulness of a low-temperature semiconductor-surface treatment technique.

We briefly review this progress below:

(1) Information Transmission with Photon-Number-Squeezed Light:[1] Several methods have been proposed for the generation of photon-number-squeezed (sub-Poisson) light by imparting to the photon stream an anticorrelation that regularizes the times of arrival of the photons. This is accomplished by means of control of the excitation or emission process or by feedback, using a copy of the photon point processes in cases [where] the emissions occur in pairs. Possible advantages of communication by photon-number-squeezed light have been evaluated. For receivers in which the photon arrival times are observed, the channel capacity cannot be improved by modifying an initially Poisson photon stream and making it sub-Poisson. For photon-counting receivers, however, improvement of the channel capacity is possible. The bit-error-rate of an on-off keying communication system

using sub-Poisson photons created by introducing anticorrelation into an initially Poisson beam may or may not be smaller than the error rates of the Poisson channel, depending on where the maximum-power constraint is placed.

(2) Performance of Lightwave Systems Incorporating Cascaded Optical Amplifiers:[2] The photon-number distribution (PND) at the output of a *cascade* of erbium-doped fiber amplifiers (EDFAs), with coherent light at the input, turns out to be the noncentral-negative-binomial (NNB) distribution, even in the presence of intervening loss, provided that the normalized bandwidth is the same for all amplifiers. The probability of error (PE) for a cascade of several high-gain EDFAs is essentially the same as that for a single EDFA. The performance of a sequence of postamplifiers is superior to that of a sequence of preamplifiers.

(3) Fractal Renewal Processes as a Model of Charge Transport in Amorphous Semiconductors:[3] We have constructed two relatively simple fractal renewal processes that provide a framework for understanding charge transport in amorphous semiconductors. These processes exhibit fractal behavior, with power spectral densities that vary as $1/f^D$, deriving from interevent-time probability density functions that themselves decay in a power-law fashion.

Fractal renewal processes and their generalizations provide useful models for a wide variety of physical phenomena, since power-law behavior and serial independence are ubiquitous. We have focused on charge transport through amorphous semiconductors, although other applications include electronic burst noise, zero crossings of Brownian motion, the decay of ordered systems, movement in systems with fractal boundaries, the digital generation of $1/f^D$ noise, cache misses, self-organized criticality, and ionic currents in cell membranes.

(4) Strained InGaAs Quantum Wells and HgCdTe Quantum Wires and Boxes:[4,5] A new approach for enhancing the exciton absorption and increasing the saturation limit in quantum wells (QWs), using tensile strain has been proposed. Because of the valence-band mixing in a strained QW, the in-plane hole mass can become very large or negative. This leads to a heavy electron-hole reduced mass (exciton mass), and therefore to a small exciton radius. Exciton absorption is substantially increased because of the increased electron-hole overlap probability in these small-radius excitons. The effects of saturation are also substantially reduced because of decreased charge-screening effects for small-radius excitons and because the rapid dispersal of the photon-generated excitons reduces the Pauli exclusion effect.

Quantum-wire and quantum-box structures for narrow-gap materials with small effective masses, such as HgCdTe, can readily be fabricated using current lithographic techniques. We have calculated the Auger-recombination carrier lifetimes in HgCdTe quantum-wire and quantum-box structures, with band gaps in the 2-5 μm wavelength range. Quantum confinement is generally believed to increase the carrier lifetimes. However, we have found that the Auger recombination lifetime in a HgCdTe quantum wire is shorter than that in a quantum well, and it decreases as the wire width decreases because of the corresponding increase in the density of states. On the other hand, band-to-band Auger recombination is zero in a quantum box because the overlap functions vanish and because of the discrete nature of the energy levels. Therefore, within the confines of our model, we predict improved temperature performance from long-wavelength quantum-box lasers but not from quantum-wire lasers. Furthermore, these conclusions are applicable for all types of band-to-band Auger processes and semiconductor materials.

(5) GaSb-Oxide Removal and Surface Passivation Using an ECR Source:[6] We have described the use of a low-temperature technique, based on H atoms from a microwave electron cyclotron resonance H_2 plasma, to remove surface oxides and carbon from a

single-crystal GaSb surface. Our experiments indicate that oxide removal occurs at a temperature of ~250°C, much lower than that for thermal evaporation of the oxide. In addition, we have found that subsequent exposure to N atoms from a N_2 plasma leaves a thin nitride layer, which p. evants degradation of the H-cleaned surface. To demonstrate this technique, we have applied it to the processing of an AlGaSb p-i-n photodiode, which is fabricated with molecular-beam epitaxy material. Our electrical measurements show that the leakage current, after surface Sb-oxide removal, is significantly reduced from that before the treatment.

This research was supported by the Joint Services Electronics Program.

References:

1. B. E. A. Saleh and M. C. Teich, "Information Transmission with Photon-Number-Squeezed Light," Proc. IEEE **80**, 451 (1992).
2. T. Li and M. C. Teich, "Performance of a Lightwave System Incorporating a Cascade of Erbium-Doped Fiber Amplifiers," Opt. Commun. **91**, 41 (1992).
3. S. B. Lowen and M. C. Teich, "Fractal Renewal Processes as a Model of Charge Transport in Amorphous Semiconductors," Phys. Rev. B **46**, 1816 (1992).
4. Y. Jiang, M. C. Teich, and W. I. Wang, "Enhanced Exciton Absorption and Saturation Limit in Strained InGaAs/InP Quantum Wells," J. Appl. Phys. **71**, 769 (1992).
5. Y. Jiang, M. C. Teich, W. I. Wang, and J. R. Meyer, "Auger Recombination in HgCdTe Quantum Wires and Quantum Boxes," J. Appl. Phys. **71**, 3394 (1992).
6. Z. Lu, Y. Jiang, W. I. Wang, M. C. Teich, and R. M. Osgood, Jr., "GaSb-Oxide Removal and Surface Passivation Using an Electron Cyclotron Resonance Hydrogen Source," J. Vac. Sci. Tech. B **10**, 1856 (1992).

PUBLICATIONS (Research Area I, Work Unit 1)

B. E. A. Saleh and M. C. Teich, "Information Transmission with Photon-Number-Squeezed Light," Proc. IEEE **80**, 451 (1992) [Special issue on quantum electronics edited by J. Whinnery].

T. Li and M. C. Teich, "Performance of a Lightwave System Incorporating a Cascade of Erbium-Doped Fiber Amplifiers," Opt. Commun. **91**, 41 (1992).

S. B. Lowen and M. C. Teich, "Fractal Renewal Processes as a Model of Charge Transport in Amorphous Semiconductors," Phys. Rev. B **46**, 1816 (1992).

Y. Jiang, M. C. Teich, and W. I. Wang, "Enhanced Exciton Absorption and Saturation Limit in Strained InGaAs/InP Quantum Wells," J. Appl. Phys. **71**, 769 (1992).

Y. Jiang M. C. Teich, W. I. Wang, and J. R. Meyer, "Auger Recombination in HgCdTe Quantum Wires and Quantum Boxes," J. Appl. Phys. **71**, 3394 (1992).

Z. Lu, Y. Jiang, W. I. Wang, M. C. Teich, and R. M. Osgood, Jr., "GaSb-Oxide Removal and Surface Passivation Using an Electron Cyclotron Resonance Hydrogen Source," J. Vac. Sci. Tech. B **10**, 1856 (1992).

1.2 NEW OPTICAL MATERIALS AND SOURCES

Irving P. Herman, Principal Investigator (212) 854-4950
Research Area I, Work Unit 2

The focus of this work unit is to understand the structural, optical and electronic properties of semiconductor materials, including superlattices and heterostructures, using optical spectroscopy and high pressure tuning. This work unit also includes optical diagnostics that are important in the fabrication of these materials. Significant advances were made during this past reporting period.

We continued our study of the optical spectroscopy of II-VI semiconductors. The demonstration of current-driven diode lasers of ZnCdSe quantum wells in ZnSe at various laboratories this past two years[1,2] demonstrates the importance of these materials for blue/green and yellow lasers and the recent major advances in the materials science and optical physics of II-VI semiconductors.

The final measurements of photoluminescence (PL) vs. pressure of $ZnSe/Zn_{1-x}Mn_xSe$ strained layer superlattices (SLS) were made for x = 0.23, 0.33 and 0.51, which clearly indicate Type I alignment (Figure 1). (These samples were obtained from R. Gunshor at Purdue University.) This has improved our understanding of the properties of these materials at very high pressure over that which we reported last year. We also extended the PL measurements of a ZnSe strained layer on GaAs (obtained from Purdue and Philips) up to pressures where the ZnSe is no longer compressive but under tensile strain. The lh and hh exciton features reverse, as is shown in Figures 2 and 3. Work on other II-VI semiconductor superlattices began. The PL spectrum of ZnTe/ZnCdTe superlattices obatined from R. Feldman at AT & T Bell Laboratories is shown in Figure 4.

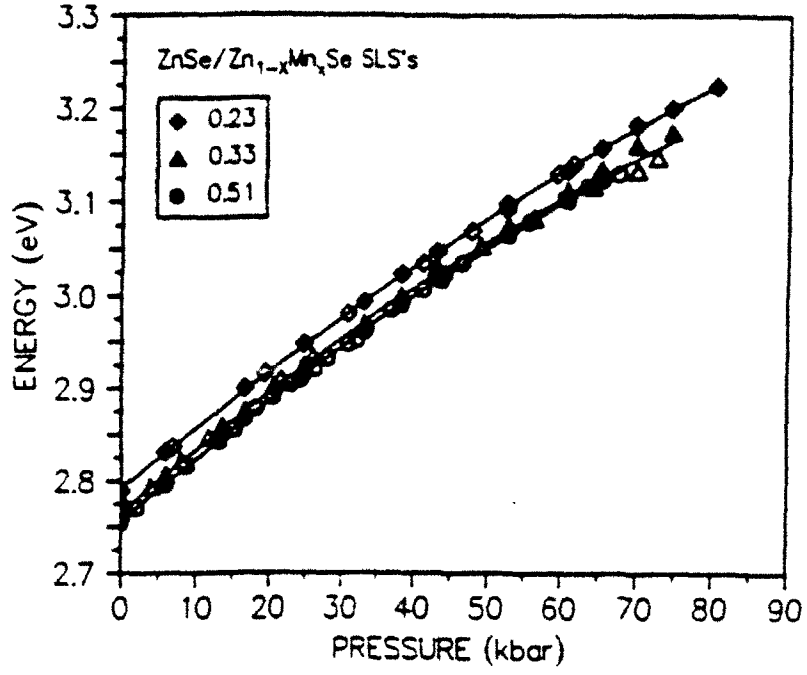

Figure 1. Peak energy of photoluminescence vs. pressure of $ZnSe/Zn_{1-x}Mn_xSe$ strained layer superlattices (SLS) for x = 0.23, 0.33 and 0.51.

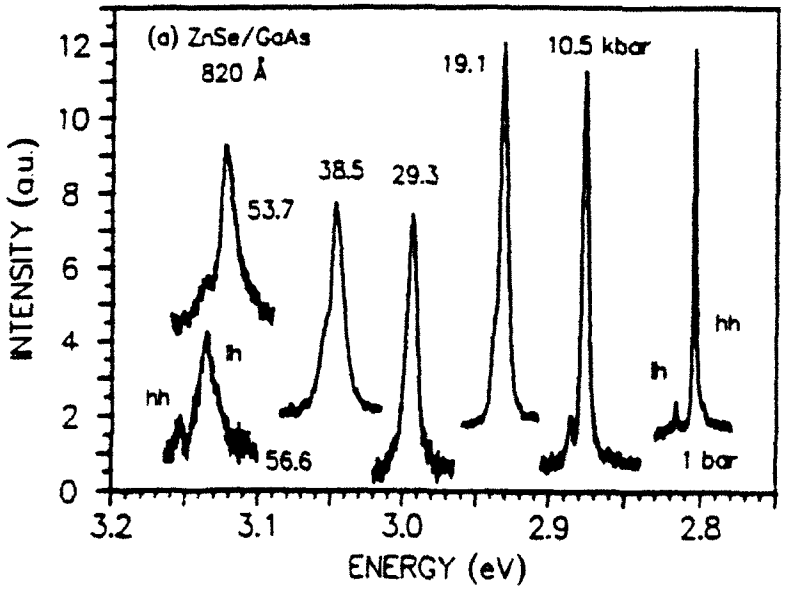

Figure 2. PL spectrum showing light and heavy hole exciton recombination radiation at 9 K in a thin strained layer of ZnSe on GaAs.

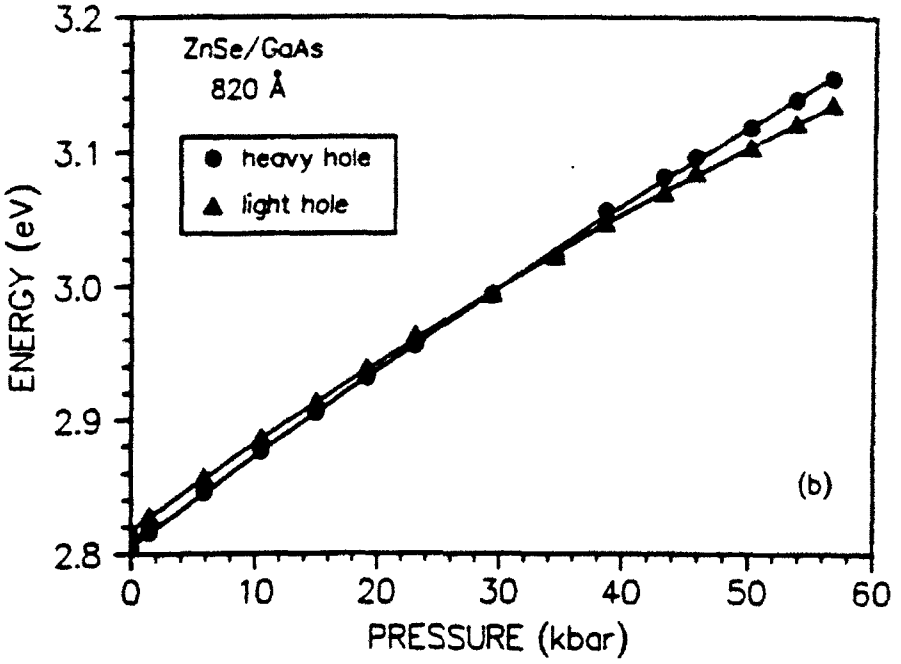

Figure 3. Variation of lh and hh peaks for ZnSe strained layer on GaAs vs. pressure.

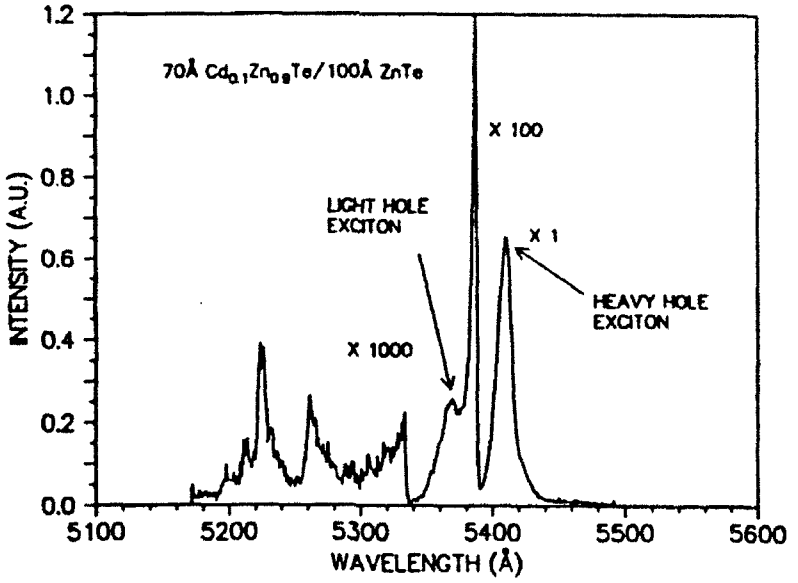

Figure 4. Photoluminescnece of ZnTe/ZnCdTe superlattices.

Work continued on Si/Ge-based heterostructures, including that on short-period Si/Ge superlattices and SiGe alloys. The temperature dependence of optical phonon

frequencies in SiGe alloys was examined for each of the three local modes, due to Si-Si, Si-Ge and Ge-Ge vibrations, as is seen in Figure 5 vs. the fraction of silicon in the alloy (x). The Si-Si modes are similar to the c-Si optical phonon mode, while the Ge-Ge modes are similar to the c-Ge phonon mode.

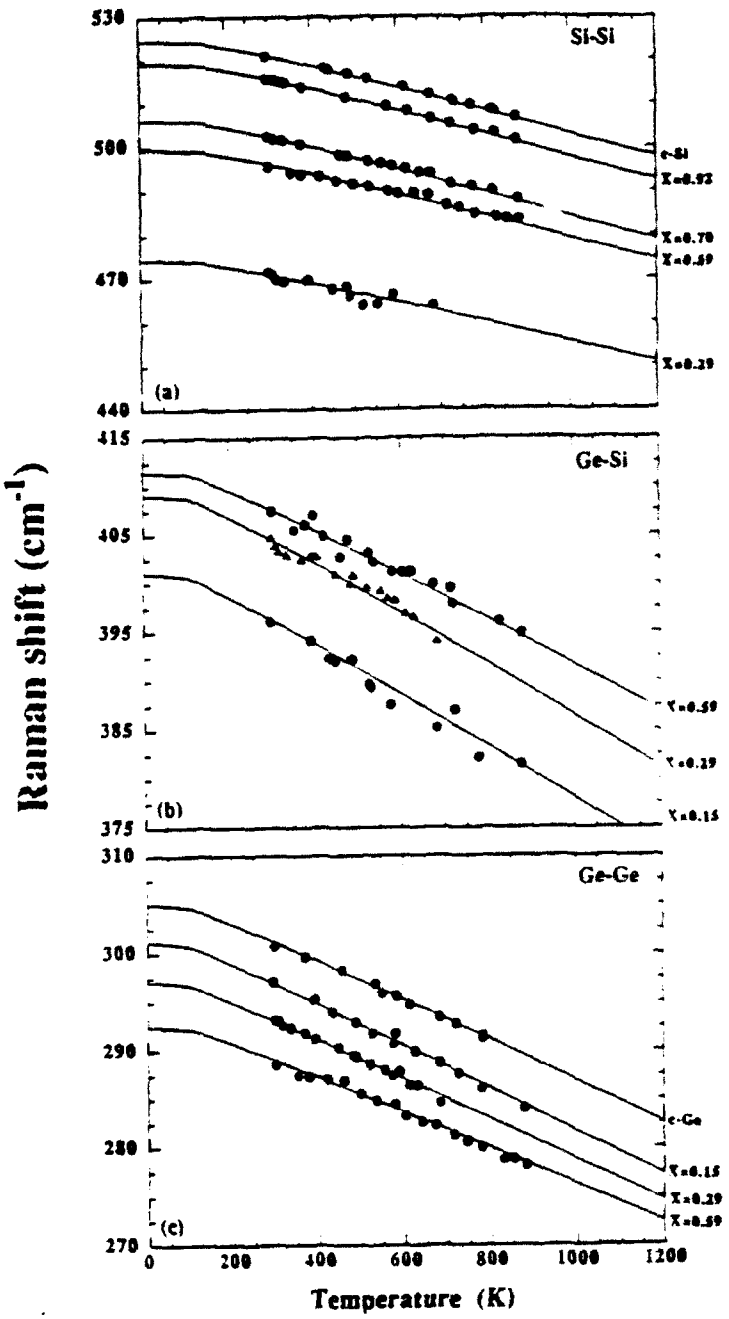

Figure 5. The temperature dependence of the frequencies of the Si-Si, Ge-Si, and Ge-Ge optical phonon modes in bulk Ge-Si alloys.

To support our studies of phonons in strained layer Si/Ge heterostructures we have performed lattice dynamics calculations to study these materials, and also unstrained structures, at ambient and elevated pressure. The first method we adopted was the Keating model, which has two force constant parameters, α and β. The effect of strain was included by adding three parameters to modify α and β. Results obtained using this modified Keating model are shown in Figures 6 and 7 and Table I. It offers a good description of many features of optical phonons, which can be used to explain properties of ultrathin Si/Ge superlattices by considering the comfinement of optical phonons within the layers. Improvements in this model are underway that will allow a more precise treatment of optical phonons, as well as a better description of acoustic phonons and the elastic constants. One improvement is the inclusion of more interactions, than the two in the Keating model, as in valence bond force methods. The second is the analysis of cubic anharmonic terms, rather than the use of ad hoc strain-modified harmonic force constants.

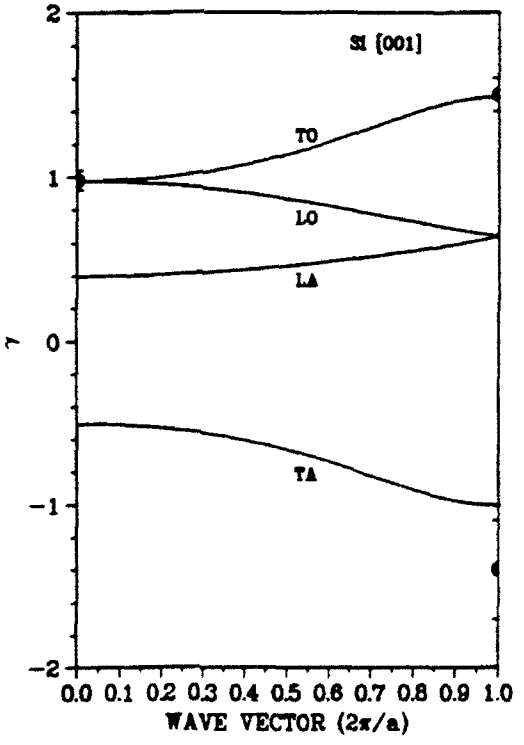

Figure 6. Grüneisen parameters for Si using the modified Keating model.

TABLE 1

	Theoretical	Si	Ge
$\gamma_{LO,TO}(\Gamma)$	$-\frac{n\alpha_0+m\beta_0}{6(\alpha_0+\beta_0)}$	0.98 ± 0.06	0.96 ± 0.05
$\gamma_{LO}(X)$	$-\frac{n\alpha_0+2m\beta_0}{6(\alpha_0+2\beta_0)}$		
$\gamma_{TO}(X)$	$-\frac{n}{6}$	1.5 ± 0.2	(1.43)
$\gamma_{LA}(X)$	$-\frac{n\alpha_0+2m\beta_0}{6(\alpha_0+2\beta_0)}$		
$\gamma_{TA}(X)$	$-\frac{m}{6}$	− 1.4 ± 0.3	− 1.5 ± 0.1
$\gamma_{LO}(L)$	$-\frac{6n\alpha_0+m\beta_0}{6(6\alpha_0+\beta_0)}$		1.2 ± 0.2
$\gamma_{TO}(L)$	$-\frac{2n\alpha_0+m\beta_0}{6(2\alpha_0+\beta_0)}$	1.3 ± 0.2	0.9 ± 0.1 (1.43)
$\gamma_{LA}(L)$	$-\frac{2n\alpha_0+13m\beta_0}{6(2\alpha_0+13\beta_0)}$		0.5 ± 0.1
$\gamma_{TA}(L)$	$-\frac{m}{6}$	− 1.3 ± 0.3	− 0.4 ± 0.3

Table I. The Grüneisen parameters obtained from the Keating model, along with available experimental for Si and Ge. Selected calculated values are given in parenthesis.

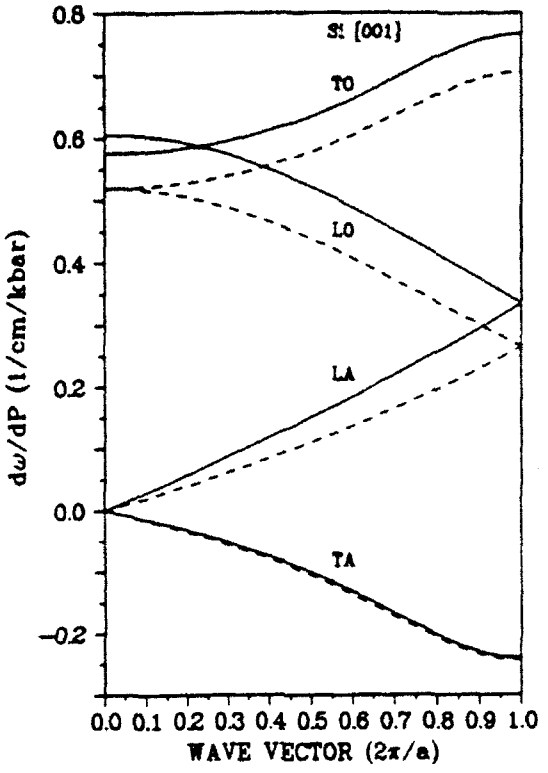

Figure 7. The change of optical phonon frequency with pressure for strained Si epilayers on Ge and for bulk Si, using the modified Keating model.

We began a collaboration with D. Lowndes and co-workers at Oak Ridge National Laboratory in which we have used photoluminescence to examine ZnSe and ZnS films they deposited by pulsed laser ablation (PLA). This study has shown that the PLA-grown ZnSe films seem to have more impurities than MBE-grown films (Figure 8). The ZnS films seem to have fewer features due to impurities. The photoluminescence spectra of PLA-grown ZnS films seems to indicate that they are very pure (Figure 9).

This past year Professor Herman moved his laboratory to the new Schapiro Center for Engineering and Physical Sciences Research, which houses several of the Columbia Radiation Laboratory JSEP activities. His new facilities are twice as large as his previous space and are much more modern.

This research was supported by the Joint Services Electronics Program.

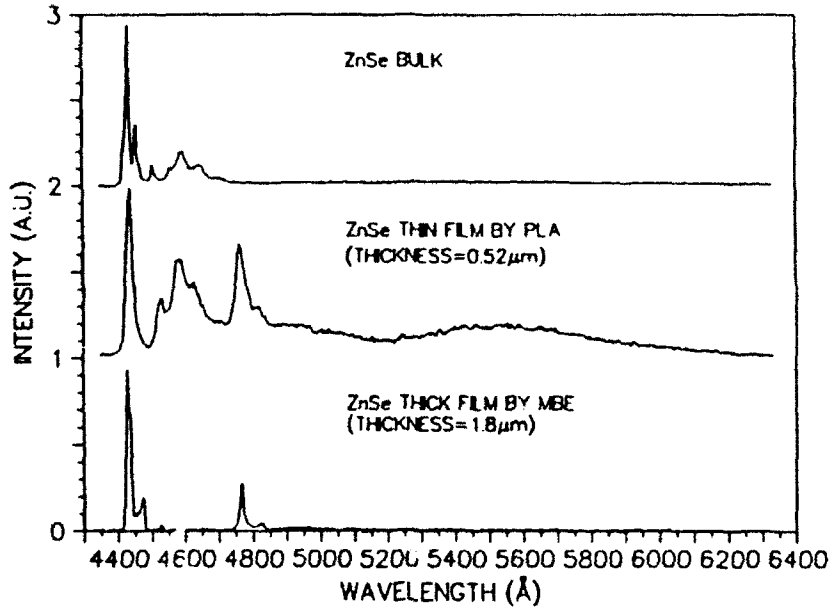

Figure 8. Comparison of photoluminescence in MBE-grown, bulk and laser-ablation grown ZnSe.

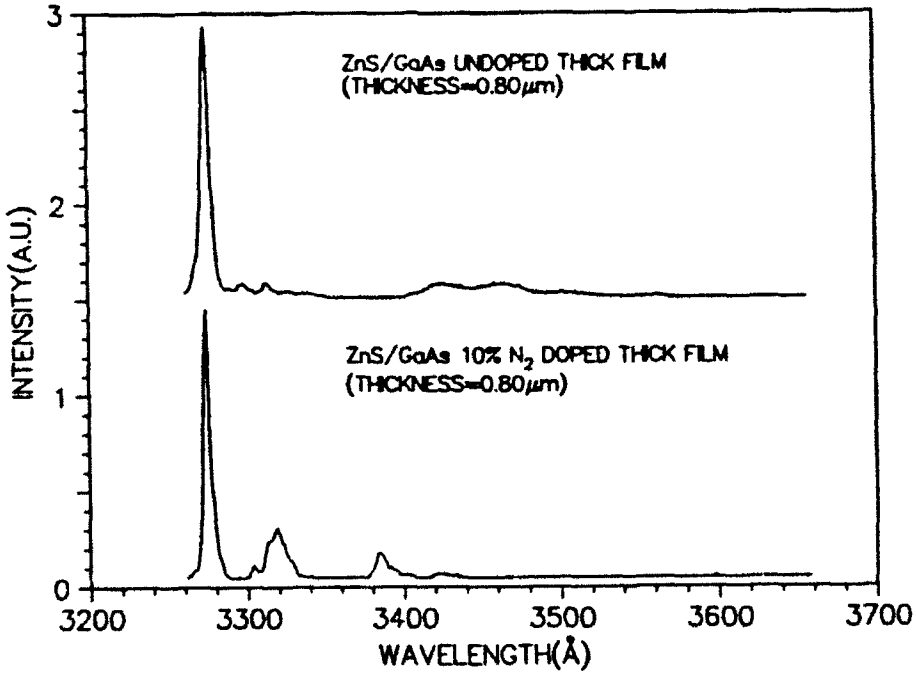

Figure 9. *Photoluminescence in laser-ablation grown ZnS.*

References:

1. M. A. Haase, J. Qiu, J. M. DePuydt, and H. Cheng, Appl. Phys. Lett. **59**, 1272 (1991).
2. H. Jeon, J. Ding, A. V. Nurmikko, H. Luo, N. Samarth, and J. Furdyna, Appl. Phys. Lett. **59**, 1293 (1991).

PUBLICATIONS (Research Area I, Work Unit 2)

Z. Sui, P. P. Leong, I. P. Herman, G. S. Higashi, and H. Temkin, "Raman Analysis of Light-Emitting Porous Silicon," Appl. Phys. Lett. **60**, 2086 (1992).

J. A. Tuchman and I. P. Herman, "General Trends in Changing Epilayer Strains through the Application of Hydrostatic Pressure," Phys. Rev. B **45**, 11 929 (1992).

J. A. Tuchman and I. P. Herman, "General Trend in the Effect of Hydrostatic Pressure on Mismatch Strains in Semiconductor Heterostructures," Bull. Am. Phys. Soc. **37**, 688 (1992).

Z. Sui, P. P. Leong, I. P. Herman, G. S. Higashi, and H. Temkin, "Raman Analysis of Light-emitting Porous Silicon," Bull. Am. Phys. Soc. **37**, 564 (1992).

Z. Sui, P. P. Leong, I. P. Herman, G. S. Higashi, and H. Temkin, "Analysis of the Structure of Porous Silicon by Raman Scattering,". Mat. Res. Soc. Symp. Proc. **256**, 13 (1992).

J. A. Tuchman, S. Kim, Z. Sui and I. P. Herman, "Exciton Photoluminescence of Bulk ZnSe and ZnSe Epilayers under Hydrostatic Pressure," Phys. Rev. B **46**, 13 371 (1992).

J. A. Tuchman, Z. Sui, S. Kim and I. P. Herman, "Photoluminescence of ZnSe/ZnMnSe Superlattices under Hydrostatic Pressure." J. Appl. Phys. (1992), accepted.

2 ELECTRONICS MATERIALS AND PROCESSING

2.1 ULTRAVIOLET TWO-PHOTON LASER PHOTOELECTRON STUDIES OF EXCITED SEMICONDUCTOR SURFACES

Richard M. Osgood, Jr., Principal Investigator (212) 854-4462

Research Area II, Work Unit 1

A. Preparation of Pristine Semiconductor Surfaces by ECR Atom Chemistry

Recently in a series of experiments, we have shown that atoms generated in a remote, low pressure plasma can be used to remove the native oxide and other atmospheric-induced impurities from the surface of III-V semiconductor wafers. This is an extremely important finding for future and present GaAs-based device technology because the process is low-temperature and it acts only on the top monolayer of the wafer surface. Both characteristics are important for precise in situ manufacture of MESFET and HEMT circuits.

The importance of this research was underscored at a recent American Vacuum Society meeting at which engineers from AT&T described experiments which used the ECR atom chemistry technology which was developed at Columbia. In these talks, they explained that the ECR surface preparation work, which they carried out in a prototype in situ manufacturing system, could be used for the low-temperature cleaning of AlGaAs surfaces as well as GaAs surfaces. We feel that this experiment represents the first step in the transfer of our technique into the manufacturing environment.

Work on this technique continued this year supported by JSEP funding. The emphasis of these most recent experiments was to show that the technique could be applied to the surfaces of GaSb. This material and its related alloys form the basis of three very new and important electronics technologies: (1) low noise photodetectors, (2) multispectral imaging systems, and (3) quantum tunnelling devices. Our results, shown in Figure 1, show that hydrogen and nitrogen atoms can be used to remove oxides and carbon, and to seal the passivated surfaces, respectively. More details of the work in this project are described in a collaborative paper by Professors Osgood, Teich and Wang.[1]

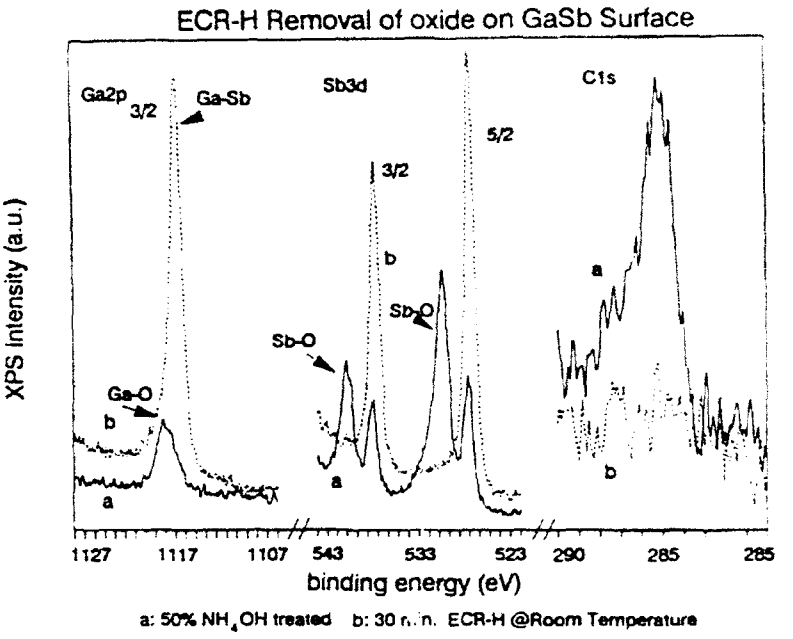

Figure 1a. XPS spectra of the Ga $2p_{3/2}$, Sb 3*d*, C 1*s* core levels for a GaSb surface (a) chemically cleaned (solvent cleaning plus 50% NH_4OH for 1 min); (b) after exposure to a 30 min. ECR-H plasma at room temperature.

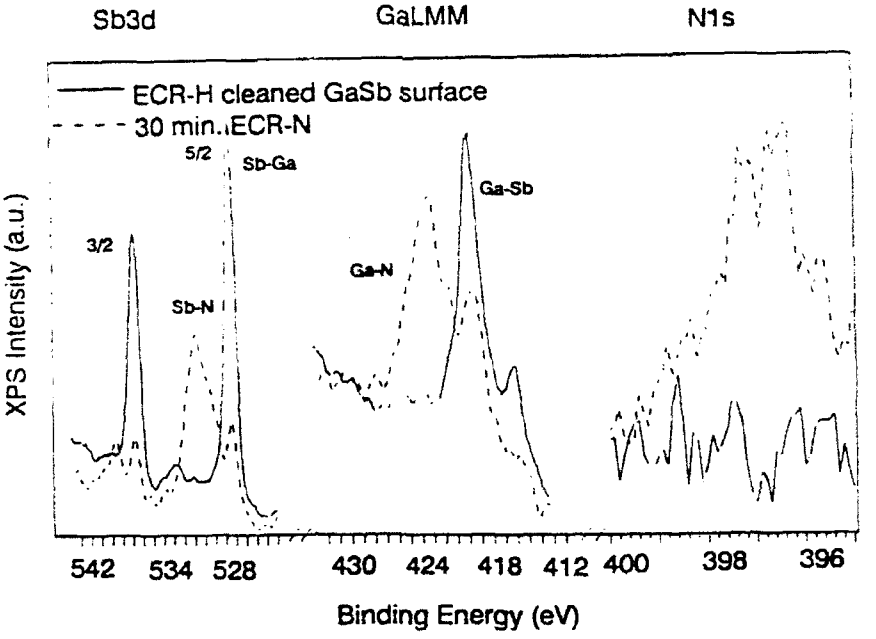

Figure 1b. XPS spectra of the Sb 3*d*, Ga *LMM*, and N 1*s* features for a clean GaSb surface before and after exposure to an ECR-N plasma for 30 min.

Reference:

1. Z. Lu, Y. Jiang, W. I. Wang, M. C. Teich, and R. M. Osgood, Jr., "GaSb-oxide Removal and Surface Passivation Using Hydrogen Atoms from an Electron Cyclotron Resonance Source," J. Vac. Sci. Tech. **B10**, 1856 (1992).

B. Optical Investigation of Image-Potential-Induced Surface Resonances on Cu(110)

One of our major recent accomplishments in the area of two-photon-photoemission (2PPE) spectroscopy was the application of this technique for observation of very-short-lived excited electronic states. We utilized a nanosecond light source to observe states with lifetimes on the order of a femtosecond, thus enhancing the utility of 2PPE spectroscopy as a surface probe. This ability to see short lived states is important for better understanding of metal surfaces as well as for the ability to probe excited states in semiconductor interfaces.

In particular, we have measured the photoemission spectra from surface resonances resulting from strong mixing of an image-potential (IP) state with a bulk energy band. These strong image resonances have recently become of interest since they provide a clear example of a well defined, calculable surface resonance system. In contrast to an image state which is formed by an electron reflecting between the Coulombic and the crystal barrier, an image resonance is formed by reflection between the same surface Coulombic barrier and an inner discontinuity in the surface potential. Quantum mechanically we would expect an increased broadening of the image feature as the degree of coupling to the bulk is increased, a phenomena which has been discussed in conjunction with the dependence on the principal quantum number of image states[1-3] and the analogous broadening of discrete energy levels of an adsorbed atom on a metal surface.[4-6] While several papers have investigated these resonances theoretically, there have been only a very limited set of corresponding experimental measurements. Typically these have relied on inverse photoemission and thus have generally had low resolution. In our experiments we were able to measure the short lived image surface resonance on the surface of Cu(110) using the two-photon photoemission, thus providing the necessary accuracy for further theoretical development on IP-induced resonances.

Comparison of IP features on three low index surfaces of copper is shown in Figure 2.

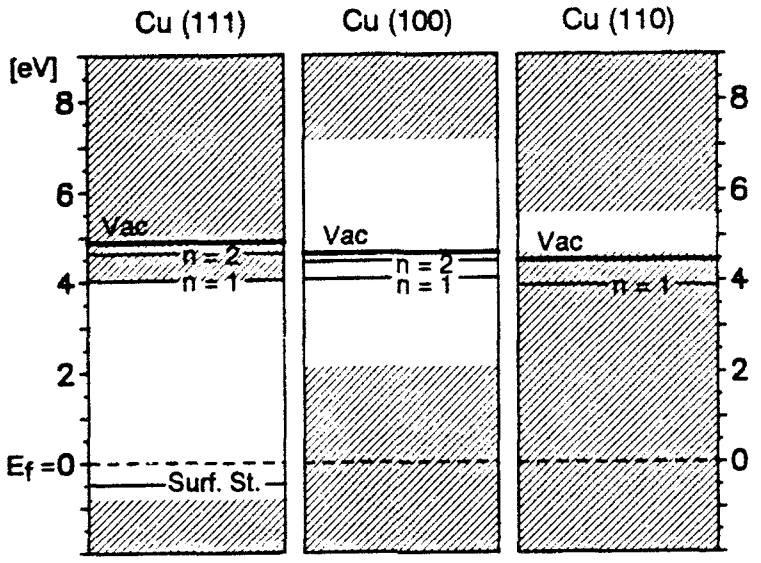

Figure 2. Energy band diagrams for Cu(111),[10] Cu(100),[12] and Cu(110).[7,8] $K_{||} = 0$, projected $k_{\perp}$. The hashed area represents the projection of the bulk band structure. Image potential states and resonances are designated by "n = 1" and "n = 2".

IP states and resonances presented in the figure have all been observed with 2PPE technique, but the three observations differed in the character of the initial or intermediate state. To probe the IP state on Cu(111), a narrow surface state that lay below E_F in the band gap of the projected band structure was used as the initial source of electrons in the 2PPE process.[9,10] Because of the surface character of the initial state, the 2PPE signal was particularly strong as the density of states for the narrow surface state is much higher than that of the bulk continuum initial levels, which are important in the cases of Cu(110) and Cu(100). Also, the transition matrix element is bigger for the overlap of a surface state wave function than for the overlap of the bulk wave function with the IP state.[11,12] In 2PPE on Cu(100)[12,13] the initial state was the bulk band, thus the intensity of the signal for this surface was an order of magnitude lower than from the (111) faces for comparable light intensities.

For the case of the Cu(110) there is also no initial surface state in the 2PPE process, and furthermore the IP resonance is fully mixed with the bulk continuum resulting in a further reduction of 2PPE signal intensity. Despite the consequently weak 2PPE signal, we were able to observe the Cu(110) n = 1 IP resonance and measure its position and width.

The experimental procedure and set-up used to carry out our experiments were described in a previous report.[14]

A typical EDC for normal emission and hν = 4.14 eV, is presented in Figure 3 (the EDC has been corrected neither for the sample bias, -5 volts, nor for the spectrometer contact potential). Three peaks appear at 5.8 eV, 7.3 eV, and 9.3 eV kinetic energy.

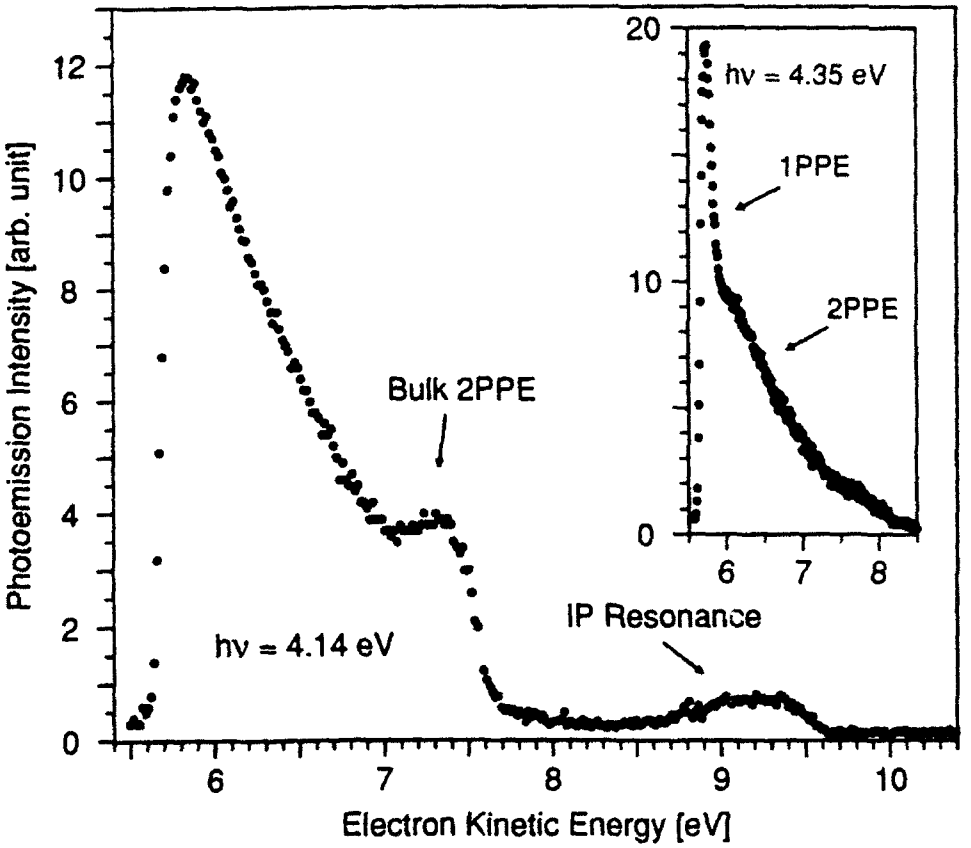

Figure 3. Typical two-photon photoemission energy distribution curve for Cu(110) (normal emission, hν = 4.14 eV). Single-photon photoemission as well as two-photon photoemission features are observed. The inset shows the 5.8 eV peak scanned at a higher photon energy, hν = 4.35 eV, for which two components of this peak are clearly distinguishable.

The peak at 5.8 eV is due to the single-photon photoemission process from thermally excited states just above the Fermi level, in the vicinity of the Σ_1 band (inset Figure 4), to free-electron-like states above the vacuum level. The high energy tail of this peak arises in part from 2PPE from bulk states 3~4 eV below E_F. The inset of Figure 3 clearly shows the two contributions to the 5.8 eV peak. This data was taken with higher incident photon energy than in Figure 3, which caused the 1PPE peak to be enhanced over the 2PPE tail in comparison to the results shown in the figure.

The small broad peak at 7.3 eV (Fig. 3) stemmed from 2PPE excitation from a 3d-like bulk band of copper.[15] Figure 4 shows the variation in kinetic energy position of this feature with the change in the incident photon energy. The data lies on the straight line with slope 2 ($\Delta E_{kin} = 2\Delta h\nu$), which indicates that this feature is due to a fixed initial state. The fact that the EDC signature of this state was also observed on contaminated Cu(110) surfaces established that a bulk state is the initial level in this transition, specifically 3d-like bulk band of Cu.

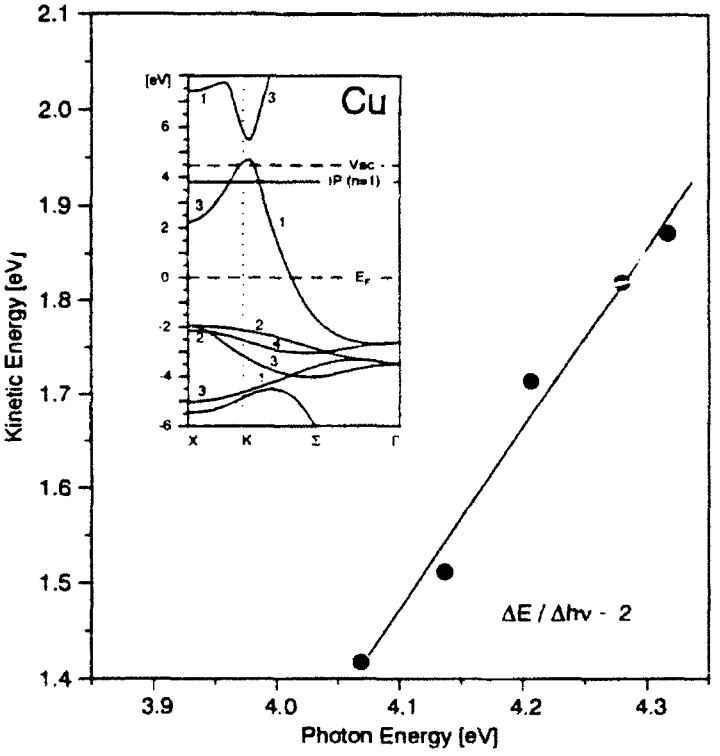

Figure 4. Variation of the kinetic energy of the 3d-like bulk band peak with change in photon energy. The $\Delta E_{kin} = 2\Delta h\nu$ dependence indicates a fixed initial state. The inset shows the bulk energy bands of Cu.[7,8,16]

The high kinetic energy of the 9.3 eV EDC peak (Figure 3) indicated that this feature was due to a two-photon process. The position of the rising edge of this peak was monitored as the incident photon energy was varied, and it was established that the kinetic energy change of the peak was equal to the change in the incident photon energy, concluding that the 9.3 eV feature used a fixed intermediate state in the two-photon process. The photoemission intensity of this peak was sensitive to the quality of the prepared surface indicating a surface state, while its binding energy was in the expected range for n = 1 IP state, and our angle resolved 2PPE study of this state confirmed that it had positive dispersion. Since previous studies have not reported other surface states in this energy range, we concluded that the 9.3 eV feature was due to the IP state of Cu(110).

The slope of the high energy side of the IP state EDC feature is step-like. We have determined that it reflects a Fermi energy cut-off, i.e., the rapid decrease of occupied energy states above the Fermi energy level. Figure 5 gives a schematic representation of the 2PPE process for a broadened intermediate state indicating that the final EDC is the product of the actual image-state feature multiplied by the Fermi function.

As is clear from Figure 5, it is possible, in principle, to measure the entire image-potential feature by increasing the photon energy. In practice, however, as the photon energy was increased, the 5.8 eV peak grew, and for $\lambda < 285$ nm ($h\nu > 4.35$ eV) significant distortion of the EDC occurred due to space charge.

The Cu(110) IP resonance data for $\lambda = 285$ nm ($h\nu = 4.35$ eV) is shown in Figure 6, where the energy axis is referenced to the vacuum level.

Numerical analysis revealed that this IP feature can be approximated as two Lorentzians with an exponential background multiplied by the Fermi function and convoluted with a Gaussian resolution of our detector. The lower energy Lorentzian was assigned to the n = 1 IP-induced resonance, and its binding energy was determined to be 0.68 ± 0.1 eV. The FWHM of this feature was measured to be 0.66 ± 0.06 eV which reflects a lifetime of 1.00 ± 0.09 fs. Lack of detail on the IP EDC feature did not allow for

individual resolution of higher IP states. The observed broad energy signature and the short lifetime was due to the resonant nature of Cu(110) IP states.

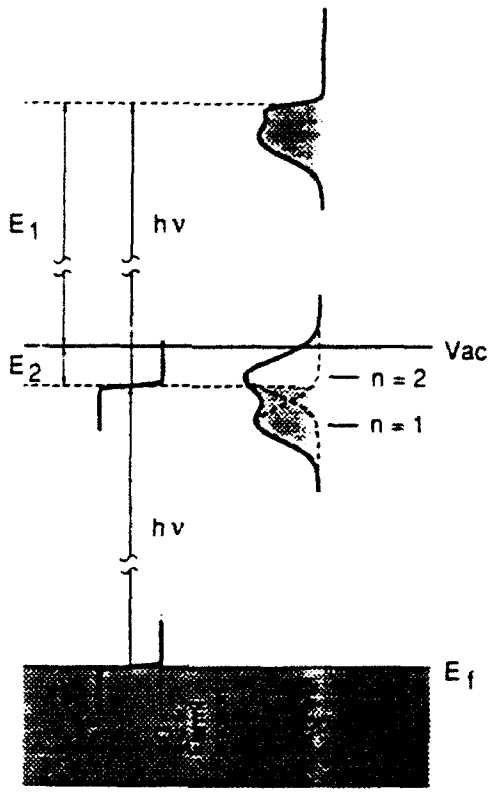

Figure 5. Two-photon excitation process for a broad intermediate state. Due to the Fermi distribution function, the states below $E_F + h\nu$ are predominantly populated by the first photoexcitation. The resultant EDC is a modified signature of the broad intermediate state (in our case, image potential resonance).

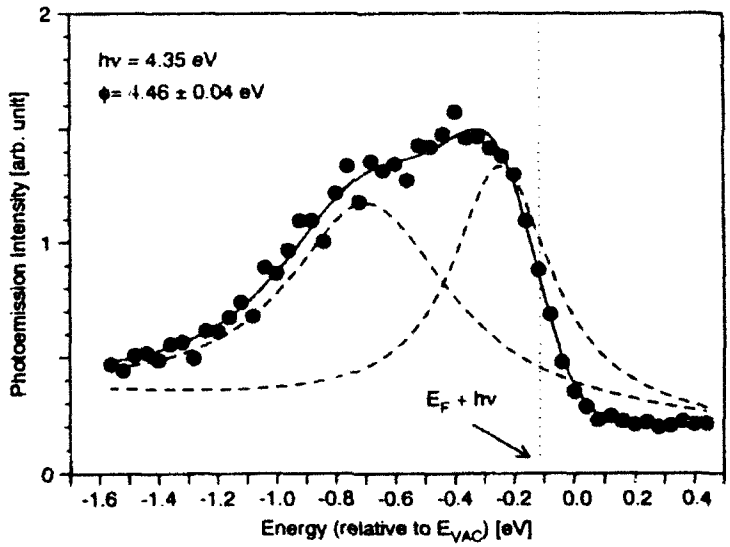

Figure 6. Image potential induced EDC peak on Cu(110) (normal emission, $h\nu = 4.35$ eV) composed of two broad, image resonances which have blended into a single feature. The $E_F + h\nu$ level has been indicated. The resultant work function is $\phi = 4.46 \pm 0.04$ eV.

Image potential features on Cu(110) surface, with their binding energies of less than 1/16 Ry, are expected to be energy degenerate with states of the bulk (Figure 2), and thus exhibit broad linewidths. Previous theoretical work on resonant states of generic (111) and (100) fcc crystal surfaces predicted an energy width of n = 1 IP state of up to 1 eV.[2,17,18] Similarly broadened linewidths are to be expected for resonant states of (110) metal surfaces, specifically Cu(110) in our case. Considering that consecutive members of Rydberg-like image state series are at most a fraction of an eV apart, we conclude that broadened IP states would overlap and blend into each other, producing a single, very broad feature as observed in our data.

The significance of our measurements can be seen in Table 1, which summarizes the currently available inverse photoemission (IPE) and 2PPE data for IP states on Cu(110). The accuracy of measurements performed by other groups did not allow for the resolution of individual IP states that form the broad IP feature; therefore, they report lower binding energies than those observed in our 2PPE measurement. The Cu(110) work function is indicated for each entry, since the IPE technique refers all the measurements to the Fermi level.

Table 1

E_{bind} [eV]	Work Function Used [eV]	Method	Reference
0.0± 0.2[a)]	4.50[b)]	IPE	19
0.18 ± 0.4	4.48[b)]	IPE	20
0.1 ± 0.4[c)]	4.50[b)]	IPE	21
0.3 ± 0.2	4.50[b)]	IPE	7
0.48 ± 0.15	4.87[d)]	IPE	22
0.68 ± 0.1 (n = 1)	4.46[e)]	2PPE	our measurement

a) Extrapolated in Ref. 7
b) Assumed value
c) Extrapolated by us from results of Ref. 21
d) Measured in situ by a Kelvin probe
e) Measured in situ from the EDC spectra (see text and Figure 5)

Table 1. *Binding energies for Cu(110) image potential resonance determined by inverse photoemission (IPE) and two-photon photoemission (2PPE).*

An interesting result of the work presented here is that the 2PPE EDC curve provided a useful method of in situ measurement of the work function ϕ, when $h\nu < \phi$. In particular, numerical fits to the data in Figure 6 provide us with the energy position of the $E_F + h\nu$ line relative to the vacuum level, which is reflected in energy E_2 from Figure 5. Using the value of E_2, the work function can be expressed as $\phi = E_2 + h\nu = 2h\nu - E_1$, and for our data, $\phi = 4.46 \pm 0.04$ eV, a value which is in agreement with other data in literature.[23] It is important to realize that the breadth of the IP state enabled us to observe clearly the $E_F + h\nu$ level. Thus, such a 2PPE work function measurement is not possible for surface systems with narrow, intermediate states. For the electron detector resolution used in Figure 6, the cutoff corresponding to the transposed Fermi function is sufficiently abrupt to provide for accurate (up to 0.1 eV) determination of the work function even without the employment of numerical fits. Furthermore, our work function measurement was sufficiently precise that it could be used for monitoring the surface quality throughout the experiment. For example, a sample that had been sitting in ~8 x 10^{-10} Torr for ~8 hours exhibited a work function difference of about 0.1 eV, and also a reduced image peak, as compared to that seen on a freshly sputtered/annealed sample.

In conclusion, we have observed a broad EDC feature that corresponded to the image potential states of Cu(110). The resonant nature of these states was responsible for their short lifetime and the consequent broad energy signature. The broadening of the Rydberg-like IP state series resulted in an overlap of individual states which merged into a single feature. Since IP states were located very close to the E_{VAC} we were not able to scan the whole IP peak without space charge distortions. With the measurement of the binding energy of n = 1 IP state ($E_B = 0.68 \pm 0.1$ eV) and its linewidth ($\Delta E = 0.66 \pm 0.06$ eV), we have demonstrated that the observation of energy-broadened surface resonances is possible with the 2PPE technique despite their short lifetimes. This is a significant step in the evolution of the 2PPE spectroscopy as a surface resonance probe. The 2PPE spectroscopy on broadened IP states also presented a simple method of measuring the work function.

References:

References 1 - 23 are listed at the end of the next section (Section C).

C. Image-Potential States and Surface Plasmons: Temperature Dependence

We report significant progress in theoretical study of surface plasmons, derived from the results of our previous experimental work on the dependence of image-potential states with the variation of surface temperature.[24]

In the past decade, IP induced electronic states have been the subject of a considerable amount of experimental research work.[25] One important characteristic of this special class of surface states is their being pinned to the vacuum energy level. In our previous work,[26] and work by other researchers,[27] it has been shown that the binding energies of IP induced states on transition metal surfaces are independent of temperature or atomic adsorption. This result led us to further explore the well known intimate connection between image-potential induced states and surface plasmons, and allowed us to derive an expression for the temperature dependence of the eigenfrequencies of surface plasmons. As surface plasmons influence the surface charge density, their thorough understanding is necessary for determining the behavior of carriers localized at the surface. Our derived expression is very general and applies to complex transition metals as well as to free-electron-like metals. This examination on metal surfaces is the natural first step in further work on surface plasmons at semiconductor surfaces.

The long-range action of a semi-infinite solid upon an external charge is believed to be solely due to the polarization of the electronic surface collective excitations, i.e., in the case of a metal surface, by its surface plasmons.[28] It has been shown,[4] that the strength of the interaction between an electron outside a metallic surface and a surface plasmon with two-dimensional wavevector $\mathbf{k}$ is, in second-quantization formalism and with the notations of [4, pp. 141-144], given by:

$$g_k\left(a_k + a_{-k}^{\dagger}\right) e^{ik\cdot r_{\parallel}} \; e^{-kz}, \tag{1}$$

where:

$$g_k = -\frac{e^2}{2\varepsilon_o}\sqrt{\frac{\hbar N}{2m_e A}} \quad \sqrt{\frac{1}{k\omega_s(k)}} \tag{2}$$

and where A is the area of the metallic surface, N is the effective free electron density, $\omega_s(\mathbf{k})$ is the **k**-surface-plasmon eigenfrequency and $k = |\mathbf{k}|$. The interaction energy between the metallic surface, represented by its surface plasmons, and the electron, at a distance z, is then given by:

$$V(z) = -\sum_k \frac{g_k^2}{\hbar\omega_s(k)} e^{-2k|z|} \tag{3}$$

Providing that the electron is sufficiently far away from the surface, the long-wavelength terms (small k) dominate in the above summation over the different modes, therefore, in this summation, $\omega_s(\mathbf{k})$ can be approximated by $\omega_s(\mathbf{0}) \equiv \omega_s$ to yield:

$$V(z) = -\frac{\pi E_o \hbar^2}{m_e} \; \frac{N}{\omega_s^2} \; \frac{1}{z}, \tag{4}$$

where E_o is the hydrogen atom ground state binding energy, i.e. $E_o \approx 13.6$ eV. In the simplest model for the surface potential, which is taken infinitely repulsive for $z < 0$ and equal to the above V(z) for $z > 0$, we obtained the image-potential induced n^{th} state binding energy as:[29]

$$E_B(n) = \frac{\pi^2 E_o^2 \hbar^2}{2m_e^3} \left(\frac{N}{\omega_s^2}\right)^2 \frac{1}{n^2} \tag{5}$$

We recognized that in the above expression binding energies depend on the nature of the metallic surface only through the ratio of N to ω_s^2. Since it was observed in our

experiments that E_B is independent of temperature variations, i.e., $\Delta E_B/\Delta T = 0$, this yielded $\Delta(N/\omega_s^2)/\Delta T = 0$. This expression can be rewritten as:

$$\frac{\Delta \omega_s}{\Delta T} = -\frac{3}{2}\alpha \omega_s \quad , \tag{6}$$

since, in the case of metals, $-(\Delta N/\Delta T)/N$ is, to an excellent approximation, equal to 3α, where α is the linear expansion temperature coefficient.[31]

We confirmed the validity of the above expression by comparing the value of $\Delta\omega_s/\Delta T$ measured on Ag(100) by M. Rocca *et al.* :[30] $\Delta\omega_s/\Delta T = -(8.9\pm0.9)\times10^{-5}$ eV/K to the numerical value which is retrieved from (6) with $\alpha = 19\times10^{-6}$ K^{-1},[31] and $\omega_s = 3.69$ eV:[30] $\Delta\omega_s/\Delta T = -10.5\times10^{-5}$ eV/K. The agreement is remarkable if one considers the simplicity of the model we used to derive (6).

To further refine the expression of Equation 6, we utilized a modified expression for the binding energies of the image-potential induced states from the phase-shift model,[32] i.e., we replaced n in Equation 5 by n+a, where a is a "quantum defect" given by: $a = (1-\phi_c/\pi)/2$. In the case of Ag(100), the phase of the energy-dependent reflectivity of the crystal barrier, $\phi_c \approx \pi/2$ (i.e. $a \approx 1/4$) for energies in the image-potential states range. An estimate of the correction to $\Delta\omega_s/\Delta T$ of Equation 6, is obtained by considering the n=1 image-potential state:

$$\frac{\Delta \omega_s}{\Delta T} = -\frac{3}{2}\alpha \omega_s + \left(\frac{\omega_s}{2\pi(n+a)} \frac{\Delta \phi_c}{\Delta T}(E) \right)_{n=1} . \tag{7}$$

Here we consider a maximum value for $\Delta\phi_c/\Delta T$, given by:[24,26]

$$\left.\frac{\Delta \phi_c}{\Delta T}\right|_{max.} \approx \frac{\pi}{E(X_1) - E(X_4)}\beta \quad , \tag{8}$$

β being the coefficient for the temperature variations of bulk energy bands. For the case of silver, $\beta \approx 10^{-5}$ eV/K, a typical value for d-band metals,[33] and $E(X_1)-E(X_4') \approx 5.1$eV.[34]

Therefore, the above correction term allows us to give the following range for the numerical value of $\Delta\omega_s/\Delta T$ for Ag(100): -10.5×10^{-5} eV/K $< \Delta\omega_s/\Delta T < -7.6\times10^{-5}$ eV/K. This range is in excellent agreement with the experimental data of M. Rocca *et al.*[30]

References:

1. F. Finocchi, C. M. Bertoni and S. Ossicini, Vacuum **41**, 535 (1990).
2. M. Radny, Surf. Sci. **247**, 143 (1991).
3. P.M. Echenique and M. E. Uranga, Surf. Sci. **247**, 125 (1991).
4. A. Zangwill, Physics at Surfaces, p. 214 (Cambridge University Press, 1988).
5. J. W. Gadzuk, Surf. Sci. **43**, 44 (1974).
6. D. M. Newns, Phys. Rev. **178**, 1123 (1969).
7. W. Jacob, V. Dose, U. Kolac, Th. Fauster and A. Goldmann, Z. Phys. **B63**, 459 (1986).
8. A. Goldmann, Surf. Sci. **178**, 210 (1986).
9. K. Giesen, F. Hage, F. J. Himpsel, H. J. Riess and W. Steinmann, Phys. Rev. **B33**, 5241 (1986).
10. G. D. Kubiak, Surf. Sci. **201**, L475 (1988).
11. W. Steinmann, Appl. Phys. **A49**, 365 (1989).
12. K. Giesen, F. Hage, F. J. Himpsel, H. J. Riess and W. Steinmann, Phys. Rev. **B 35**, 971 (1987).
13. Z. Wu, B. Quiniou, J. Wang and R. M. Osgood, Jr., Phys. Rev. **B45**, 9406 (1992).
14. Joint Services Electronics Program Annual Progress Report No. 40, Columbia Radiation Laboratory.
15. T. Wegehaupt, D. Rieger and W. Steinmann, Phys. Rev. **B37**, 10086 (1988).
16. E. Dietz and F. J. Himpsel, Solid State Comm. **30**, 235 (1979).
17. M. Radny, Surf. Sci. **231**, 43 (1990).
18. P. de Andrew, P. M. Echenique and F. Flores, Phys. Rev. **B 35**, 4529 (1987).
19. R. A. Bartynski, T. Gustafsson and P. Soven, Phys. Rev. **B 31**, 4745 (1985).
20. B. Reihl and K. H. Frank, Phys. Rev. **B 31**, 8282 (1985).
21. A. Goldmann, V. Dose and G. Borstel, Phys. Rev. **B 32**, 1971 (1985).
22. D. Straub and F. J. Himpsel, Phys. Rev. **B 33**, 2256 (1986).
23. CRC Handbook of Chemistry and Physics, 66th Edition, E-86 (CRC Press, 1986) and C. Kittel, Introduction to Solid State Physics, 6th Edition, 537 (John Wiley & Sons, 1986).
24. Z. Wu, B. Quiniou, J. Wang and R. M. Osgood, Jr., Phys. Rev. **B45**, 9406 (1992).

25. see for example, S. L. Hulbert, P. D. Johnson, N. G. Stoffel, W. A. Royer and N. V. Smith, Phys. Rev. **B31**, 6815 (1985); D. Straub and F. J. Himpsel, Phys. Rev. **B33**, 2256 (1986); W. Steinmann, Appl. Phys. **A49**, 365 (1989); and S. Schuppler, N. Fisher, Th. Fauster and W. Steinmann, Appl. Phys. **A51**, 322 (1990).
26. Z. Wu, B. Quiniou, J. Wang and R. M. Osgood, Jr., Phys. Rev. **B45**, 9406 (1992).
27. V. Dose, W. Altmann, A. Goldmann, U. Kolac and J. Rogozik, Phys. Rev. Lett. **52**, 1919 (1984); A. Goldmann, Surf. Sci. **178**, 210 (1986); and R. Schneider, H. Dürr, Th. Fauster and V. Dose, Phys. Rev. **B42**, 1638 (1990).
28. J. R. Manson and R. H. Ritchie, Phys. Rev. B 24, 4867 (1981); R. Ray and G. D. Mahan, Phys. Lett. **42 A**, 301 (1972); and R. H. Ritchie, Surf. Sci. **34**, 1 (1973).
29. D. Straub and F. J. Himpsel, Phys. Rev. **B33**, 2256 (1986).
30. M. Rocca, F. Moresco and U. Valbusa, Phys. Rev. **B45**, 1399 (1992).
31. R. C. Weast, ed., Handbook of Chemistry and Physics (CRC Press, 1986), p. D-185.
32. N. V. Smith, Phys. Rev. **B32**, 3549 (1985).
33. J. A. Knapp, F. J. Himpsel, A. R. Williams and D. E. Eastman, Phys. Rev. **B19**, 2844 (1979).
34. D. A. Papaconstantopoulos, Handbook of the Band Structure of Elemental Solids (Plenum Press, New York, 1986).

D. Bicromatic Two-Photon Photoemission Spectroscopy on Cu(100)

We have further improved our two-photon photoemission experimental setup, making it suitable for performance of bichromatic 2PPE (Bi2PPE) studies. The advantage of Bi2PPE spectroscopy technique is in its improved signal to noise ratio as compared to conventional 2PPE.

The first step in a two-photon photoemission process is promotion of an electron from its ground state to an excited state through an absorption of a photon. Absorption of a second photon, within the lifetime of the excited state, promotes the electron to a level above E_{VAC}. At this final level, the electron's kinetic energy can be measured, and information about the intermediate excited state can be extracted.

In conventional 2PPE spectroscopy, frequency doubled photons of energy 2hv are responsible for both electron-promotion steps. Experimentally, though, problems with this technique arise when intermediate states that lie very close to E_{VAC} are probed, as the

photon energy 2hν has to be very close to material's work function ϕ. In this case one-photon photoemission (1PPE) can provide a significant contribution to the photoemission spectra, generating space charge distortions and spectral background.

Bichromatic 2PPE spectroscopy, first introduced by Schoenlein *et al.*,[1] and further discussed by Schuppler, *et al.*,[2] circumvents this problem. As in the conventional 2PPE the first excitation step is done by frequency doubled light of energy 2hν, but the second excitation step is performed with laser's fundamental wavelength of energy hν. The hν-light intensity is chosen much stronger than that of 2hν-light, while the signal counting rate is kept constant by preserving the product of the two intensities. Decrease in the 2hν-light intensity decreases the 1PPE spectral contribution as well as the background and space charge distortions. Furthermore, second step excitation with the light of lower energy is more efficient, due to the increased cross section, resulting in more prominent 2PPE feature. All of this contributes to better signal to noise ratio, that was shown by Schupler *et al.* to be improved by up to one order of magnitude.

In our experiments on resonant image potential states of Cu(110) (discussed in section 2) we encountered the problem of low signal to noise ratio. Bi2PPE seemed to be a feasible method for improving the quality of our measurements, and thus we have redone our experimental setup to allow us to incident both the frequency doubled and the fundamental light on the same spot on the sample. The bichromatic setup was tested on Cu(100), which exhibits a prominent IP feature (the resultant EDC spectra is shown in Figure 7). Numerical fit indicated that first two IP states were scanned, and their binding energies were in good agreement with results obtained by Geisen *et al.*[3] using conventional 2PPE. As a good indicative of signal to noise ratio we compared the relative size of image-potential induced peak to the size of the low energy peak. Conventional 2PPE experiments performed by Geisen *et al.* give this ratio as 0.039 ± 0.010 for $2h\nu = 4.30$ eV, while for our data in Figure 7 the ratio is 0.50 ± 0.01 with $h\nu = 2.20$ eV

(2hν = 4.40 eV). We thus observe an improvement by a factor of ~13 despite the higher 2hν energy, used in our experiment, which should produce a higher background.

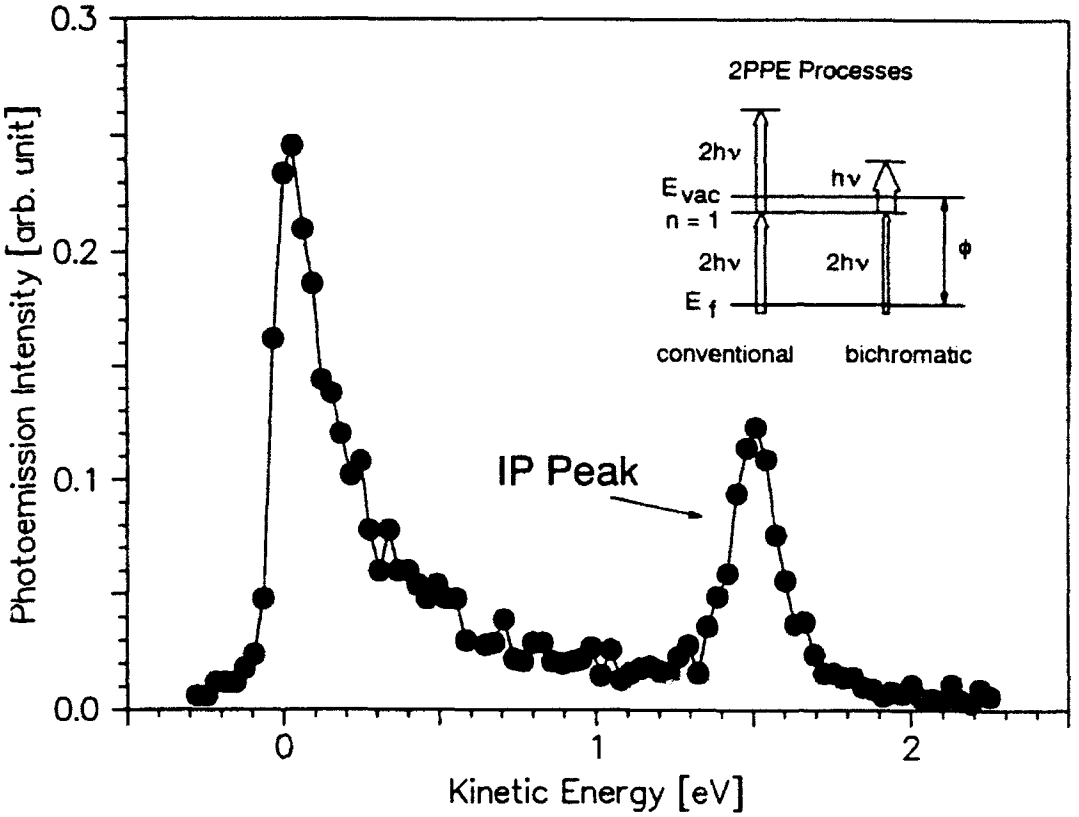

Figure 7. Bichromatic 2PPE EDC spectra of Cu(100) (normal emission, hν = 2.2 eV). IP state feature is indicated. The inset compares the conventional and the bichromatic 2PPE process. The arrow thicknesses symbolize light intensities.

References:

1. R. W. Schoenlein, J. G. Fujimoto, G. L. Eesley and T. W. Capehart, Phys. Rev. Lett. **61**, 2596 (1988).
2. S. Schuppler, N. Fischer, Th. Fauster and W. Steinmann, Appl. Phys. **A51**, 322 (1990).
3. K. Geisen, F. Hage, F. J. Himpsel, H. J. Riess and W. Steinmann, Phys. Rev. **B35**, 971 (1987).

E. Theoretical Calculations of Image Potential Resonances

Since image resonances arise from the quenching of image states by coupling to the bulk continuum, their observation indicates that the surface electrons in these states are not immediately lost to the bulk but rather reflect several times from potential energy discontinuities at the surface of the metal. Thus, we might hope to use the shape of these resonances to act as probes of the magnitude and form of the surface potential-energy barrier.

In order to accomplish this goal, we have developed the necessary theoretical tools for calculating the wave functions and the density of states for the image potential resonances on simple metals. This work was done in collaboration with an undergraduate from Bard College at Annadale-on-Hudson. Several approaches were used in the work including those reported by L. Jurczyszyn[1,2] and M. Radny.[3,4] The results were compared with other theoretical treatments of image resonances.[5,6]

These calculations have shown clearly that the magnitude of the image resonance as well as its binding energy is very sensitive to the shape of the surface potential. For example, in Figure 1, we show that the resonance position and its amplitude change with the position of a free electron-like metal band with respect to the position of the unperturbed image-state resonance. We are currently attempting to use these calculations to match data which we have recently obtained on the shape and position of resonances on Al(111) surfaces.

References:

1. L. Jurczyszyn, Surf. Sci. **247**, 158 (1991).
2. L. Jurczyszyn, Surf. Sci. **259**, 65 (1991).
3. M. Radny, Surf. Sci. **231**, 43 (1990).
4. M. Radny, Surf. Sci. **247**, 143 (1991).
5. S. Papadia, M. Persson, and L.-A. Salmi, Phys. Rev. **B41**, 10237 (1990).
6. S. A. Lindgren and L. Wallden, Phys. Rev. **B40**, 11546 (1989).

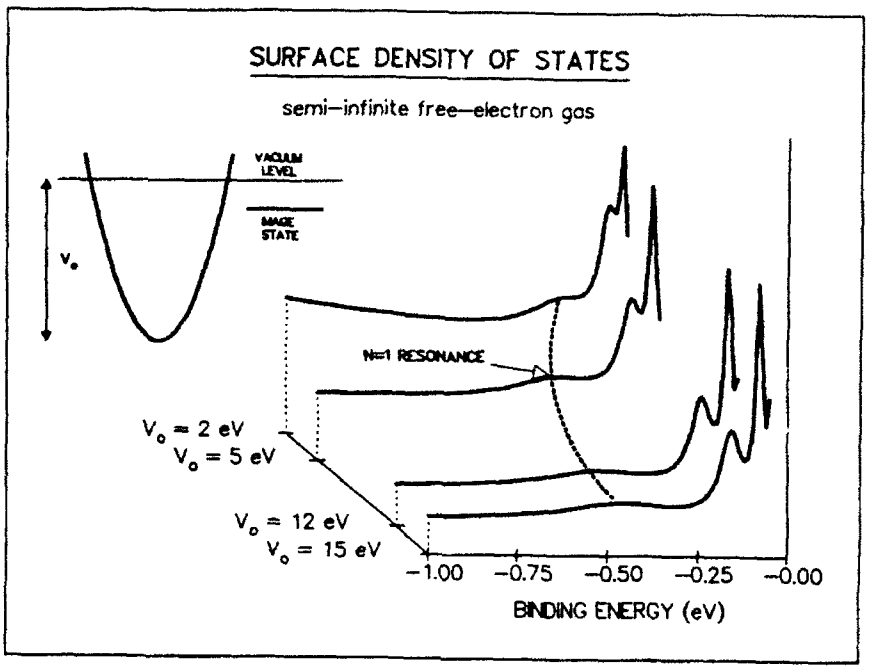

Figure 8. Density of states distributions for n = 1, n = 2 and n = 3 resonance image states, calculated for different values of parameter V_0. The parameter V_0 represents the energy difference between the bottom of the free electron-like bulk band and the vacuum level, which is pictorially represented in the inset of this figure.

This research was supported in part by the Joint Services Electronics Program.

PUBLICATIONS (Research Area II, Work Unit 1)

B. Quiniou, W. Schwarz, Z. Wu and R. M. Osgood, Jr., "Photoemission from Thick Overlying Epitaxial Layers of CaF_2 on Si(111)," Appl. Phys. Lett. **60**, 183 (1992).

Z. Wu, B. Quiniou, J. Wang and R. M. Osgood, Jr., "Temperature and Adsorbate Dependence of the Image-Potential States on Cu(100)," Phys. Rev. **B45**, 9406 (1992).

B. Quiniou and R. M. Osgood, Jr., "Image-Potential States and Surface Plasmons: Temperature Dependence," accepted for publication in Phys. Rev. **B** (January 1993).

B. Quiniou, V. Bulovic and R. M. Osgood, Jr., "Observation of Image-Potential-Induced Resonances on Cu(110) Using the Two-Photon Photoemission Technique," submitted for publication in Phys. Rev. **B** (November 2, 1992).

B. MacDonald, C. Guest, M. Freiler, R. Scarmozzino, A. Smith, R. Hunter, Jr., and R. M. Osgood, Jr., "Efficient Multiple via Etching of Polyimide Films using Fresnel Phase Zone Plate Arrays," submitted for publication in Appl. Opt. (November 18, 1992).

2.2 INVESTIGATION AND CONTROL OF COLLISION PROCESSES FOR QUANTUM ELECTRONICS AND MICROELECTRONICS

George W. Flynn, Principal Investigator (212) 854-4162

Research Area II, Work Unit 2

A. Scanning Tunneling Microscopy of Molecular Adsorbates

1. Introduction

The next generation of electronic and opto-electronic devices will require molecular films with very specific mechanical and electronic properties. Advances in organic synthetic methods as well as in assembly techniques are making feasible the production of films with specific electronic and chemical properties. Non-destructive probes are also required to investigate such films and to establish the relationship between structure at the atomic or molecular level and the function of these films at the macroscopic level. These structure-function relationships are certain to play a major role in the development of thin polymer films for use in microelectronics packaging applications. The scanning tunneling microscope has proven to be a remarkable tool for studying surface features and surface electronic structure as well as changes in these features due to chemical reactions. The original objective of the STM was to image structure and electronic properties of surfaces.[1] The method of operation is similar to stylus profilometry where a tip in contact with a surface is scanned over the surface to determine its topography. However, in the STM the tip is scanned with a few angstroms separation between the surface and tip, and electron tunneling is achieved between these elements by applying a voltage difference between the tip and the surface. Because the tunneling current is a sensitive (exponential) function of the tip to surface distance, vertical features can be imaged with angstrom resolution.[2] Lateral resolution is obtained with piezoelectric materials and by proper preparation of the tunneling tip. Atomic resolution is achieved when tunneling from a single tip atom to the surface is dominant and has become routinely possible for many conducting and semiconducting materials.

The STM is a very versatile instrument as images can be taken under ultrahigh vacuum conditions, in air, under liquids (both conducting and insulating) and over a wide temperature range. More recently a number of attempts have been made to image molecules and aggregates which are either adsorbed on or bonded to well characterized surfaces. Examples of species which have been imaged in this way include DNA,[3] the liquid crystal molecule 4'-octyl-4-biphenylcarbonitrile (8CB),[4] and small organic molecules such as azulene, benzene, and naphthalene.[5] Clearly this particular use of the STM is in its earliest stages but holds tremendous potential for the characterization of the structure and properties of a number of chemically important species.[6]

At this point in time little is known about the properties of adsorbate molecules which lead to successful STM imaging. There are indications that molecules which can be well localized, either due to packing constraints or to strong interactions between the molecules and the surface, are the ones that can be successfully imaged. A common feature of these systems seems to be the ability to keep adsorbates from moving on the surface, especially due to the influence of the tunneling tip. The tunneling processes contributing to the individual molecule images are not well understood.[4(b-d),7] It is however recognized that STM images reveal how the adsorbed molecules locally affect the electronic structure of the underlying substrate.

Our STM efforts have been aimed at using the scanning tunneling microscope to image molecules which can be adsorbed on or bonded to passive surfaces. In particular our research is being conducted along two basic lines. The first is to investigate a series of similar molecules and surface substrates in which small structural variations in the molecules can be used to establish the capabilities and limitations of imaging molecular adsorbates with the STM. These experiments are being directed at both a series of substituted long chain alkane molecules and a series of synthetic polymers. The second line of effort, which follows from the first set of experiments, is to use the STM to image more complicated molecular structures, especially those which are difficult to directly

characterize using X-ray diffraction techniques. These experiments are being directed at imaging a series of Starburst dendrimer polymers.[8]

2. Experimental

Our STM laboratory is now well equipped to undertake the various experiments necessary to study thin layers of surface adsorbates on well characterized surfaces. Available for these studies are two commercial scanning tunneling microscopes and a home built low temperature microscope which is currently close to being operational. All of these microscopes can be operated with either the Digital Instruments Nanoscope II or the Nanoscope III control electronics and image processing hardware/software presently in our laboratory.[9] Additional image processing and modeling calculations are being done using an available IBM RS/6000 workstation with molecular modeling software. The low temperature microscope which will be operated under high vacuum and at liquid nitrogen temperature, will provide conditions which reduce surface diffusion and vibrational motion of the adsorbed molecules making single molecule imaging studies possible. In addition, plans are being developed to construct a simple variable temperature enclosure (room temperature - 100°C) which could house either of the commercial microscopes and allow for the investigation of two dimensional phase transitions and other temperature dependent surface phenomena.

3. STM Imaging of Terminally Substituted n-Alkanes

A wide variety of organic molecules ranging from small molecules to large polymers have been imaged with the STM. In our research, we have been especially successful in imaging terminally substituted alkane molecules physisorbed to the basil plane of graphite (HOPG). Figure 1 is an STM image of dotriacontane (n-$C_{32}H_{66}$) molecules on HOPG taken in our laboratory. These experiments are performed by placing a few microliters of a dilute organic solution containing the long chain alkane on the HOPG

surface and locating the STM tunneling tip directly in this drop. The resulting images reflect the structure and orientation of the adsorbate molecules at the solution/solid interface.

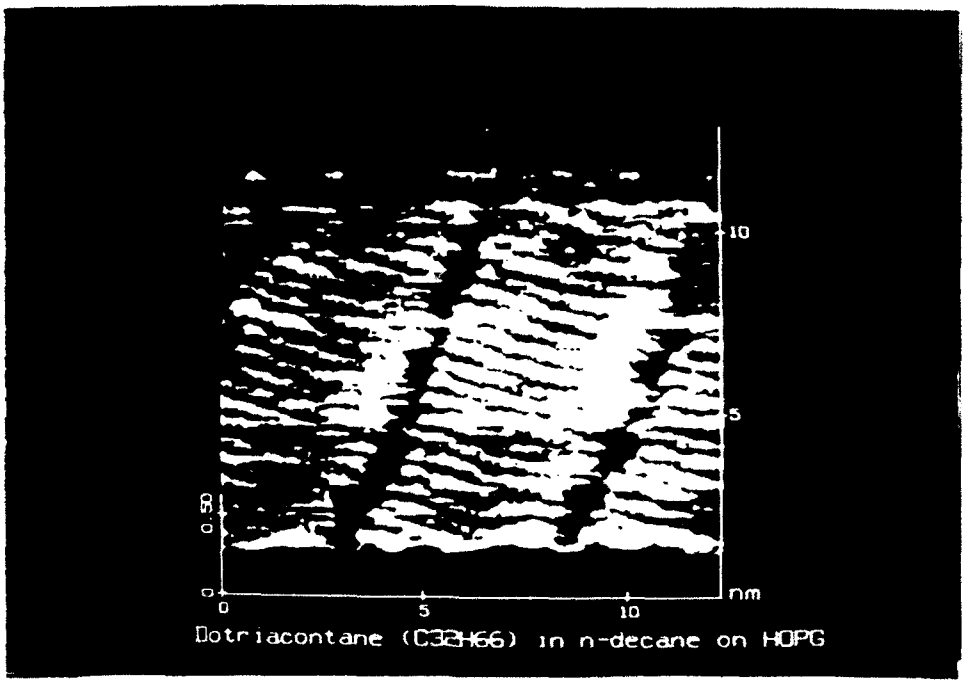

Figure 1. A 3D surface plot of dotriacontane (n-$C_{32}H_{66}$) molecules on a HOPG surface. The molecules are arranged in parallel arrays, termed lamellae, oriented perpendicular to the lamellae boundaries and are in the all *trans* configuration.

Information concerning adsorbate molecule structures at the solid/liquid interface are relevant for a number of macroscopic scale surface phenomena such as microelectronics packaging, molecular epitaxy, lubrication, and adhesion.[10] On the atomic scale issues such as the underlying substrate structure and its effect on the orientation of surface adsorbates are critical in developing electronic devices based on liquid crystal molecules and chemically functionalized surfaces which rely on molecular recognition for chemical sensors and chromatography.[11] In addition, studies of molecular monolayers and their two dimensional structures are of theoretical interest because true crystalline order at finite temperatures is not possible in a two dimensional system.[12] A considerable amount of data obtained from both classical thermochemistry experiments[13] and more modern surface analytical techniques[14] is available in the literature which provides information complimentary to that obtained from STM images.

These long chain alkanes provide a system which can be investigated relatively easily and reproducibly with the STM. This is largely due to the relatively strong adhesion of the molecules to the graphite surface which results from similarities between the alkane structure and the HOPG surface structure. The alkanes are saturated linear hydrocarbons with their carbon atoms arranged in a zigzag chain having a C-C bond length of 1.54 Å and an angle of 109° 28'. More importantly for the high surface affinity of these molecules and their commensurate adsorption, the length of a C-C-C unit is 2.51 Å, only 2% longer than the 2.46 Å spacing between the hollows in the hexagonal structured graphite surface.[13(e)] This is shown pictorially in Figure 2. For a particular hydrocarbon such as dotriacontane ($C_{32}H_{66}$), the experiments measuring the heat of adsorption (ΔH_{abs}) reveal that this quantity can vary from 50 kJ/mole for n-heptane solutions to 120 kJ/mole in isooctane solutions.[13(e)] Other experiments in which ΔH_{abs} was measured for a series of alkanes in n-heptane have shown that ΔH_{abs} increases by 6.28 kJ/mole per -CH_2- linkage.[13(e)]

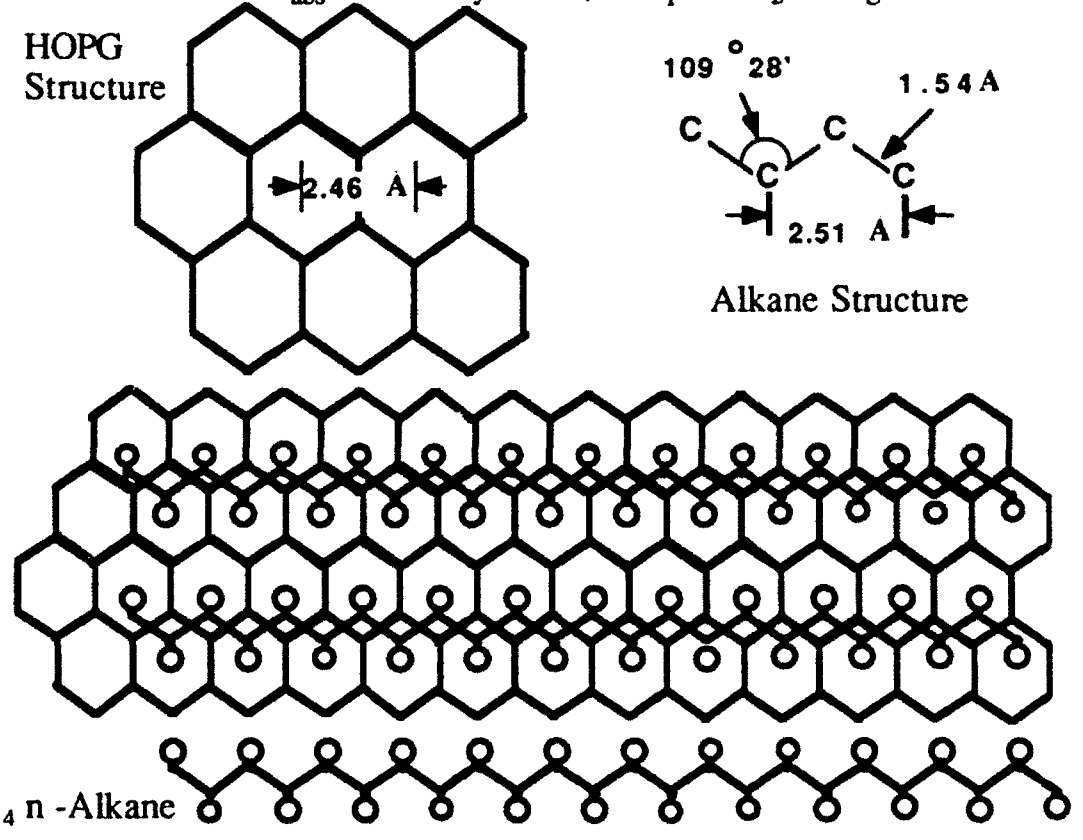

Figure 2. A schematic drawing containing the structure of a n-alkane, a portion of the basil plane of HOPG, and a graphic representation of how a C_{24}-alkane is thought to rest on the HOPG surface.

A number of other research groups have reported results from molecular imaging studies of these types of molecules.[15] The experiments reported so far involve investigations of CH_3-$(CH_2)_n$-R molecules where R = CH_3, OH, COOH, C_6H_6; n ranges from 17 - 50; and all use the HOPG substrate. These molecules have either been investigated at the interface between the surface and a dilute organic solution of the long chain molecules or the interface between the surface and a neat liquid of the molecule itself. Images reveal that the alkanes form highly ordered lamellae with the extended alkyl chains parallel to the substrate surface. Subtle details concerning the individual adsorbate structure and the orientation of the lamellar lattice relative to the graphite surface are also apparent. Some very exciting results have come from experiments using a fast scanning STM capable of capturing room temperature monolayer dynamics of didodecylbenzene on the millisecond time scale.[15(e),15(f),16] The high surface affinity and propensity for self ordering on the HOPG surface of these long chain alkyl species offers a potential means to immobilize interesting molecules through the attachment of the long alkyl chains to the molecules.

Thus far in our research on these long chain alkanes, we have largely concentrated our STM imaging efforts on a series of terminally substituted C_{30} n-alkanes on a HOPG surface. These molecules include triacontane (n-$C_{30}H_{62}$), 1-triacontanol (n-$C_{30}H_{61}$-OH), 1-triacontanoic acid (n-$C_{29}H_{59}$-COOH), and 1-chlorotriacontane (n-$C_{30}H_{61}$-Cl). All of these molecules are commercially available except the chlorinated alkane which we prepared in a one step quantitative reaction from the alcohol using thionyl chloride ($SOCl_2$). Figures 3 and 4 are STM images of 1-triacontanol (n-$C_{30}H_{61}$-OH) and 1-triacontanoic acid (n-$C_{29}H_{59}$-COOH) taken in our lab, which establish our ability to obtain high resolution images of this class of molecule. In each of these images, submolecular scale features are apparent which we tentatively attribute to the structure of the carbon backbone of the molecule lying parallel to the surface. In future experiments we plan to build on our preliminary results and address important issues regarding the STM contrast mechanism,

the role played by intermolecular forces in producing two dimensional ordered structures, and the effects of solvent, temperature and substrate material on the resulting images.

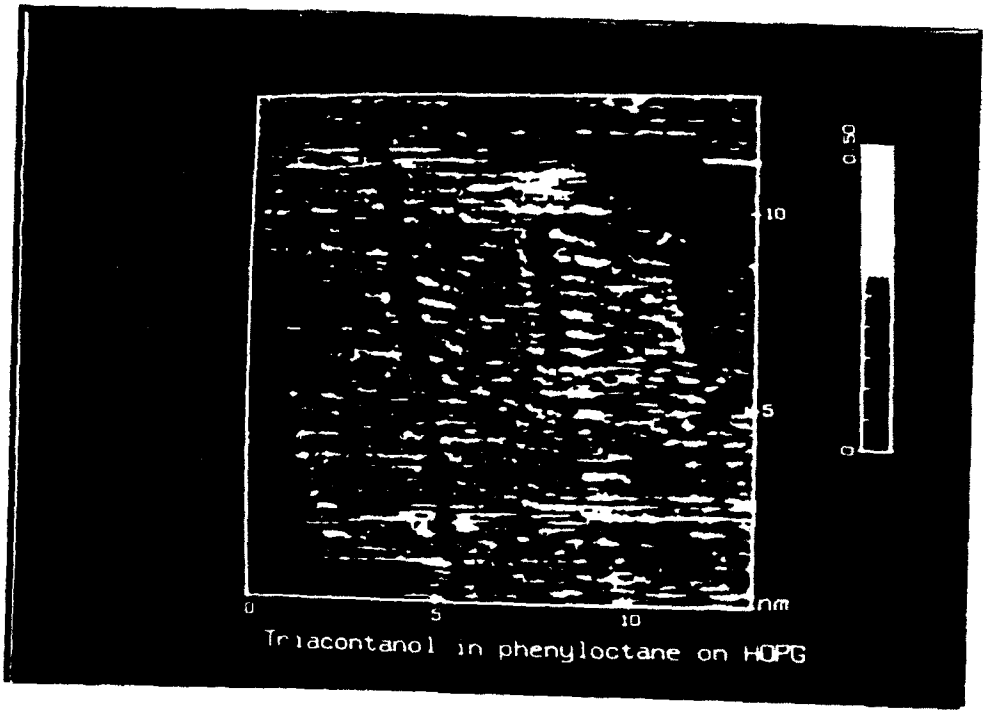

Figure 3. A high resolution topographic image of some 1-triacontanol (n-$C_{30}H_{61}$-OH) molecules on the HOPG surface.

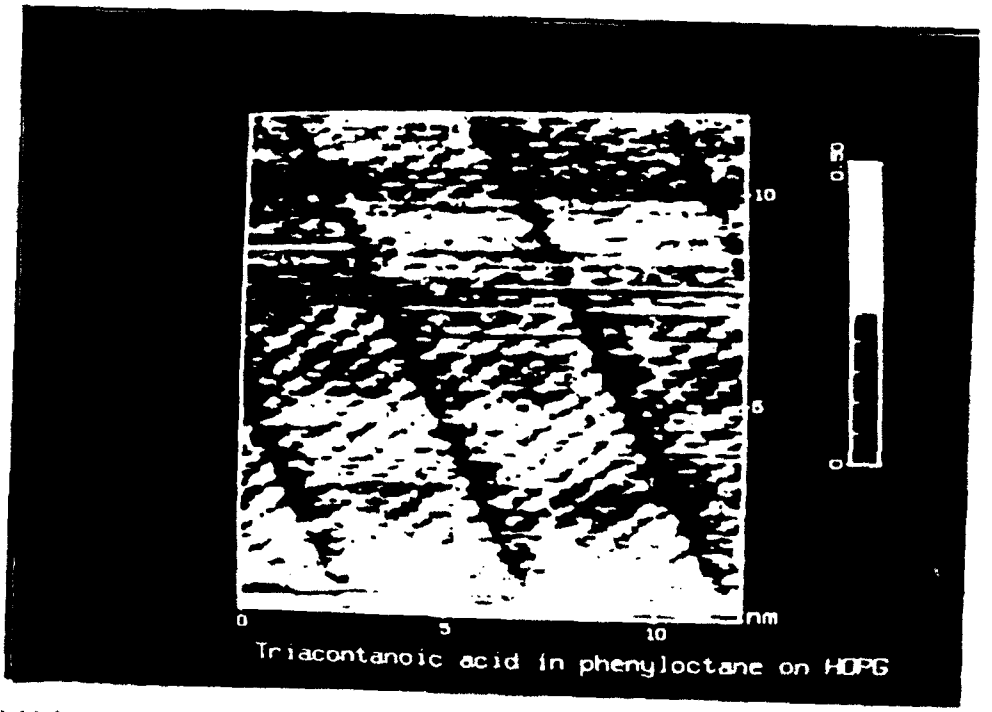

Figure 4. A high resolution topographic image of some 1-triacontanoic acid (n-$C_{29}H_{59}$-COOH) molecules on the HOPG surface.

One of our initial objectives in these STM studies was to examine a series of similar compounds to test our ability to recognize a particular molecular species. The ability to distinguish different molecules on the surface could result from differences in the observed STM features for an individual molecule, which in a simplified model are dependent on the polarizability of the molecular adsorbate, or alternatively, the STM features observed for a collective assembly of molecules on the surface could differ due to long range order reflecting the competition between surface-molecule forces and molecule-molecule forces. Figures 5 and 6 are STM images of triacontane (n-$C_{30}H_{62}$) and 1-triacontanol (n-$C_{30}H_{61}$-OH) taken in our laboratory which display dramatic differences in the extent of long range order.

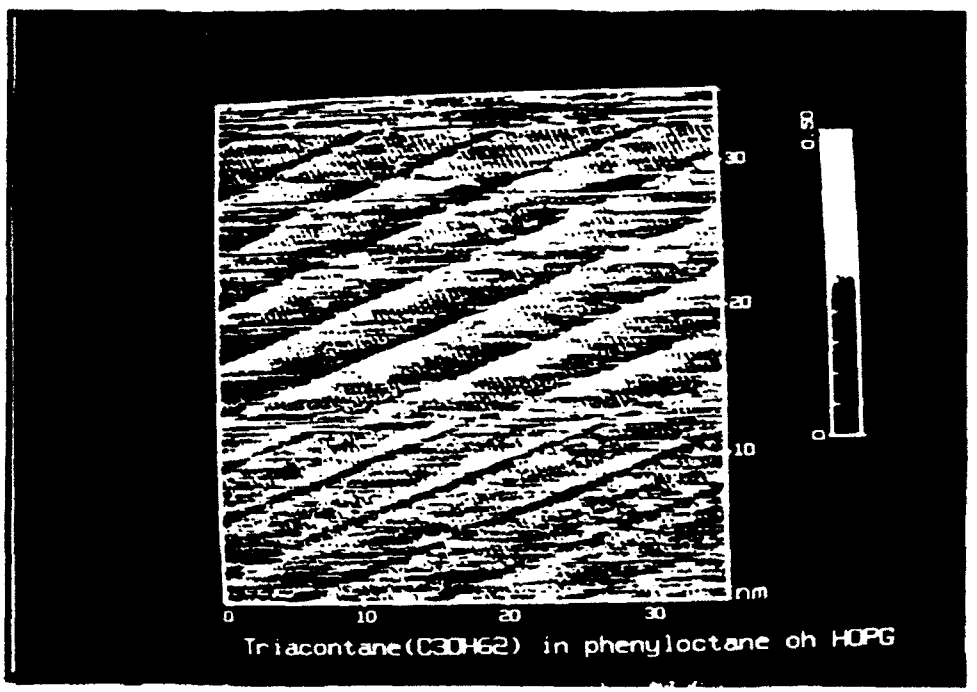

Figure 5. A topographic image of a large array of triacontane (n-$C_{30}H_{61}$-OH) molecules on the HOPG surface.

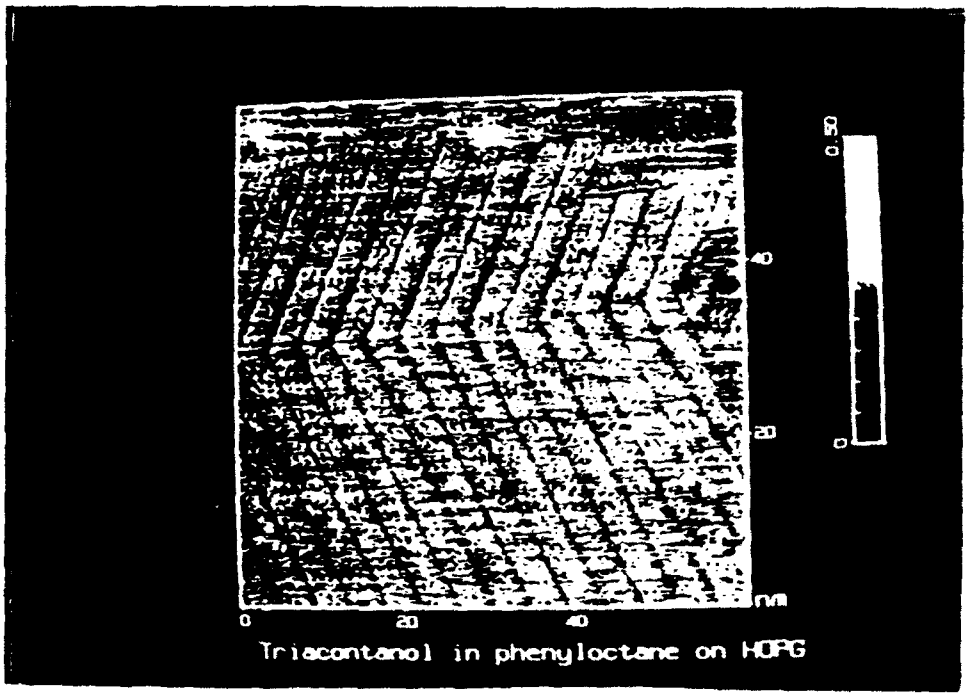

Figure 6. A topographic image of a large array of 1-triacontanol (n-$C_{30}H_{61}$-OH) molecules on the HOPG surface. Note the domain boundary where the direction of the lamellae change by 60^{o}.

While the above experiments emphasize individual molecule properties, we are very anxious to investigate as well the effects of solvent, substrate and temperature on the extent of long range surface order for adsorbed molecules observed with the STM. Depicted in Figure 7 is a large scale STM image of 1-triacontanoic acid (n-$C_{29}H_{59}$-COOH) in phenyloctane on HOPG. Evident in this image is an ≈ 100 nm scale domain of molecules in an ordered array oriented at 60^{o} with respect to the array of other molecules in the image. The depicted domain is characteristic of many images taken for this molecule and the ≈ 100 nm size is smaller than typical grains in the HOPG surface.[17] The size and orientation of the domains reflect the forces between the individual adsorbate molecules, the forces between the surface and the adsorbate, and the rate at which the molecules are adsorbed.

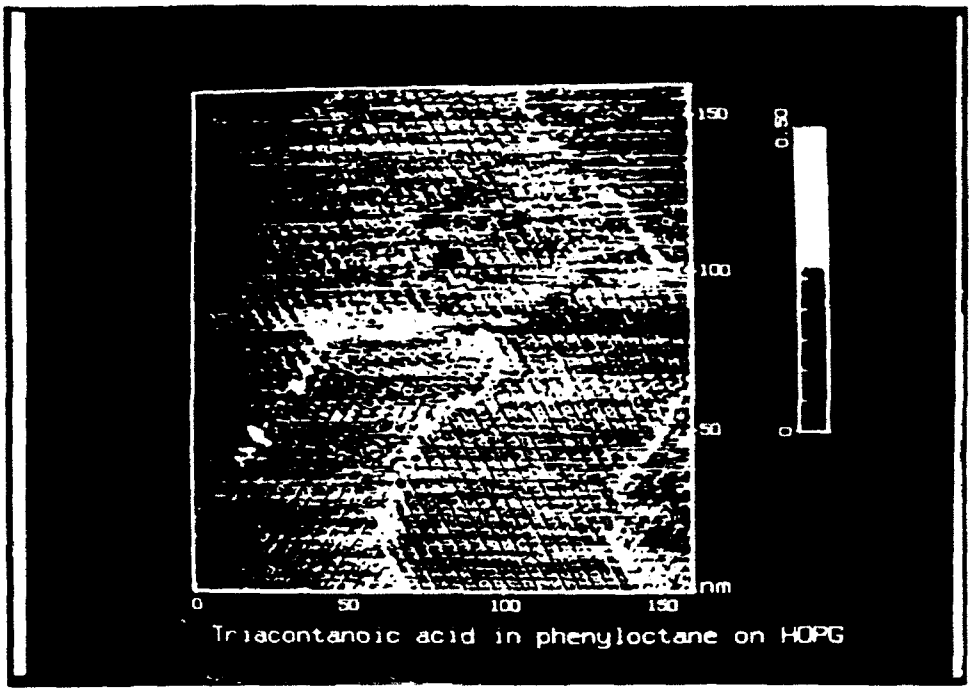

Figure 7. A large scale topographic image of 1-triacontanoic acid (n-$C_{29}H_{59}$-COOH) molecules on the HOPG surface. The image reveals a number of smaller domains oriented at multiples of 60^{o} with respect to one another.

Calorimetry measurements for dotriacontane (n-$C_{32}H_{66}$) *in n-heptane solutions in* contact with two other hexagonal structured layered materials, molybdenum disulfide (MoS_2) and tungsten disulfide (WS_2), reveal reductions in ΔH_{abs} greater than 65% as compared to graphite.[13(b)] In addition, the ΔH_{abs} for dotriacontane (n-$C_{32}H_{66}$) on HOPG can vary from 50 kJ/mole for n-heptane solutions to 120 kJ/mole for isooctane solutions.[13(e)] This solvent dependence of ΔH_{abs} can be accounted for by considering both the gain in energy due to the adsorption of the C_{32} molecules on the surface compared to their solvation energy and the energy cost due to the displacement of the surface bound solvent molecules.[13(e)] Clearly the choice of substrate will affect the interactions of the molecules with the surface and both the choice of solvent and the system temperature will affect the rate of adsorption. We have already obtained a small number of MoS_2 samples, and we are currently adapting our STM to allow studies at elevated temperatures. Further STM experiments on 1-triacontanoic acid and other alkane molecules will provide details of the adsorption process and the participating forces. In addition, molecular dynamics

calculations on these systems will provide complementary information useful in interpreting the STM results.[15(g)]

4. STM Imaging of Synthetic Polymers

Another molecule which is very amenable to study using the STM is the synthetic polymer poly-γ-benzyl-L-glutamate (PBLG).[18(a),19] In our own investigations of this polymer, we were able to directly correlate the features of PBLG liquid crystalline films in the STM images to the molecular structure using the molecular modeling program MacroModel.[20] Figure 8 is an image of PBLG obtained in our laboratory. Our results clearly reveal that the features observed in the STM image are largely due to the dominant contributions of the benzyl groups which surround the helical backbone formed by the amide linkages. This molecular species is both a prototypical rigid rod polymer and α-helical molecule in certain solvents.[21] In addition, PBLG demonstrates well known lyotropic phase behavior in both concentrated solutions and thin films.[22] This liquid crystal character, which is driven by the interaction of the side-chains, is the principal reason this molecule is so amenable to study using diffraction techniques and the STM.

In our STM experiments, commercially available[23] PBLG (MW ≥ 85,000 amu) is imaged as a film on the HOPG surface. These films are prepared by depositing a few drops of a dilute N,N-dimethylformamide solution of the polymer (0.5 mg/ml) on HOPG and allowing it to sit in ambient conditions for a period of ≈ eight hours. Resulting films are cloudy in appearance and suitable for examination with the STM. These films consist of an assembly of α-helical molecules in the thermodynamically stable 18/5 conformation.[24] The metastable 7/2 conformation of the polymer can also be prepared as a film but requires greater care and slow removal of the excess solvent.[24] Imaging is done under ambient conditions by placing the tunneling tip in the film and commencing the tunneling experiment. Although these films are certainly much greater than a monolayer thick, the tunneling process and

resulting images discriminate against all but the layer of molecules in direct contact with the surface.

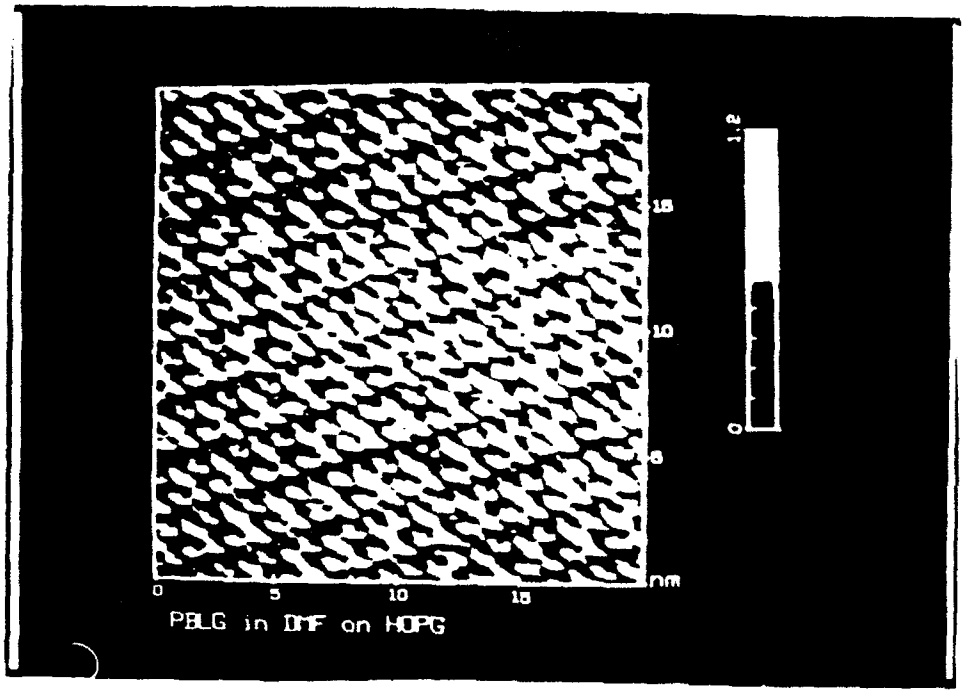

Figure 8. A topographic image of a small portion of an array of poly-γ-benzyl-L-glutamate (PBLG) molecules (M.W. ≥ 85,000) on the HOPG surface. The image features observed are due largely to the benzyl substituents of the polymer side chains.

5. STM Imaging of Starburst Dendrimer Polymers

In recent years considerable attention has been focused on the synthesis of structurally defined macromolecules, especially for the examination of guest-host molecular relationships.[25] One extensively developed molecular system is the "Starburst Dendrimer" polymer pioneered by Tomalia and co-workers, which is schematically depicted in Figure 9.[8] These polymers, which are prepared using controlled branching reactions from an initiator core molecule, can be synthesized in a range of sizes (generations) and with various types of surface terminating groups. The "Starburst Dendrimer" macromolecules provide a unimolecular prototype for both endo-receptor and exo-supramolecular controlled morphogenesis.[25(e)]

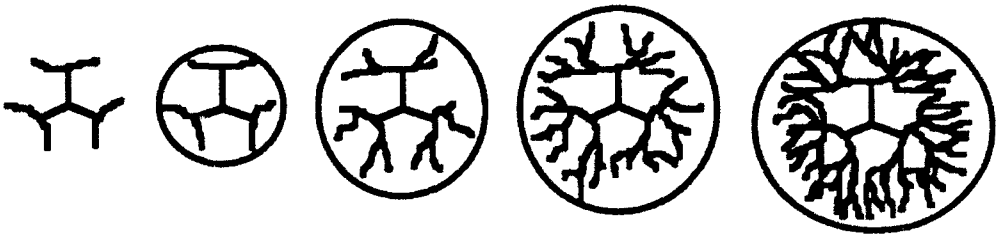

Generation	1.5	2.5	3.5	6.5	9.5
Diameter(nm)	3.6	4.8	7.8	12.7	21.0

Figure 9. A schematic drawing of the carboxylate-terminated Starburst dendrimers. The hydrodynamic diameters have been determined by size-exclusion chromatography.

Detailed experimental structural information is currently unavailable for these dendrimer polymers due to their fractal nature. This fractal nature leads to disorder in the spatial configuration from dendrimer to dendrimer and hence a lack of long range order which is necessary for X-ray diffraction studies. Other methods such as size exclusion chromatography and low angle laser light scattering have provided information concerning the hydrodynamic diameters and molar masses for a series of dendrimer generations.[26] The combination of NMR experiments, which probe the interactions of guest molecules in solution with the dendrimers, and molecular modeling calculations has provided the most extensive information concerning the morphological changes as a function of generation and the predicted internal voids in the higher generation dendrimers.[27] These latter experiments and calculations on the carbomethoxy-terminated β-alanine dendrimers reveal that the smaller generations (1-3) form highly asymmetric, domed shaped open structures. A transition to more dense, spheroid-like topologies, with connecting networks of solvent filled interior hollows, occurs at generation 4.

We are using the STM as a way of directly characterizing the shape and structure of these dendrimer macromolecules. Displayed in Figure 10 is an STM image (taken in our laboratory) observed when a dilute methanol solution containing generation 2.5 carboxylate-terminated dendrimers is deposited on the HOPG surface. Evident in this image is an array of features with a characteristic spacing of 2-3 nm, considerably less than

the reported hydrophobic diameter of 4.8 nm. This is a very preliminary result and currently we are trying to interpret these image features and their relationship to the possible conformations and packing geometries for these early generation dendrimers.

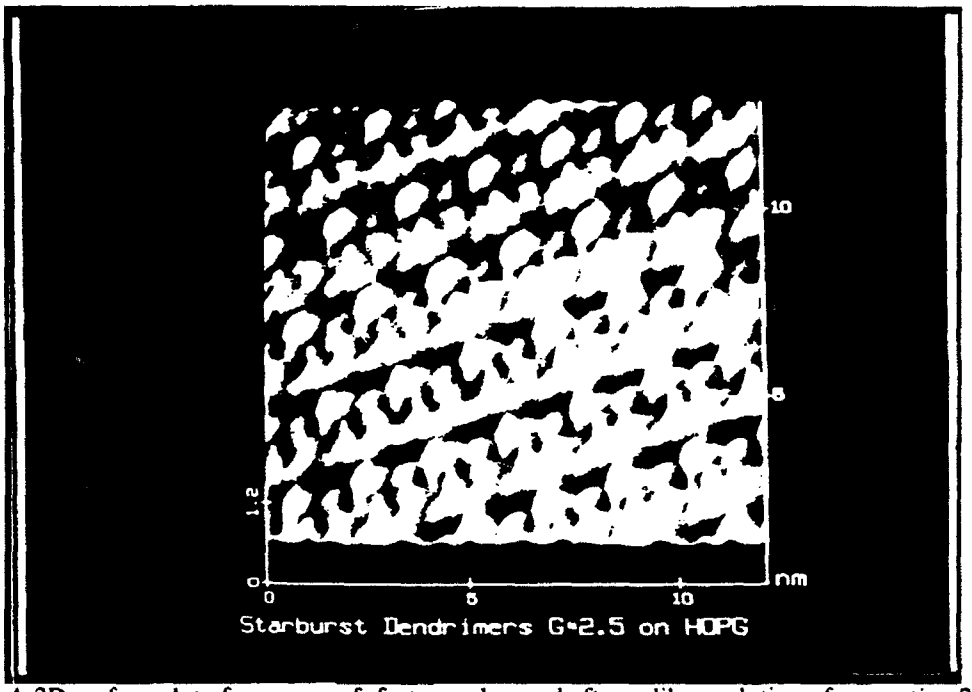

Figure 10. A 3D surface plot of an array of features observed after a dilute solution of generation 2.5 carboxylate-terminated Starburst dendrimers is deposited on a HOPG surface.

Additional imaging experiments will also be necessary to establish the capabilities of the STM to act as a structural probe of these molecules. Currently we have a small amount of the carboxylate-terminated dendrimers in generations 1.5, 2.5, 3.5, 4.5, and 6.5 which were generously provided by Professor Nicholas Turro of our department. A selection of Starburst dendrimers is also commercially available from Polysciences, Inc..[28] Due to the ionic nature of the terminal groups, these dendrimers are soluble only in strongly polar solvents, especially water. Some effort will be required to develop reproducible deposition and sample preparation techniques, but our preliminary results indicate that this is possible.

The principle objective of our experiments is to obtain a direct probe of the shape and structure of the dendrimer macromolecules on various surfaces. This will be a significant aid for investigations of host-guest chemistry and other experiments requiring

well defined molecular geometries. Because the STM is a local probe capable of revealing site specific structural details, it is well suited to investigate the dendrimers. Since both the initiator core molecules and surface terminating molecules can be varied, a wide variety of dendrimer systems are potentially available for investigation. These include polythioether dendrimers, polyamide dendrimers, polyamido alcohol dendrimers (arborols), and polyarylamine dendrimers.[8] Additionally all-hydrocarbon based dendrimers, such as those based on benzene, triptycene or phenylacetylene,[30] will be amenable for investigation with the STM. These dendrimer systems provide an excellent research area to test the abilities of the STM for molecular structure characterization where other direct structural characterization techniques cannot be applied.

Summary

The enormous potential for the STM to contribute to important problems in molecule-surface interactions and molecular structure determination will be realized only if techniques are developed which make the imaging of molecular adsorbates routine. To this end, it will be important to gain a better understanding of the adsorbate's contribution to the tunneling processes, which make imaging molecules possible, and the extent to which small changes in an adsorbate's structure can be detected. By using the STM to perform systematic investigations of terminally substituted alkanes, synthetic polymers, and starburst dendrimer polymers, we can begin to test the limits of this instrument and the factors which lead to the successful imaging of molecular adsorbates. In addition, the application of the STM to these systems will also reveal details of molecule-surface interactions and molecule-molecule interactions, as well as their role in molecular epitaxy and the formation of two dimensional crystal structures.

This work was supported in part by the Joint Services Electronics Program.

References:

1. H. Rohrer, Proc. Natl. Acad. Sci. USA **84**, 4666 (1987).

2. (a) G. Binnig, H. Rohrer, Ch. Gerger and E. Weibel, Phys. Rev. Lett. **49**, 57 (1982). (b) R. Hamers, Annu. Rev. Phys. Chem. **40**, 531 (1989). (c) J. Tersoff and D. Hamann, Phys. Rev. B **31**, 805 (1985).

3. (a) G. Binnig and H. Roher in Trends in Physics (eds. J. Janta and J. Pantoflicek) 38 - 46 (European Physical Society, The Hague, 1984). (b) G. Travaglini, H. Rohrer, M. Amrein, and H. Gross, Surf. Sci. **181**, 380 (1987). (c) S. M. Lindsay and B. Barris, J. Vac. Sci. Technol. A **6**, 544 (1988). (d) T.P. Beebe, Jr., T. E. Wilson, D. F. Ogletree, J. E. Katz, R. Balhorn, M. B. Salmeron, and W. J. Siekhaaus, Science **243**, 370 (1989). (e) M. Salmeron, T. Beebe, J. Odriozola, T. Wilson, D.F. Ogletree and W. Siekhaus, J. Vac. Sci. Technol. A **8**, 635 (1990). (f) M. Amrein, R.Durr, A. Stasiak, H. Gross, and G. Travaglini, Science **243**, 1708 (1989). (g) P.G. Arscott, G. Lee, V.A. Bloomfield and D.F. Evans, Science **244**, 475 (1989). (h) P.G. Arscott, G. Lee, V.A. Bloomfield and D.F. Evans, Nature **339**,484 (1989). (i) P.G. Arscott and V.A. Bloomfield, Ultramicroscopy **33**, 127 (1990). (j) S.M. Lindsay, T. Thundat, L. Nagahara, U. Kipping, and R.L. Rill, Science **244**, 1063. (1989). (k) S.M. Lindsay, L. A. Nagahara,T. Thundat, U. Kipping, R.L. Rill, B. Drake, C. B. Prater, A. L. Weisenhorn, S. A. C. Gould, and P. K. Hansma, J. Biomol. Struct. Dyn. **7**, 279 (1989). (l) L. Nagahara, T. Thundat, P. I. Olden, S. M. Lindsay, Ultramicroscopy **33**, 107 (1990). (m) A. Cricenti, S. Selci, A. C. Felici, R. Generosi, E. Gori, E. Djaczenko, and G. Chiarotti, Science **243**, 1226 (1989). (n) D.D. Dunlap and C.Bustamante, Nature **342**, 204 (1989). (o) D. Keller, C. Bustamante,and R. W. Keller, Proc. Natl. Acad. Sci. U.S.A. **86**, 5356 91989). (p) R.J. Driscoll, M.G. Youngquist and J.D. Baldeschwieler, Nature **346**, 294 (1990). (q) Y. Kim, E. C. Long, J. K. Barton, and C. M. Lieber, Langmuir **8**, 496 (1992).

4. (a) J.S. Foster and J.E. Frommer, Nature **333**, 542 (1988). (b) J.K. Spong, H.A. Mizes, L.J. LaComb Jr., M.M. Dovek, J.E. Frommer and J.S.Foster, Nature **338**, 137 (1989). (c) D.P.E. Smith, H.Horber, Ch. Gerber and G. Binnig, Science **245**, 43 (1989). (d) D.P.E. Smith, J.K.H. Horber, G. Binnig, and H. Nejoh, Nature **344**, 641 (1990). (e) A. Okumura, K. Miyanura and Y. Goshi, J. Vac. Sci. Technol. A **8** , 625 (1990). (f) T.J. McMaster, H. Carr, M.J. Miles, P.Cairns and V.J. Morris, J. Vac. Sci. Technol. A **8**, 672 (1990). (g) M. Hara, Y. Iwakabe, K. Tochigi, H. Sasabe, A.F. Garito and A.Yamada, Nature **344**, 228 (1990). (h) H. Shindo, M. Kaise, Y. Kawabata, C. Nishihara, H. Nozoye and K. Yoshio, J. Chem. Soc., Chem. Commum., 760 (1990).

5. (a) H. Ohtani, R.J. Wilson, S. Chiang and C.M. Mate, Phys. Rev. Lett. **60**, 2398 (1988). (b) V.M.Hallmark, S. Chiang, J.K. Brown, and Ch. Woll, Phys. Rev. Lett. **66**, 48 (1991). (c) V.M. Hallmark, S. Chiand, Ch. Woll., J. Vac. Sci. Technol. B **9**, 1111 (1991). (d) S. Chiang, D.D. Chambliss, V.M. Hallmark, R.J. Wilson, and , Ch. Woll, Springer Ser. Surf. Sci. **24**, 204 (1991)

6. For a recent reviews see (a) Engel, A., Annu. Rev. Biophys. Chem., 1991, 20, 79. (b) Proceedings of the Annual International Conference on Scanning Tunneling Microscopy/Spectroscopy published each year in J. Vac. Sci. Technol.

7. R. Garcia and N. Garcia, Chem. Phys. Lett. **173**, 44 (1990).

8. D.A. Tomalia, A.M. Naylor and W.A. Goddard III, Angew. Chem. Int. Ed. Engl. **29**, 138 (1990).

9. Digital Instruments, 6780 Cortona Drive, Goleta, California 93117

10. J.N. Israelachvilli, Intermolecular and Surface Forces, Academic Press, London, 1985.

11. J. D. Swalen, D.L. Alllara, J.D. Andrade, E.A. Chandross, S. Garoff, J. Israelachvilli, T.J. McCarthy, R. Murray, R.F. Pease, J.F. Rabolt, K.J. Wynne, and H.Yu., Langmuir **3**, 932 (1987).

12. R.E. Peierls, Helv. Acta Suppl. **7**, 81 (1934).

13. (a) A.J. Groszek, Nature **196**, 531 (1962). (b) A.J. Groszek, Nature **204**, 680 (1964). (c) G.D. Parfitt and E. Willis, J. Phys. Chem. **68**, 1780 (1964). (d) D.H. Everett and G.H. Findenegg, Nature **233**, 52 (1969). (e) A.J. Groszek, Proc. Roy. Soc. Lond. A **314**, 473 (1970).

14. J. Suzanne in Adsorption at the Gas-Solid and Liquid-Solid Interface, edited by J. Rouqerol and K.S.W. Sing (Elsevier, Amsterdam, 1982). (b) J. Suzanne, J. L. Seguin, H. Taub, and J.P. Biberian, Surf. Sci. **125**, 153 (1983). (c) J. Krim, J. Suzanne, H. Shechter, R. Wang and H. Taub, Surf. Sci. **162**, 446 (1985).

15. (a) G.C. McGonigal, R.H. Bernhardt, and D.J. Thomson, Appl. Phys. Lett. **57**, 28 (1990). (b) R.H. Bernhardt, G.C. McGonigal, R. Schneider, and D.J. Thomson, J. Vac. Sci. Technol. A **8**, 667 (1990). (c) G.C. McGonigal, R.H. Bernhardt, Y.H. Yeo, and D.J. Thomson, J. Vac. Sci. Technol. B, 1107, (1991). (d) S. Buchholz and J.P. Rabe, J. Vac. Sci. Technol. B, 1126 (1991). (e) J.P. Rabe and S. Buchholz, Phys. Rev. Lett. **66**, 2096 (1991). (f) J.P. Rabe and S. Buchholz, Science **253**, 424 (1991). (g) R. Hentschke, B.L. Schurmann, and J.P. Rabe, J. Chem. Phys. **96**, 6213 (1992). (h) S. Buchholz and J.P. Rabe, Angew. Chem. Int. Ed. Engl. **31**, 189 (1992). (i) R. Kuroda, E. Kishi, A. Yamano, K. Hatanaka, H. Matsuda, K. Eguchi, and T. Nakagiri, J. Vac. Sci. Technol. B. **9**, 1180 (1991).

16. J.P. Rabe and S. Buchholz, results presented at the Meeting of the American Physical Society, Indianapolis, IN, March 1992

17. (a) P.A. Thrower, Chem. Phys. Carbon **5**, 217 (1969).(b) A.W. Moore, Chem. Phys. Carbon **5**, 217 (1969). (c) A.W. Moore, Chem. Phys. Carbon **11**, 69 (1973). (d) M.R. Soto, Surf. Sci. **225**, 190 (1990). (e) O. Marti, G. Binnig, H. Rohrer and H. Salemaink, Surf. Sci. **181**, 230 & 139 (1987),

18. (a) J.J. Breen and G.W. Flynn, "STM Studies of the Synthetic Polypeptide: Poly-γ-benzyl-L-glutamate," The Journal of Physical Chemistry, July 1992. (b) J.J. Breen and G.W. Flynn, "STM Studies of the Organic Conductor Formed from DMTTT and TCNQ", submitted to Chemistry of Materials. (c) J.J. Breen, J. S. Tolman and G.W. Flynn, "Scanning Tunneling Microscopy Studies of Vapor Deposited Films of Tetrathiafulvalene and Iodine", submitted to Applied Physics Letters. (d) "Scanning Tunneling Microscopy Studies of Charge Transfer Salts and Molecular Adsorbates" presented at the 203rd National Meeting of the American Chemical Society; San Francisco, CA; April 1992; Symposium Title: Novel Structural, Mechanical and

Electrical Aspects of Chemical Interfaces organized by the Division of Colloid and Surface Chemistry.

19. (a) T.J. McMaster, H. Carr., M.J. Miles, P. Cairns, V.J. Morris, J. Vac. Sci. Technol. A **8**, 648 (1990). (b) M.J. Miles, T. McMaster, H.J. Carr, A.S. Tatham, P.Shewery, J.M.Field, P.S.Belton, D. Jeenes, B. Hanley, M. Whittman, P.Cairns, V.J. Morris and N.Lambert, J. Vac. Sci. Technol. A **8**, 698 (1990).

20. MacroModel V3.0, Department of Chemistry, Columbia University, New York, NY 10027

21. (a) P. Doty, J.H. Bradbury, and A.M. Holtzer, J. Am. Chem. Soc. **78**, 947 (1956). (b) H. Kihara, Polymer J. **9**, 443 (1977).

22. (a) D.A.D. Parry and A. Elliott, J. Mol. Biol. **25**, 1 (1967). (b) I.M. Squire and A. Elliott, Mol. Cryst. Liq. Cryst. **7**, 457 (1969). (c) E.L. Wee and W.G. Miller, J. Phys. Chem. **75**, 1446 (1971). (d) A.J. McKinnon and A.V. Tobolsky, J. Phys. Chem. **70**, 1453 (1966).

23. Sigma Chemical Company, St. Louis, MO 63178-9916

24. (a) E.T. Samulsky and A.V. Tobolsky, Biopolymers **10**, 1013 (1971). (b) J. Watanabe, K. Imai, R. Gehani and I. Uematsu, J. Polym. Sci. Polym. Phys. Ed. **19**, 653 (1981). (c) J. Watanabe, R. Gehani, and I. Uematsu, J. Polym. Sci. Polym. Phys. Ed. **19**, 1817 (1981). (d) J. Watanabe and I. Uematsu, Polymer **25**, 1711 (1984).(e) J. Watanabe, K. Imai, and I. Uematsu, Macromolecules **19**, 1491 (1986).

25. (a) C.J. Pederson, J. Am. Chem. Soc. **89**, 7017 (1967). (b) C.J. Pederson, H.K. Frensdorff, Angew. Chem. Int . Ed. Engl. **11**, 16 (1972). (c) C.J. Pederson, H.K. Frensdorff, Angew. Chem. Int . Ed. Engl. **27**, 1029 (1988).(d) J.M. Lehn, Struct. Bonding (Berlin), **16**, 1 (1973). (e) J.M. Lehn, Acc. Chem. Res. **11**, 49 (1978). (e) J.M. Lehn, Angew. Chem. Int . Ed. Engl. **27**, 89 (1988). (f) F. Vogtle, Angew. Chem. Int. Ed. Engl. **18**, 753 (1979). (g) D.J. Cram and J.M. Cram, Acc. Chem. Res. **11**, 8 (1978). (h) D.J. Cram., Angew. Chem. Int . Ed. Engl **25**, 1039 (1986).(i) D.J. Cram., Angew. Chem. Int . Ed. Engl. **27**, 109 (1988).(j) D.J. Cram, Science **240**, 760 (1988).

26. (a) M.C. Moreno-Bondi, G. Orellana, N.J. Turro, and D.A. Tomalia, Macromolecules **23**, 912 (1990). (b) P.L. Dubin, S. L. Edwards, J. I. Kaplan, M. S. Mehta, D. A. Tomalia, and J Xia, submitted to Analytical Chemistry.

27. A.N. Naylor, W.A. Goddard III, G.E. Kiefer, and D.A. Tomalia, J. Am. Chem. Soc. **111**, 2339 (1989).

28. Polysciences. Inc., Warrington, PA, 18976 - 2590

29. (a) M.J. Allen, M. Balooch, S. Subbiah, R.J. Tench, W. Siekhaus and R. Balhorn, Scanning Microscopy **5**, 625 (1991). (b) M. Allen, R. Balhorn, M. Balooch, W.J. Siekhaus, R.J. Tench and S. Subbiah, AIP Conf. Proc. **241**, 176 (1992).

30. J. Zhang, J.S. Moore, Z. Xu, R.A. Aguirre, J. Am. Chem. Soc. **114**, 2273 (1992).

B. Translationally and Rotationally Resolved Excitation of $CO_2(00^02)$ by Collisions with Hot Hydrogen Atoms

1. Introduction

State resolved energy transfer scattering experiments provide fundamental information about the potential surfaces that govern collision dynamics.[1] The simplest systems, where diatomic or triatomic molecules are ro-vibrationally excited by collisions with translationally "hot" hydrogen atoms (H*), have been the subject of extensive investigation[2] using a variety of transient detection techniques. The system of interest here, $H^* + CO_2$, has strong inelastic and reactive channels as well as a number of stable HOCO intermediates and has been the subject of numerous theoretical and experimental investigations. In an ambitious theoretical study, Schatz and co-workers employed a quasi-classical trajectory approach to calculate final state distributions for both reactive and inelastic scattering.[3] The reactive channel has been studied experimentally by measurements of ro-vibrational excitation in both the OH[4-7] and CO[8] fragments. A number of these reaction studies have employed $HX \cdot CO_2$ van der Waals complexes as reactants, using supersonic expansion techniques to prepare $HX \cdot CO_2$ and UV lasers to dissociate HX. Both the rotational distribution of the OH fragment[5-7] and the time scale[9] for HOCO break-up have been measured in separate studies using this method. In recent years, diode laser absorption spectroscopy has been employed in our laboratory to obtain CO_2 ro-vibrational distributions for several important inelastic scattering channels in this system.[10-17]

In this study, diode laser spectroscopy has been used to measure translational and rotational excitation of CO_2 (00^02) by collisions with hot hydrogen atoms. UV photolysis of H_2S gives reasonably monoenergetic "hot" hydrogen atoms (H*) with 2.1 eV of

translational energy, which collisionally excite CO_2 into (among others) the 00^02 vibrational state:

$$H_2S + h\nu(\lambda=193\ nm) \rightarrow HS + H^* \qquad \text{(Hot Atom Production)}$$

$$CO_2 + H^* \rightarrow CO_2\ (00^02;J;V) + H \qquad \text{(Collisional Excitation)}$$

where J is the rotational angular momentum and V the recoil velocity of CO_2. High resolution time-resolved diode laser spectroscopy is used to measure the nascent (*i.e.* unrelaxed) rotational population distribution in this vibrational level via transitions of the type

$$CO_2\ (00^02;J;V) + h\nu(\lambda\sim4.3\ \mu m) \rightarrow CO_2\ (00^03;J\pm1;V)\ , \qquad \text{(Diode Laser Probing)}$$

which share the large oscillator strength of the ν_3 fundamental.

The experimental results can also be compared with the predictions based on Schatz's theoretical treatment of high energy H (1.9-2.6 eV)-CO_2 collisions. This work[3] developed a potential energy surface and used *ab initio* quasi classical trajectory methods to determine cross-sections for ro-vibrational excitation and for chemical reaction in this system. Agreement between theory and experiment is excellent for this system for reactive scattering; however, substantial discrepancies exist between theoretical and experimental inelastic cross sections and rotational distributions. Inelastic scattering data thus provides a rigorous test for the potential energy surface developed for this complicated 4-body system.[3,18]

Two theoretical approaches have recently been developed in this laboratory to model rotationally resolved inelastic scattering for the system H^*/CO_2 in which the final CO_2 vibrational state is the first asymmetric level 00^01. The first employs an inversion procedure based on the infinite order sudden (IOS) approximation to extract *state-to-state* cross-sections from the experimental data for this system.[19] It was found that the ro-

vibrationally inelastic cross-sections for $00^00,J' \rightarrow 00^01,J$ exhibit a large degree of rotational inelasticity, with a peak at $\Delta J = 41$. Later in this report, we point out the similarities between scattering events which produce 00^01 and 00^02 and draw conclusions about the scattering process, $00^00,J' \rightarrow 00^02,J$. The second study treated the H atom as a point particle, CO_2 as a 3-dimensional "breathing ellipsoid", and modeled their interaction employing classical impulsive scattering.[20] For collisions which produce $CO_2(00^01)$, this approach results in a correlation between features of the experimental data (rotationally resolved population distribution and translational recoil) and specific "types" of collisional trajectories. Specifically, $CO_2(00^01)$ is found to be excited only by trajectories which are near normal to the ellipsoid surface and strike near the end of the CO_2 molecule. We might expect the requirements for exciting 00^02 to be even more stringent than those for exciting 00^01.

The relative or absolute probability of exciting the CO_2 (00^01) and (00^02) levels cannot be predicted using the classical "breathing ellipse" model, but rather requires a quantum mechanical treatment of the scattering process.[21-25] In a very recent study, Hensley, Green, and Flynn[25] have used a simple repulsive, atom-atom potential approximation to the ellipsoid model in a more exact IOS/quantum mechanical calculation of the $CO_2(00^01)$ and $CO_2(00^02)$ excitation probabilities for hot H/CO_2 encounters. They also find that the transition probability for excitation of $CO_2(00^01)$ has its optimum value near the end of the CO_2 molecule, but they observe a small, secondary maximum between the C and O atoms. Physically, this is quite reasonable since H atom trajectories that strike between the C and O atoms, which naturally force the C and O atoms apart in a repulsive potential approximation, can be expected to have a significant excitation probability for the $CO_2(00^01)$ asymmetric stretch level. Since the H atoms strike nearer the CO_2 center of mass for such collisions, these trajectories produce less CO_2 angular momentum than end on collisions. As a result, the atom-atom quantum approach, not surprisingly, predicts slightly cooler 00^01 rotational profiles than the classical trajectory, ellipsoid model. The

atom-atom repulsive potential approach, unlike the breathing ellipsoid model, can also be used to predict differences in the excitation probality for the $00^0 1$ and $00^0 2$ levels. It is thus particularly relevant to the present experimental study.

2. Experimental

The UV/IR double resonance apparatus has been described in detail elsewhere.[10,11] Time domain absorption signals were measured for the following absorption lines at 292 K:

$$00^0 2 \rightarrow 00^0 3, \text{ R}(6, 14, 20, 24, 30, 34, 38, 40, 48, 52, 54).$$

Typical signals exhibit a prompt rise following the excimer pulse (limited by the ~700 ns response time of the IR detector), followed by a slowly varying component which corresponds to rotational relaxation within the $00^0 2$ level.

3. Summary of Results and Conclusions

The translationally and rotationally resolved population distribution has been measured for $CO_2(00^0 2)$ produced by collisions of CO_2 with hot hydrogen atoms. The conclusions drawn from this study are:

(1). The magnitude of population scattered into $00^0 2$ is ~21 times smaller than that scattered into $00^0 1$.

(2). A simple repulsive force quantum scattering model predicts a much smaller probability for the excitation of $00^0 2$ compared to $00^0 1$ than that observed experimentally.

(3). The $00^0 2$ rotational population distribution and rotationally resolved linewidths are remarkably similar to those previously obtained for $00^0 1$. Within the context of the "breathing ellipsoid" model, the similar rotational distributions and translational recoils

for 00^01 and 00^02 suggest that these two states are excited by similar collision trajectories, wherein asymmetric stretching excitation is optimized when H strikes near the end of the O-C-O molecule.

(4). It appears that the rotational and translational degrees of freedom of CO_2 can be treated classically for H*-CO_2 collisions which produce either the one quantum 00^01 state or the two quantum 00^02 state. The overall probability for excitation of one or two quanta of asymmetric stretching vibration, however, requires a quantum mechanical approach with a proper potential energy surface.

This research was sponsored in part by the Joint Services Electronics Program.

References:

1. S. R. Leone, Ann. Rev. Phys. Chem. **35**, 109 (1984).

2. G. W. Flynn and R. E. Weston, Jr., Ann. Rev. Phys. Chem. **37**, 551 (1986).

3. G. C. Schatz, M. S. Fitzcharles, and L. B. Harding, Faraday Discuss. Chem. Soc. **84**, 359 (1987); G. C. Schatz and M. S. Fitzcharles, in: *Selectivity in Chemical Reactions*, ed. J. C. Whitehead (Kluwer Academic Publishers, Dordrecht, 1988), pp. 353-365.

4. K. Kleinermanns and J. Wolfrum, Chem. Phys. Lett. **104**, 157 (1984); Laser Chem. **2**, 339 (1983); K. Kleinermanns, E. Linnebach, and J. Wolfrum, J. Phys. Chem. **89**, 2525 (1985); A. Jacobs, M. Wahl, R. Weller, and J. Wolfrum, Chem. Phys. Lett. **158**, 161 (1989).

5. G. Hoffmann, D. Oh, Y. Chen, Y. M. Engel, and C. Wittig, Israel J. Chem. **30**, 115 (1989).

6. Y. Chen, G. Hoffmann, D. Oh, and C. Wittig, Chem. Phys. Lett. **159**, 426 (1989).

7. S. Buelow, G. Radhakrishnan, J. Catanzarite, and C. Wittig, J. Chem. Phys. **83**, 444 (1985);.G. Radhakrishnan, S. Buelow, and C. Wittig, J. Chem. Phys. **84**, 727 (1986); S. Buelow, G. Radhakrishnan, and C. Wittig, J. Phys. Chem. **91**, 5409 (1987); S. Buelow, M. Noble, G. Radhakrishnan, H. Reisler, C. Wittig, and G. Hancock, J. Phys. Chem. **90**, 1015 (1986); C. Wittig, S. Sharpe and R. A. Beaudet, Accounts Chem. Res. **21**, 341 (1988); J. Rice, G. Hoffmann, and C. Wittig, J. Chem. Phys. **88**, 2841 (1988).

8. J. K. Rice, Y. C. Chung, and A. P. Baronavski, Chem. Phys. Lett. **167**, 151 (1990).

9. N.F. Scherer, L.R. Khundkar, R.B. Bernstein, and A.H. Zewail, J. Chem. Phys. **87**, 1451 (1987).

10. F. A. Khan, T. G. Kreutz, G. W. Flynn, and R. E. Weston, Jr., J. Chem. Phys. **92**, 4876 (1990).

11 J. A. O'Neill, C. X. Wang, J. Y. Cai, G. W. Flynn, and R. E. Weston, Jr., J. Chem. Phys. **88**, 6240 (1988).

12. J. F. Hershberger, J. Z. Chou, G. W. Flynn, and R. E. Weston, Jr., Chem. Phys. Lett. **149**, 51 (1988); J. F. Hershberger, S. A. Hewitt, S. K. Sarkar, G. W. Flynn, and R. E. Weston, Jr., J. Chem. Phys. **91**, 4636 (1989).

13. J.O. Chu, G.W. Flynn, and R.E. Weston, Jr., J. Chem. Phys. **78**, 2990 (1983).

14. J. O. Chu, C. F. Wood, G. W. Flynn, and R. E. Weston, Jr., J. Chem. Phys. **80**, 1703 (1984); **81**, 5533 (1984); S. A. Hewitt, J. F. Hershberger, G. W. Flynn, and R. E. Weston, Jr., J. Chem. Phys. **87**, 1894 (1987).

15. F. A. Khan, T. G. Kreutz, Lei Zhu, G. W. Flynn, and R. E. Weston, Jr., J. Phys. Chem. **92**, 6171 (1988).

16. F. A. Khan, T. G. Kreutz. J. A. O'Neill, C. X. Wang, G. W. Flynn, and R. E. Weston, Jr., J. Chem. Phys. **93**, 445 (1990).

17. S. A. Hewitt, J. F. Hershberger, J. Z. Chou, G. W. Flynn, and R. E. Weston, Jr., J. Chem. Phys. **93**, 4922 (1990).

18. George Schatz, private communication.

19. T. G. Kreutz, F. A. Khan, and G. W. Flynn, J. Chem. Phys. **92**, 347 (1990).

20. T. G. Kreutz and G. W. Flynn, J. Chem. Phys. **93**, 452 (1990).

21. R. N. Schwartz, Z. I. Slawsky, and K. F. Herzfeld, J. Chem. Phys. **20**, 1591 (1952).

22. J. L. Stretton, Trans. Faraday Soc. **61**, 1053 (1965).

23. J. T. Yardley and C.B. Moore, J. Chem. Phys. **49**, 1111 (1968).

24. D. Rapp and T.E. Sharp, J. Chem. Phys. **38**, 2641 (1963).

25. J. M. Hensley, S. Green, and G. W. Flynn, Chem. Phys. Letts. **177**, 508 (1991)

PUBLICATIONS (Research Area II, Work Unit 2)

J. Park, Y. Lee, J. F. Hershberger, J. M. Hossenlopp, and G. W. Flynn, "Chemical Dynamics of the Reaction between Chlorine Atoms and Deuterated Cyclohexane," J. Am. Chem. Soc. **114**, 58 (1992).

J. J. Breen and G. W. Flynn, "STM Studies of the Synthetic Polypeptide: Poly-γ-benzyl-L-glutamate," J. Phys. Chem. **96**, 6825 (1992).

R. E. Weston, Jr. and G. W. Flynn, "Relaxation of Molecules with Chemically Significant Amounts of Vibrational Energy: The Dawn of the Quantum State Resolved Era," Ann. Rev. Phys. Chem. **43**, 559-589 (1992).

C. K. Ni and G. W. Flynn, "Correlation between Molecular Recoil and Molecular Orientation in Collisions of Symmetric Top Molecules with Hot Hydrogen Atoms," Chem. Phys. Lett. **193**, 69 (1992).

S. A. Hewitt, L. Zhu, and G. W. Flynn, "Diode Laser Probing of CO_2 and CO Vibrational Excitation Produced by Collisions with High Energy Electrons from 193 nm Excimer Laser Photolysis of Iodine," J. Chem. Phys. **97**, 6397 (1992).

J. J. Breen, J. S. Tolman, and G. W. Flynn, "STM Studies of Vapor Deposited Films of TTF and Iodine," accepted for publication.

L. Zhu and G. W. Flynn, Diode Laser Probing of OCS and N_2O Vibrational Excitation Produced by Collisions with High Energy Electrons from 193 nm Excimer Laser Photolysis of Iodine," J. Phys. Chem., accepted for publication.

F. A. Khan, T. G. Kreutz, G. W. Flynn, and R. E. Weston, Jr., "Translationally and Rotationally Resolved Excitation of $CO_2(00^02)$ by Collisions with Hot Hydrogen Atoms," accepted for publication.

2.3 INTERFACE STUDIES AND DEVICE APPLICATIONS OF MULTI-LAYERED SCHOTTKY BARRIER AND HETEROJUNCTION STRUCTURES

Edward S. Yang, Principal Investigator (212) 854-3120
Research Area II, Work Unit 3

A. Surface Passivation of GaAs/AlGaAs Heterojunctions by Electron Cyclotron Resonance Plasmas

One of the major limitations of the AlGaAs/GaAs technology is the current gain degradation associated with the scaling of the emitter-base junction size.[1] The current degradation is known to be related to the high surface recombination velocity of GaAs. Several methods have been developed to reduce this recombination current, e.g., using graded base structure[2] or passivating the emitter-base periphery with sulfide treatments.[3,4] Unfortunately, the graded base introduces unnecessary process complexity and the sulfide treated surface is not stable. We report here the first experiment of electron cyclotron resonance (ECR) hydrogen and nitrogen plasma surface passivation of the AlGaAs/GaAs heterojunction bipolar transistor (HBT). As a result of the plasma treatment, the low-current current gain is enhanced by a hundred-fold, and the collector and base current ideality factors are improved. We present in situ x-ray photoelectron spectroscopy (XPS) of the surface before and after each ECR plasma step, and the surface spectroscopy is then correlated with the electrical measurements of the HBT. In addition, we provide new experimental data with ECR ammonia plasma, which further enhances the device characteristics.

The experiments were carried out in an ultrahigh vacuum (UHV) system with two independent chambers equipped with a monochromatic Al $K\alpha$XPS, a residual gas analyzer (RGA) and a custom made ECR plasma source. The base pressure is $1X10^{-8}$ and $<5X10^{-10}$ Torr for the processing chamber and the analysis chamber, respectively. The ECR plasma is produced with a 120-W, 2.45 GHz microwave source. A 1.5-in.-diam quartz cell on the UHV system, surrounded by a microwave cavity and an electromagnet,

allows the microwave power to be absorbed by the gas in an 875-G magnetic field. The processing gas is introduced at the base of the quartz cell, and the typical chamber pressure is $1X10^{-3}$ and $5X10^{-4}$ Torr for hydrogen and nitrogen (or ammonia), with a flow rate around 7 sccm. Samples used in our experiment are *Npn* AlGaAs/GaAs HBTs with a two-dimensional elecron gas (2DEG) emitter. A GaAs wafer is used as a control sample for the XPS surface analysis. The 2DEG-emitter HBT has a high current gain, a low offset voltage, but large leakage currents.[5] Samples are positioned 22 cm from the center of the plasma source. Typical ion energies in the ECR plasma are around 20 eV, and the ion-current density at the sample position is measured using a Faraday cup to be $I_{sat} = 0.4\ \mu m/cm^2$ for hydrogen with absorbed microwave power of 80 W. The sample may be biased to eliminate either positive or negative particles from being incident on the sample, which allows modification of the reaction conditions. Under the typical XPS data acquisition conditions, the Au $4f_{7/2}$ peak at 84.0 eV binding energy (BE) has a full width at half-maximum (FWHM) of 1.0 eV. The run-to-run energy position resolution is within ± 0.05 eV. The analyzer settings and acquisition time for each run were kept constant in order to make meaningful comparisons of the peak areas, which correspond to the elemental concentrations. Before loading into the UHV system, the samples were cleaned by $NH_3OH:H_2O$ (1:1) to remove the native oxide. The ECR hydrogen plasma treatment was set for 30 min at 250 °C with a sample bias of -22 V. Half of the hydrogen plasma treated samples were treated with a nitrogen plasma for 10 min and the others were treated with a 10 min ammonia plasma at room temperature. The collector current-voltage characteristics and the junction reverse leakage currents were measured by HP4145B.

The XPS spectrum of the GaAs sample before hydrogen plasma treatment shows a strong oxygen signal, indicating the surface is covered by native oxide. Expanded spectra of the As2p and Ga2p core levels are shown in Fig. 1. For As bound to GaAs, the As2p core level produces emission at binding energy around 1322 eV. For Ga in GaAs, the Ga2p core level is positioned around 1117 eV. The oxide composed of As_2O_3 and Ga_2O_3

are characterized by chemical shifts of 3 and 1 eV toward higher binding energies, respectively. After 30 min of hydrogen plasma processing at 250 °C, the As_2O_3 signal completely disappeared and the emission intensity of the main peak As2p increased. The oxygen 01s signal decreased, indicating that the hydrogen plasma reduces the As_2O_3 with subsequent oxygen removal. For Ga, some oxygen signal Ga_2O_3 is still detectable and the observed intensity increase of the main peak is larger for Ga2p than for As2p. These results indicate that oxygen in As_2O_3 reacts with hydrogen plasma more readily than oxygen in Ga_2O_3, and the hydrogen plasma appears to have removed the excess As to re-establish a clean stoichiometric GaAs surface. This is also reflected in a slight decrease of the FWHM of the core levels.

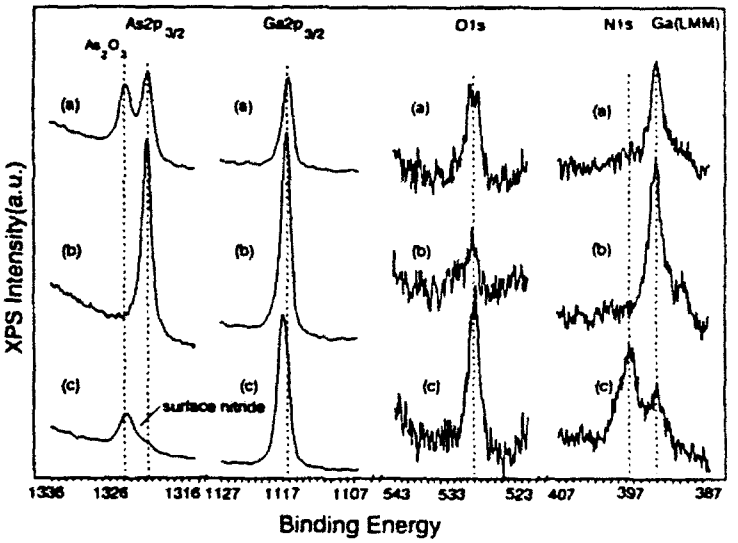

Figure 1. XPS spectrum of ECR hydrogen, nitrogen plasma treated GaAs(100) surfaces. (a) 50% NH_4OH clean (1 min), (b) 30 min ECR hydrogen plasma at 250°C, (c) 30 min ECR hydrogen and 10 min nitrogen plasma.

The effect of the nitrogen plasma on the cleaned GaAs surface is plotted in Fig 1(c). The shoulders in both the As2p and the Ga2p levels are indications of the formation of a mixed surface nitride-oxide layer. Since a surface layer is formed, the intensity of the core levels signal for GaAs decreases. The observed XPS intensity reduction of the main peak is larger for As2p than for Ga2p. This result may be interpreted as As dangling bonds

saturated by N atoms. The origin of the oxygen is likely to come from the residual moisture stuck to the chamber or the gas roughing line. In addition to baking out the chamber, a liquid nitrogen (LN_2) cold trap is wrapped around the roughing line to purify the processing gas.

The influence of the ammonia plasma on the cleaned GaSa surface is different from the case of nitrogen plasma treatment. The XPS data are shown in Fig. 2. After the ammonia plasma treatment, a mixed surface nitride-oxide layer is also formed. However, instead of detecting a strong 01s peak, we observe a slight increase in the intensity of the oxygen. The shoulders in the As2*p* and Ga2*p* levels are nitride rich. The reduction of the oxygen signal can be explained as follows: during the ammonia plasma processing, both the nitrogen and hydrogen plasma play a role in the reaction. Therefore, when the surface is nitridized, the hydrogen plasma also clean the GaAs surface.

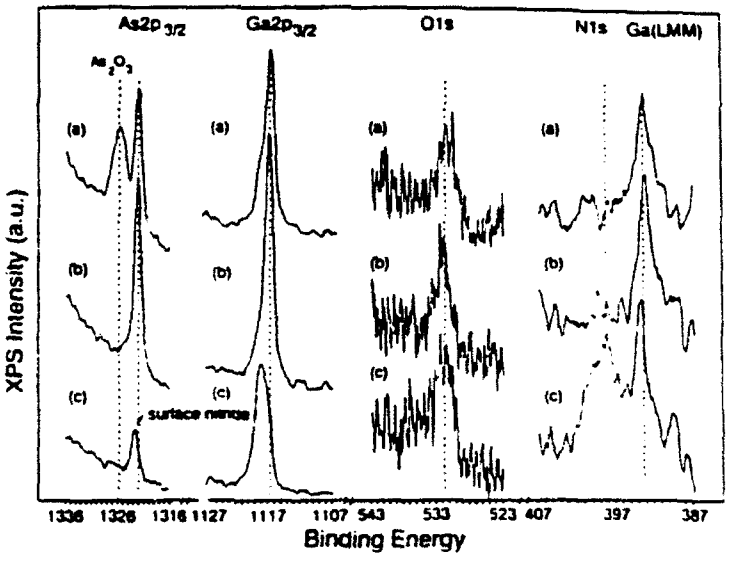

Figure 2. XPS spectrum of ECR hydrogen, ammonia plasma treated GaAs(100) surfaces. (a) 50% NH_4OH clean (1 min), (b) 30 min ECR hydrogen plasma at 250°C, (c) 30 min ECR hydrogen and 10 min ammonia plasma.

The currents as a function of the emitter junction bias (Gummel plot) of the HBT are plotted in Fig. 3. Before the ECR plasma process, the collector ideality factor is 1.26 and the base current has a large leakage component with an ideality factor of 2.67 at V_{be} less than 1.02 V. After the hydrogen and nitrogen ECR treatment, the base current and collector current ideality factors become 1.96 and 1.08, respectively, at V_{be} less than 1.08 V, which are improved further to 1.49 and 1.02 by replacing nitrogen with ammonia. These changes are proportional to the ratio of the arsenic nitride to arsenic oxide qualitatively. It is clearly seen that the shunt leakage current is reduced significantly by the ECR plasma. We found that the recombination current associated with the surface states is also reduced effectively. The corresponding current gains as a function of the collector current density are shown in Fig. 4. These data are consistent with lower junction recombination for ammonia treated samples. In other words, there appears to be fewer surface states after the ammonia treatment than after the nitrogen treatment. The current-voltage characteristic of the HBT remained the same after exposure to air for a week. Most of the devices degraded after two weeks of storage but could be recovered with another ECR treatment. It seems that the thin nitride-oxide layer is oxygen permeable The regrown As_2O_3 appears to be responsible for the device degradation with aging.

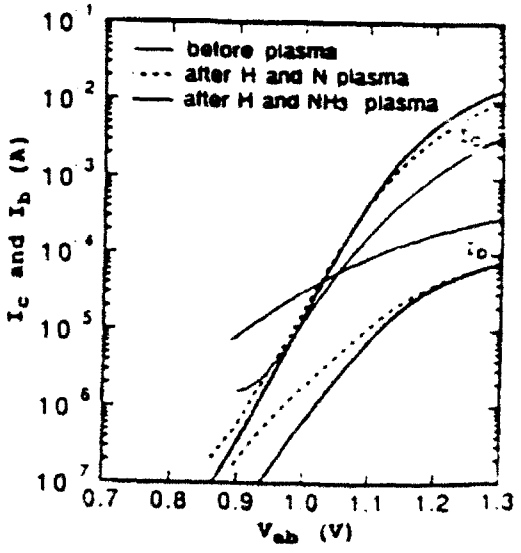

Figure 3. Gummel plot of the HBT before (dotted line) and after the ECR hydrogen and nitrogen plasma (dashed line) and ECR hydrogen and ammonia plasma (solid line).

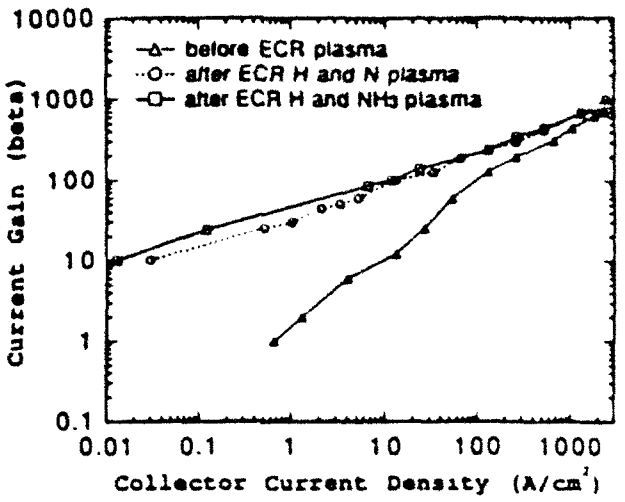

Figure 4. Common emitter current gain as a function of collector current density.

In summary, XPS analysis has been carried out on n^+-GaAs surfaces cleaned by hydrogen, nitrogen, and ammonia ECR plasma. The hydrogen plasma was found to remove the native oxide and recover the surface order. A mixed surface nitride-oxide layer was formed after the nitrogen and ammonia plasma treatments. An improved base current ideality factor of AlGaAs/GaAs HBTs is obtained. The improved device performance is due to the removal of the native oxide and passivation of As atoms on the GaAs surface. When a thicker nitride layer is obtainable, the ECR hydrogen, nitrogen, and ammonia plasma treatments could offer a practical technique for the surface passivation of AlGaAs/GaAs HBTs.

References:

1. O. Nakajima, K. Nagata, H. Ito, T. Ishibashi, and T. Sugeta, Jpn. J. Appl. Phys. **24**, 596 (1985).
2. O. Nakajima, K. Nagata, H. Ito, T. Ishibashi, and T. Sugeta, Jpn. J. Appl. Phys. **24**, 1368 (1985).
3. C. J. Sandroff, R. N. Nottenberg, J. C. Bischoff, and R. Bhat, Appl. Phys. Lett. **51**, 33 (1987).
4. H. L. Chuang, M. S. Carpenter, M. R. Melloch, and M. S. Lundstrom, Appl. Phys. Lett. **57**, 2113 (1990).
5. Q. Wang, Y. Wang, K. F. Longenbach, E. S. Yang, and W. I. Wang, Appl. Phys. Lett. **59**, 2582 (1991).

B. Low Temperature SiGe Oxidation by Electron Cyclotron Resonance

Because of interest in developing low-temperature processing methods for submicrometer integrated-circuit technology, plasma oxidation is currently being investigated as a potential alternative for thermal oxidation. Microwave electron cyclotron resonance (ECR) plasmas are receiving considerable attention from the plasma processing industry due to the capability of operating at low pressure (~10^{-4} Torr), high plasma densities, great ionization efficiency (10%-20%), and low ion energies (20-30 eV). These advantages make the technique compatible with ultrahigh vacuum (UHV) integrated processing.[1] The use of ECR oxygen plasma to grow thin oxide on single-crystal silicon substrates has been reported.[2] The physical characteristics of the ECR-grown oxides are identical to thermal oxides and the electrical characteristics are acceptable for device fabrication. Oxidation of SiGe alloys is important because SiGe promises new device applications based on its compatibility with silicon. In order to combine SiGe-based devices with state-of-the-art Si technology, a good quality SiGe oxide is necessary. Several reports on the oxidation of SiGe have been published in the literature. Previous studies of thermal oxidation of SiGe alloys revealed that either a pure SiO_2 layer[3-5] or a mixed oxide layer consisting of SiO_2 and GeO_x (x= 1,2)[6,7] was formed on top of the SiGe alloy, which was accompanied by the rejection of Ge from the oxide and thus the formation of Ge-rich layers. These Ge-rich layers greatly increase the interface trap density. Recently, Vancauwenberghe et al.,[8] reported that both Si and Ge in the SiGe alloy are fully oxidized at room temperature by low-energy ion-beam oxidation using $^{18}O_2^+$ ion beams with energies ranging from 100 eV to 1 keV. However, the ion energies used in the low ion-beam oxidation seem high enough to induce damage or defects on the surface. In this section, we report the oxidation of SiGe by ECR plasma and demonstrate that Si and Ge are fully oxidized with no additional heating. We also present XPS and Auger electron spectroscopy (AES) results at different stages of oxidation.

The experiments were carried out in an UHV system with two independent chambers equipped with a monochromatic Al Ka x-ray photoelectron spectrometer, and a custom-made ECR plasma source. The ECR plasma was produced with a 120-W, 2.45-GHz microwave source. Oxygen gas was introduced at the base of the quartz cell with a flow rate of approximately 7 sccm. Chamber pressure was kept around $5X10^{-4}$ Torr during oxidation. Samples were positioned 22 cm away from the center of the plasma source. Typical ion energies in ECR plasmas were around 20 eV.[1] The ion-current density at the sample position was measured using a Faraday cup. A value of I_{sat} = 12 $\mu A/cm^2$ for an oxygen plasma with absorbed microwave power of 120 W was observed. The substrate holder was designed for floating or dc bias operation, which could eliminate either positive or negative particles from impinging on the sample, thus allowing modification of the reaction conditions. The substrate holder contained resistive heating elements and a thermocouple for substrate temperature measurement and control. The sample temperature was varied from room temperature to 500°C. The SiGe samples (2000 Å) used in this study were grown on n-type Si(100) substrates by molecular-beam epitaxy (MBE) at 400°C. Samples were chemically cleaned and (10%) hydrofluoric acid (HF) dipped before being loaded into the UHV chamber. Both $Si_{0.8}Ge_{0.2}$ and $Si_{0.5}Ge_{0.5}$ samples were studied. XPS spectra of the Si2p, Ge2p, Ge3d, and O2s core levels were taken before and after ECR processing. The Si2p and Ge2p peaks, which have electron escape depth of 30 and 7 Å,[9] respectively, were used to determine the oxide coverage. From XPS the oxide thickness d_{ox} is given by[10]

$$d_{ox} = l_{ox} \sin\theta \ln [(I_{ox} / I_{sub}) (D_{sub} / D_{ox}) (\lambda_{sub} / \lambda_{ox}) + 1],$$

where d_{ox} is the thickness of the oxide layer, λ_{ox} and λ_{sub} are the electron mean escape depths of the oxide and the substrate, respectively, and θ is the exit angle of the detected photoelectron relative to the surface. I_{ox} and I_{sub} are the intensities of the photoelectron

from the same atomic level; D_{ox} and D_{sub} are the densities of the oxide and the substrate. Under the typical XPS data acquisition conditions, the Au $4f_{7/2}$ peak at 84.0 eV binding energy has a half-width at half-maximum (FWHM) of 1.0 eV. The run-to-run energy position resolution was within ±0.05 eV. The analyzer settings and acquisition time for each run were kept constant in order to make meaningful comparison of the peak areas, which correspond to elemental concentrations.

A systematic XPS study of the ECR oxidation of SiGe with a sample bias +7.5 V at 250°C was undertaken with representative results shown in Fig. 1. Spectra 1(a) shows a chemically cleaned $Si_{0.8}Ge_{0.2}$ surface with well-defined Si2p, Ge2p, and Ge3d substrate peaks. The Ge2p photoelectrons have a lower kinetic energy than Ge3d photoelectrons and originate from a shallower depth. They provide a signal more representative of the surface than the Ge3d photoelectrons. After a 1 min ECR oxygen plasma exposure, a 12 Å oxide is formed. The oxide is composed primarily of SiO_2 and GeO_2 which are characterized by core-level chemical shifts of 3.8 eV (for Si2p) and 4 eV (for Ge2p and Ge3d) towards higher binding energies, respectively [Fig. 1(b)]. As the exposure to the oxygen plasma increases, the Si2p signal positioned at 99.6 eV gradually decreases, while a signal at 103.4 eV corresponding to SiO_2 increases [Fig. 1(c) and 1(d)]. The same observations are made with the Ge3d signal. However, the Ge2p signal positioned at 1217.6 eV (corresponding to elemental Ge) decreases rapidly and the Ge2p signal positioned at 1221.6 eV (corresponding to Ge^{4+}) at first increases with oxidation time and reaches a maximum at the oxide thickness of about 30 Å, then gradually decreases. This phenomenon will be discussed later. It is seen from these XPS spectra that both Si and Ge are simultaneously fully oxidized forming SiO_2 and GeO_2. However, at the beginning of the ECR oxidation, suboxides can be detected for silicon. As the oxidizing process continues, these suboxides disappear completely and only fully oxidized Si and Ge are observed.

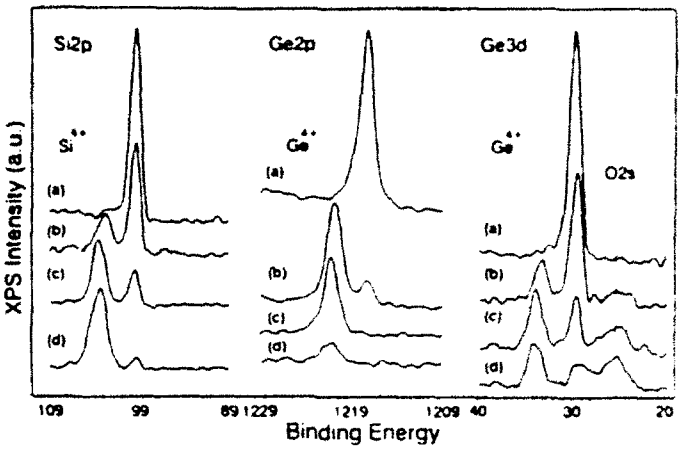

Figure 1. XPS spectrum of ECR oxidation of $Si_{0.8}Ge_{0.2}$ under a sample bias +7.5 V at 250°C. (a) Cleaned by 10% HF, (b) 1 min oxygen plasma, (c) 1 h oxygen plasma, and (d) 3 h oxygen plasma

Figure 2 is the Auger depth profile of the oxidized $Si_{0.8}Ge_{0.2}$. Ge was found to be uniformly distributed in the oxide, and the Ge peak-to-peak height is slightly lower in the oxide than in the underlying alloy. There is no enriched Ge layer formed between the oxide layer and the alloy. The Auger result showing that Ge is oxidized is consistent with the in situ XPS data.

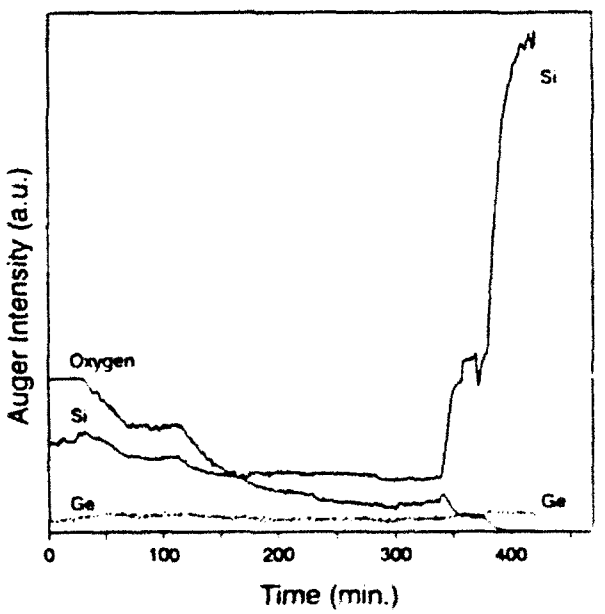

Figure 2. Auger depth profile of the ECR oxidized $Si_{0.8}Ge_{0.2}$.

The amount of Ge in the SiGe dielectric films is lower than the original Ge content of the SiGe alloy, as shown in Figs. 1(a) and 1(b), and Fig. 2. The XPS intensity of GeO_2 (from Ge2p photoelectrons) increases with time and reaches a maximum at the oxide thickness of about 30 Å, and then the XPS intensity of GeO_2 gradually decreases [Figs. 1(c) and 1(d)]. Further oxide growth results in a silicon oxide-rich surface. Since GeO_2 is a volatile oxide with a high vapor pressure, it has a lower sublimation energy than SiO_2. Therefore, some GeO_2 near the surface layer may get evaporated and preferential sputtered by the plasma.[8] This can explain why the GeO_2 component near the surface region decreases with time after the initial growth [Figs. 1(c) and 1(d)]. With increasing growth temperature up to 500°C, the oxide is stoichiometric and does not lose its GeO_2 component. After *in vacuo* (around $5X10^{-8}$ Torr) annealing at 450°C for 1 h, we found that the amount of GeO_2 in the dielectric oxide films did not change, which indicates that these alloy oxides are thermally stable.

Figure 3 shows the oxide thickness derived from the XPS data as a function of growth time. There is a fast growth regime followed by a slow growth regime. At the very initial stage of growth, the oxidation involved a reaction zone, which might be several monolayers, where the oxygen species react with the bulk SiGe directly.[11] So, the effect of bias is less clear and the oxidation rate is almost the same with either postitive or negative bias. Further oxidation is limited by the diffusion of oxygen species through the growing oxide to the bulk SiGe. The oxidation under a negative bias condition becomes self-limiting, and its saturation implies that postitive ions are not the main reaction species and a barrier is present for negative ions to prevent further oxidation. On the other hand, the positive sample bias enhances the oxidation rate which indicates that negative ions cause some additional oxidation effect.[12] These phenomena can be explained as follows: SiGe can be oxidized under a negative bias condition that attracts positive ions. Negative bias also permits injection of electrons from the SiGe substrate into the near oxide, where they can attach to interstitial oxygen to form O^-. The negative ion can readily diffuse towards

the interface and react with the bulk SiGe. When the negative electric field becomes high enough to offset the diffusion gradient, this process stops. Under the postiive bias condition, negative ions are attracted to the surface and the high density of electrons in the plasma promote electron attachment to oxygen to form O^-. The negative ion, O^-, can migrate readily through the oxide by diffusion or by drift with a positive sample bias. The result is in accord with the previous studies of the ECR plasma oxidation of Si.[12]

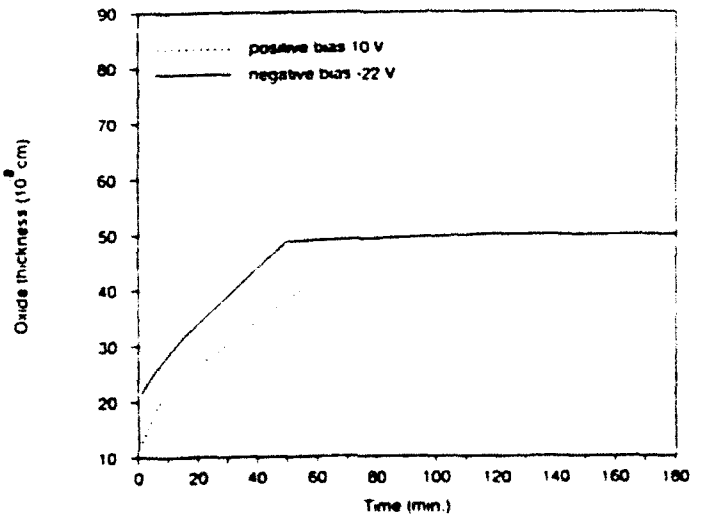

Figure 3. Growth rate of ECR oxidation $Si_{0.8}Ge_{0.2}$ at 300°C with absorbed microwave of 120 W.

In summary, we report the growth of oxide of SiGe alloy by ECR plasma oxidation at temperatures from room temperature to 500°C. The ECR oxidation of SiGe has been studied by in situ XPS and ex situ AES. The results indicate that both Si and Ge are fully oxidized, and the stoichiometry of the oxide does not change with temperature. The new SiGe oxide films have the potential for applications in advanced SiGe-based electronics and optoelectronics.

This research was supported by the Joint Services Electronics Program.

References:

1. *Handbook of Ion Beam Processing Technology, Principles, Deposition, Film Modification and Synthesis*, edited by J. J. Cuomo, S. M. Rossnagel, and H. R. Kaufman (Noyes, Park Ridge, NJ, 1989).

2. D. A. Carl, D. W. Hess, M. A. Lieberman, T. D. Nguyen, and R. Gronsky, J. Appl. Phys. **70**, 3301 (1991).
3. S. Margalit, A. Bar-Lev, A. B. Kuper, H. Aharoni, and A. Neugroschel, J. Cryst. Growth **17**, 288 (1972).
4. F. K. Legoues, R. Rosenberg, and B. S. Meyerson, Appl. Phys. Lett. **54**, 644 (1989).
5. D. Nayak, K. Kamjoo, J. C. S. Woo, J. S. Park, and K. L. Wang, Appl. Phys. Lett. **56**, 66 (1990).
6. H. K. Liou, P. Mei, U. Gennser, and E. S. Yang, Appl. Phys. Lett. **59**, 1200 (1991).
7. J. Eugene, F. K. LeGoues, V. P. Kesan, S. S. Iyer, and F. M. d'Heurle, Appl. Phys. Lett. **59**, 78 (1991).
8. O. Vancauwenberghe, O. C. Hellman, N. Herbot, and W. J. Tan, Appl. Phys. Lett. **59**, 2031 (1991).
9. H. Grant and W. Monch, Surf. Sci. **105**, 217 (1981).
10. T. A. Carlson and G. E. Mcguire, J. Electron. Spectrosc. **1**, 161 (1972/73).
11. V. Murali and S. P. Muraka, J. Appl. Phys. **60**, 2106 (1986).
12. Y. Z. Hu, J. Joseph, and E. A. Irene, Appl. Phys. Lett. **59**, 1353 (1991).

PUBLICATIONS (Research Area II, Work Unit 3)

H. K. Liou, P. Mei, U. Gennser, and E. S. Yang, "Effects of Ge Concentration on SiGe Oxidation Behavior," Appl. Phys. Lett. **59**, 1200 (1991).

H. K. Liou, X. Wu, U. Gennser, E. S. Yang, V. P. Kesan, S. S. Iyer and K. N. Tu, "Interfacial Reactions and Schottky Barriers of Pt and Pd on Epitaxial $Si_{1-x}G_x$ Alloys," Appl. Phys. Lett. **60**, 577 (1992).

P. W. Li, Q. Wang, E. S. Yang, "Chemical and Electrical Characterization of AlGaAs / GaAs Heterojunction Bipolar Transistors Treated by Electron Cyclotron Resonance Plasmas," Appl. Phys. Lett. **60**, 1996 (1992).

P. W. Li, H. K. Liou, E. S. Yang, S. S. Iyer, T. P. Smith, III, and Z. Lu, "Formation of Stoichiometric SiGe Oxide by Electron Cyclotron Resonance Plasma," Appl. Phys. Lett. **60**, 3265 (1992).

2.4 SURFACE SCIENCE STUDIES OF POLYMER THIN FILMS FOR ADVANCED INTERCONNECT AND PACKAGING TECHNOLOGY

Brian E. Bent, Co-Principal Investigator (212) 854-3041
Robert C. White, Co-Principal Investigator (212) 854-3115
Research Area II, Work Unit 4

A key issue in the development of polymer thin films for microelectronics applications is the ability to control their properties. While bulk polymers such as polyimides have highly desirable properties as insulating materials (for example, low dielectric constant, ease of fabrication, thermal stability, and adhesion), it is often found that many of these properties are degraded when the polymer is fabricated as a thin film. Similarly, when thin film polyimides are employed for wave guides in optical interconnect schemes, bulk properties such as losses are also found to degrade. Our research on polyimide and polyolefin thin films over the past year has focused on two issues: (1) controlled deposition of ultra-thin polymer films and (2) analysis of the bulk and surface structure, as well as local electrical properties of the films that are produced. It is in the thin film regime that a bulk to interphase transition occurs which has important ramifications on microelectronic device reliability and performance. We have completed the installation of infrared spectroscopy and x-ray photoelectron spectroscopy for characterizing the structure and composition of polymer films, and have implemented scanning tunneling microscopy and spectroscopy to determine the local electronic structure of polymer thin films. These accomplishments are described below.

(1.) Controlled Deposition of Polymer Thin Films: The focus of this work is the deposition of polymer films ranging in thickness from one monolayer to a few microns in thickness. This is the range over which polymer film properties are believed to transform from those of an adsorbed monolayer to those of a bulk polymer. Our goal is to develop methods for depositing polymer films under conditions where the molecular ordering and orientation can be controlled. Three approaches have been pursued over the past year: spin

coating of ultra-thin films, vapor deposition in vacuum, and synthesis of oriented hydrocarbon chains under ultra-high vacuum conditions.

As trial systems for the spin coating and vapor deposition techniques, we have studied the deposition of polyimides which result from the use of two building blocks, the dianhydride PMDA and the diamine ODA. Polyimides are insulating and thermally stable materials which have not only become accepted in microelectronics, but indeed are pervasive from the device level up to the package level. Spin coating (or dip coating) is pursued to investigate the effects of the precursor material which is an acidic solution, polyamic acid. Deposition of these materials from acidic solution which also contains a solvent has important ramifications on device fabrication, not the least of which is the effect on the substrate itself. An example is the diffusion of Cu into the polyimide film when polyamic acid is cured on Cu films. The fabrication of films by chemical vapor deposition (CVD) of the separate building blocks is attractive for two reasons, first due to the solventless nature of the process, and second because this is a method completely compatible with all semiconductor processing including the popular cluster tooling important for contamination control. The two deposition methods also result in different predominant molecular orientation within the films.

Thin films of the polyimide PMDA-ODA have been spin coated on Si, SiO_2, Al, Au, Cr, and dip-coated on graphite substrates.[1] These films should display molecular orientation parallel to the substrate surface. The metal substrates were multilayer structures similar to those used in microelectronic interconnects, with the metal vapor deposited onto Si or SiO_2. The thickness of these films was varied from approximately 25 Ångstroms to 200 Ångstroms in small steps. In addition, films of thickness 0.1, 0.5, 1.0 and 2.5 μm were spin coated on these substrates for comparison of bulk and interfacial properties. The continuity of films < 120 Ångstroms in thickness has not been verified since XPS indicates small amounts of substrate signal visible below this thickness, however STM results indicate that at worst, patch regions are coated leaving other patches uncoated, with the

degree of homogeneity depending on the substrate. Employing films of less than 120 Ångstroms thickness we have investigated substrate effects on ordering at the interphase. The electrical properties such as conductivity have been investigated using a point contact electrical measurement, referred to as scanning tunneling spectroscopy (STS). In this technique, contact is not actually made, but I vs. V is measured across a tunnel junction between an atomically sharp tip and the surface of the polymer film. Anomalous conductivity in these films has allowed for surface topographic characterization as well as electronic structure measurements.

In addition, films fabricated by chemical vapor deposition (CVD) which should have molecular orientations away from the substrate surface have been fabricated on the same substrates as the spin coated films. These films were grown in a manner intended to imitate actual processing of packaging structures, where thin native oxides existed on the substrate material. Au was employed in order to present a non-oxidized surface for CVD growth of the polymer films. Extensive XPS analysis reveals that good reactivity and film growth is accomplished for all substrates except the Au, where film quality is degraded. This result could easily be employed in device fabrication by depositing small amounts of Au in regions where one wishes not to grow a polymer film. This is otherwise a difficult problem since polyimide, once imidized, is essentially intractable and cannot be removed easily with solvents. Another interesting result is that the vapor deposited films passivate the substrates quite well to further reactivity, except in the case of Cr where oxidation of the substrate after film deposition was observed.[2]

Parallel to the deposition of polyimide thin films, we have completed a series of studies on the structure of model polyolefin thin films on copper surfaces. Last year, we reported that such films could be formed by using alkyl iodides as precursors. The disadvantage to this approach is that only half of the adsorbed species in the resulting monolayer are the desired hydrocarbon chains and the rest are iodine atoms. Since then, we have developed a more general, iodine-free method for preparing these model

monolayers. The approach, as shown in Scheme 1, is to condense onto the surface a monolayer of hydrocarbon molecules that are one H atom shy of the desired organic polymer chain. Because these are stable molecules, they are readily obtained from commercial sources and easily adsorbed onto the surface. The additional hydrogen or deuterium atom needed to make the polymer chain is subsequently added from the gas phase as shown schematically below.[3,4]

Scheme 1

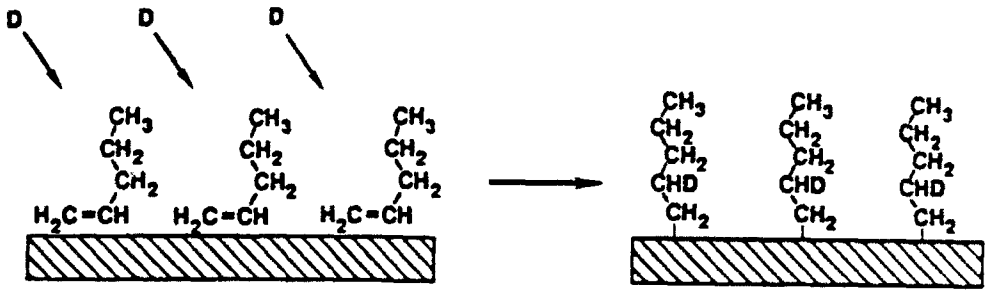

Well-defined oriented and ordered monolayers such as that shown above are important for calibrating infrared spectroscopy as an analytical tool for determining the structure and bonding of more complex polymer thin films. In this regard, the deuterium-labeling of polymer chains is particularly useful for spectroscopically identifying the vibrational modes of the hydrocarbon chain. For example, we have recently employed this technique to determine that the C-H bonds adjacent to the metal are "softened" by their interaction with the surface.[5]

(2.) Polymer Film Structures and Properties: It is well-known that bulk properties of materials are often determined by local defects and impurities. To study the compositional purity of the polyimide films deposited by spin coating and vapor deposition, we have employed x-ray photoelectron spectroscopy (XPS).

Photoemission has revealed that surface composition of spin coated materials are in general quite close to the expected stoichiometry. There is often a near surface depletion of

carbonyl groups, and we have also observed this in our spin coated films. The chemical purity is quite high, however. Similar results are found for the vapor deposited films, except that signifigant degradation of chemical composition is observed for films vapor deposited on Au. Thicker films often display less chemical degradation, indicating an interphase degradation of the polyimide near the Au substrate.

A second important issue in the deposition of ultra-thin polymer films is ascertaining whether the appropriate chemical bonds have been formed to make the desired molecular chains. Infrared spectroscopy, in being a bond-specific probe, is ideal for this determination, and over the past year we have developed single reflection infrared absorption spectroscopy (RAIRS) to make these measurements. Our initial studies have been under atmospheric conditions, but as described below in Section 3, we have also set-up an infrared spectrometer for studies under vacuum conditions.

An illustrative infrared spectrum of a 130 Å polyimide film (PMDA-ODA) that has been spin-coated onto an aluminum film evaporated on silicon is shown in Figure 1. The vibrational frequencies in this spectrum are consistent with those reported in the literature for bulk polyimides.[6] Particularly note-worthy is the imide mode at ~1380 cm^{-1}. Studies with polarized infrared light are in progress to address the average orientation of the molecular subunits within these thin films.

To address the local electronic properties of these structurally-characterized films, we have employed scanning tunneling microscopy and spectroscopy. Our most important result is that true tunneling can be established at the surface of an ultra-thin polyimide film which has been spin coated or dip coated onto a substrate. This was reported last year for spin coated films less than 200 Å thick on Si substrates. We have now established this result for all the above mentioned subtrates. Tunneling in an air atmosphere is much more difficult to establish and maintain than tunneling in vacuum. This is due to residual water which is present in the polyimide film,[1] as these materials are known to absorb water in significant amounts. This phenomenon is one reason that hermiticity is required for

packaging structures which employ these materials, and is also the basis for their use as sensors.[7]

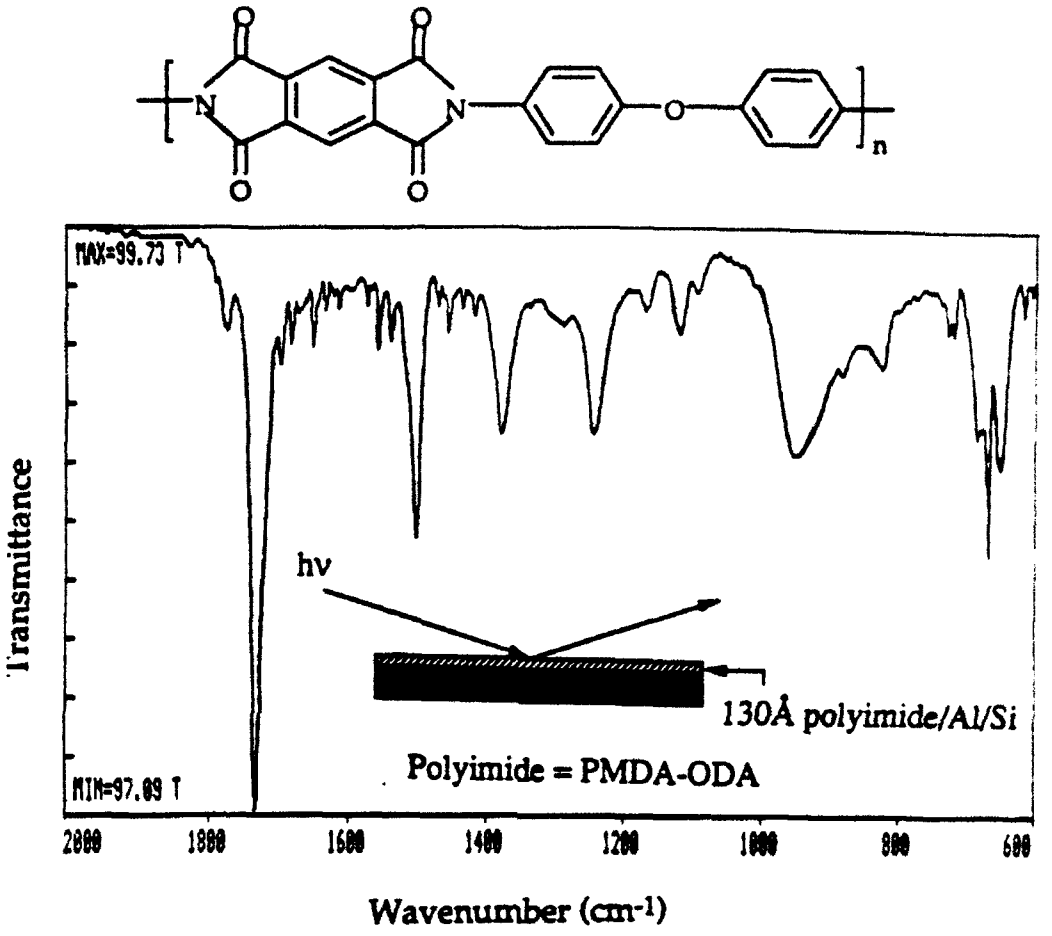

Figure 1. Single reflection Fourier transform infrared spectrum of a 130 Å polyimide film spin-coated onto an aluminum-covered silicon wafer. The film thickness was determined by ellipsometry.

We will use results from dip coated films on graphite substrates to illustrate our results to date. It should be noted that spin coated films on Si, Si with native oxide, Al, and Au all exhibit similar results, with bias voltages required for stable imaging controlled by the oxide barrier layer between substrate and the polymer film. Thus topographic imaging of polyimide on Si with a native oxide, or Al with a native oxide will require bias voltages of 3 to 4 volts, but imaging of the same material on graphite or a gold substrate can be accomplished with bias voltages of only 10 mV. Figure 2 shows a series of

topographic images obtained from a polyimide film dip coated onto a graphite substrate. These images are produced by assigning a gray scale value to the magnitude of the piezo voltage controlling the tip to sample distance. This converts a typical line scan to a depth view. Figure 2A shows a large region (1000 Å by 1000 Å) of the polyimide surface which displays a large degree of ordering in the substrate plane. Layers or step like structures can be discerned, which are shown in a "zoom" of the lower right area in figure 2B. Such ordering is not generally observed in the spin coated samples on metal or semiconductor substrates. Figure 2C shows another small region (300 Å by 300 Å) elsewhere on the surface. This image shows clearly the existence of "granular metallic regions" with diameter of approximately 20 to 30 Å . Such structure is common on all the other substrates we have observed, with the average and minimum size of these grains varying depending on the substrate. This is apparently the common surface structure exhibited by surfaces of the conducting polymer, polyaniline, as well.[8]

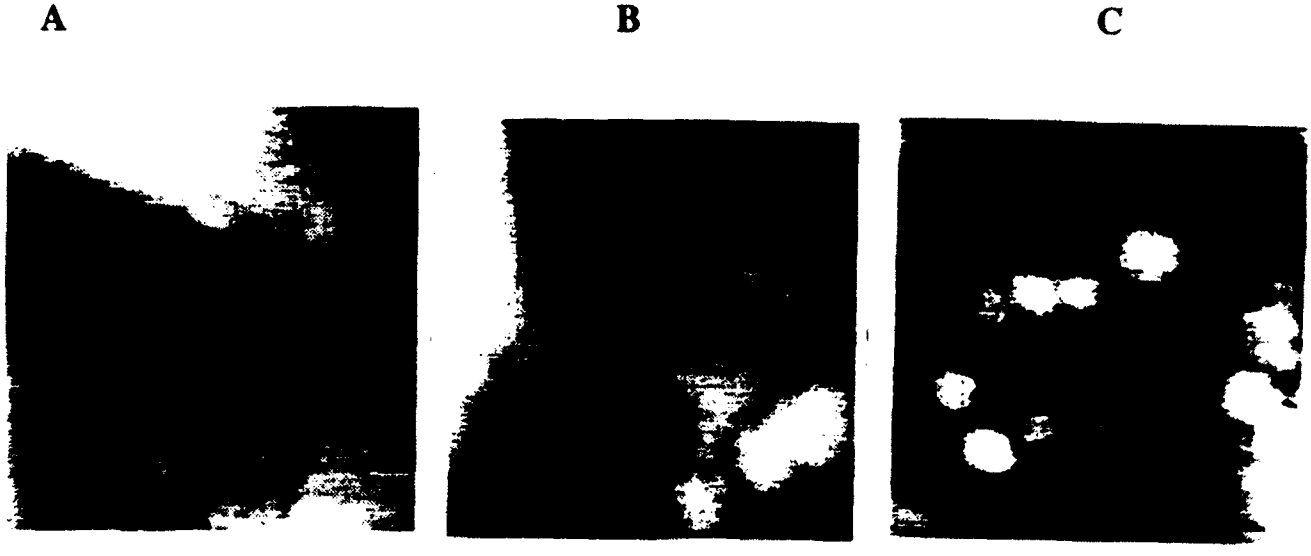

Figure 2. Topographic images of the surface of a virgin PMDA-ODA film. Tip-sample bias is +0.5V, with a tunneling current of 0.5 nA. A) area is 100 nm x 100 nm, grayscale 9 nm. B) Close-up of lower right portion of A with area 30 nm x 30 nm, grayscale 4.5 nm. C) Another region of the film under the same conditions. Area is 30nm x 30 nm, grayscale 3 nm.

Local electronic structure measurements have been made using scanning tunneling spectroscopy (STS). In this technique, I vs V_{bias} curves are obtained during topographic

imaging by stopping at a specific x-y coordinate, releasing the tip from the feedback loop control, and ramping the bias voltage while recording the tunneling current. The tunneling current sums over available electronic states as the voltage is increased, thus making a total density of state measurement. This is valid for a metal or semiconductor surface, and the normalized density of states can then be obtained by plotting (dI/dV)/(I/V) vs voltage. As shown in figure 3A, we have observed essentially metallic states for some topographic points on a film dip coated onto graphite. Other regions of the surface display a low and rather constant density of states within the "quasi-gap" expected for the polyimide. In some regions, superimposed onto this low density of states, we observe negative differential resistance (NDR) as seen in figure 3B. NDR has been associated with localized impurity states for Si(111). Additionally, in the study of polyaniline,[8] as the metallic to insulator transition was followed, NDR was observed associated with charge trapping in localized states. Thus we are on the verge of associating electronic structure with topographic features exhibited on the nanometer scale with conductivity of the film. Further study will reveal what fabrication methods yield molecular structure which exhibits dielectric loss and how this can be avoided.

(3.) New Techniques: The results described above on the fabrication, structure and properties of polyimide films have relied on the implementation of several new techniques into our laboratories over the past year. For example, to vapor deposit the polyimide films under vacuum conditions, a deposition chamber with Knudsen cells for evaporation of the monomer units has been fabricated in Prof. White's laboratory. The first results from this system were presented at the fall meeting of the American Vacuum Society and a paper is in preparation. A similar apparatus is being constructed in Prof. Bent's laboratory for combining vapor deposition with *in situ* Auger and infrared spectroscopy on the resulting polymer films. For quantitative determinations of surface composition, x-ray photoemission has been added to Prof. White's laboratory. A Kratos XSAM800

instrument with XPS, Auger, and ion beam capability for these studies was obtained by a donation from a research group at AT&T Bell Laboratories with whom we have informal interactions. For studying the structure and orientation of polymer films, Fourier transform infrared spectroscopy has been set-up in Prof. Bent's lab. Two Perkin-Elmer FT1800 spectrometers are being used for these studies. One, obtained by donation from Perkin-Elmer, has been connected to an ultra-high vacuum system that has been equipped for vapor deposition of polymer films as described above. The second, a departmental facility obtained from an NSF equipment grant, is being used to analyze the structure of spin-coated polyimide films. Finally, to study the local electronic structure of this spin-coated films, scanning tunneling spectroscopy has been implemented in Prof. White's laboratory. The first results from these studies have been described above in Section 2.

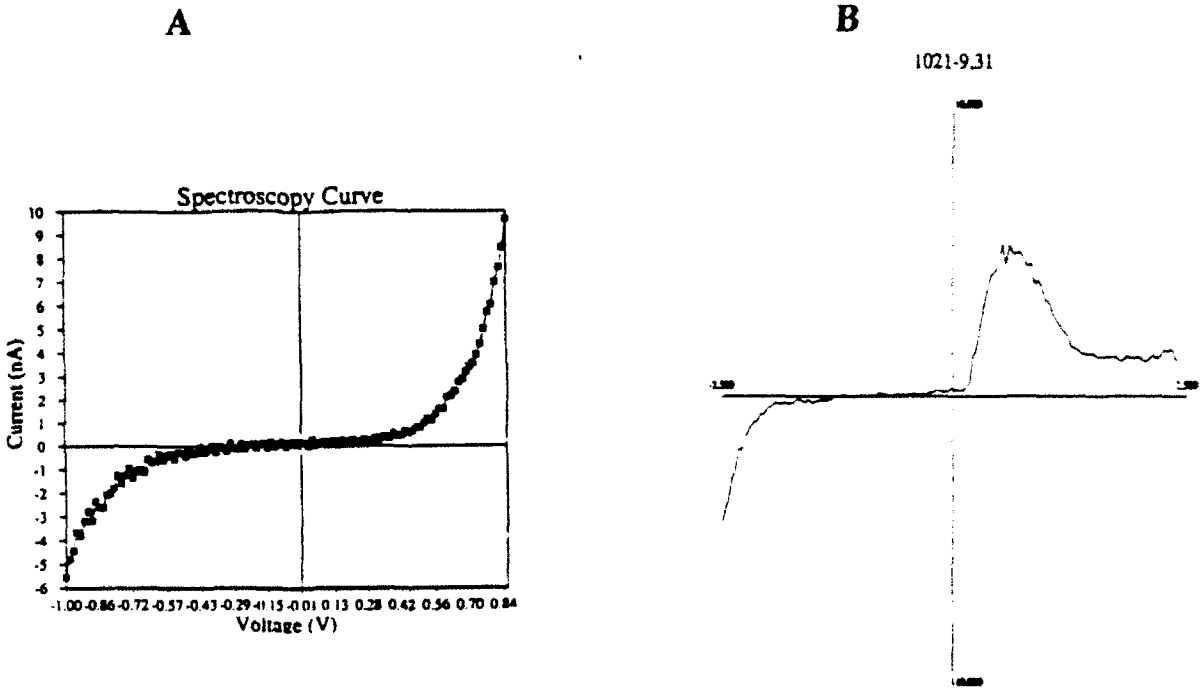

Figure 3. (A) I/V characteristic typical of metallic surface electronic structure from the film imaged in Figure 2. (B) Less typical but reproducible I/V characteristic from the same film showing background, low density of states and negative differential resistance.

(4.) New Directions: An important issue in polymer film applications, in addition to film deposition and properties, is polymer etching. A particularly promising approach is

the use of plasmas, which provide rapid etch rates at low temperatures. Our current studies on the use of hydrogen atoms to prepare organic monolayers and on the use of ion beams to enhance metal/polymer adhesion have lead us naturally into the field of plasma etching. It has become apparent from our investigations on the interaction of single atoms and ions with organic monolayers and polymer surfaces that this type of study allows us to isolate and determine the basic physical and chemical mechanisms of plasma etching. For example, in the case of hydrogen atom reactions with organic monolayers, we have found that an important mechanism is the direct addition or abstraction of an atom from the adsorbed organic molecule.[3,4] This type of direct reaction between a gas phase atom and a surface molecule (called an Eley-Rideal (E-R) mechanism) is to be contrasted with the more typical Langmuir-Hinshelwood (L-H) mechanisms where a reaction occurs between two species that are bonded to the surface. This fundamental distinction has potentially important implications for polymer etching. E-R mechanisms will produce directional etching while L-H mechanisms have the potential to etch side walls and destroy the directional nature of the etch. Our goal is to investigate the reactions of atomic beams with polymer surfaces to determine what factors favor one mechanism over another.

In the case of ion/polymer interactions, we have found that interesting effects occur even for non-reactive etching. The use of electron cyclotron resonance (ECR) plasma as a source of low energy (<20 eV) ions for etching or adhesion enhancement is common in fabrication of packaging structures. We have found that Ar ECR plasma etches faster than 500 eV Ar ion beams.[9] This could be due to the shallower depth of the damage region or reactive neutral species not present in the ion beam. In addition, use of N_2 ECR plasma has been shown to incorporate reactive N sites within the damaged region of the polymer. This is significant for several reasons, including adhesion enhancement of Au to polyimide due to chemically reactive sites formed by ion beam treatment of the polymer.[10] It is our intention to pursue the underlying mechanisms in ion and plasma treatment of polymer films by investigation of the effects of separated ions and neutrals. We were invited to

write an informal proposal which we have submitted to the high end packaging group at I.B.M. T. J. Watson Research Center in order to obtain a $1 M instrument designed and constructed specifically for this purpose. This instrument would strengthen our existing interactions (see Technology Transitions section) and includes a specially designed low energy ion source which can be pulsed, and a time of flight mass spectrometer for high resolution measurements of the etching products and their reaction times.

This research was supported by the the Joint Serviced Electronics Program.

References:

1. E. N. Schulman and R. C. White, "Observation of Nanometer Ordering in Multilayer Films of PMDA-ODA Using the Scanning Tunneling Microscope and Ultra High Vacuum," submitted to J. Vac. Sci. Technol.
2. S. Zolgharnain and R. C. White, "In-vacuum Synthesis and Characterization of Thin Aromatic Polyimide Films Prepared by a Chemical Vapor Deposition Process," submitted to J. Vac. Sci. Technol.
3. M. Xi and B. E. Bent, "Evidence for an Eley-Rideal Mechanism in the Addition of Hydrogen Atoms to Unsaturated Hydrocarbons on Cu(111)," J. Vac. Sci. and Technol. B, in press.
4. M. Xi and B. E. Bent, "Reaction of Deuterium Atoms with Cyclohexane on Cu(111): Hydrogen Abstractions Reactions by Eley-Rideal Mechanisms," submitted to J. Phys. Chem.
5. J.-L. Lin and B. E. Bent, "C-H Vibrational Mode Softening in Alkyl Groups Bound to Cu(111)," Chem. Phys. Lett. **194**, 208 (1992) .
6. H. Ishida, S. T. Wellinghoff, E. Baer, and J. L. Koenig, "Spectroscopic Studies of Poly[N,N'-bis(phenoxyphenyl)Pyromellitimide]. 1. Structures of the Polyimide and Three Model Compounds," Macromolecules **13**, 826 (1980).
7. M. T. Fertsch, R. M. White, and R. S. Muller, "Surface Acoustic Wave Vapor Sensing Device," Device Research Conference, Ithaca, N.Y., 1980.
8. D. Jeon, J. Kim, M. C. Gallagher, and R. F. Willis, "Scanning Tunneling Spectroscopic Evidence for Granular Metallic Conductivity in Conducting Polymeric Polyanaline," Science **256**, 1662 (1992).
9. H.-S. Jeong, Z. Lu, and R. C. White, "Surface Modification of Polyimide by ECR Plasma," Nuclear Inst. and Meth. B **59/60**, 1285 (1991).
10. H.-S. Jeong and R. C. White, to be published.

PUBLICATIONS (Research Area II, Work Unit 4)

Hyo-Soo Jeong and R.C. White, "Low Energy Ion Beam Modification of High Performance Electronic Polymer," Mater. Res. Soc. Symp. Proc. **236**, pp. 324-330 (1992).

J.-L. Lin and B.E. Bent, "Iodomethane Dissociation on Cu(111): Bonding and Chemistry of Adsorbed Methyl Groups," J. Vac. Sci. Technol. A **10**, 2202 (1992).

C.-M. Chiang, T.H. Wentzlaff, C.J. Jenks, and B.E. Bent, "Carbon-Carbon Bond Forming Reactions on Cu(11) Surfaces," J. Vac. Sci. Technol. A **10**, 2185 (1992).

J.-L. Lin and B.E. Bent, "C-H Vibrational Mode Softening in Alkyl Groups Bound to Cu(111)," Chem. Phys. Lett. **194**, 208 (1992).

M. Xi. and B.E. Bent, "Evidence for an Eley-Rideal Mechanism in the Addition of Hydrogen Atoms to Unsaturated Hydrocarbons on Cu(111)," J. Vac. Sci. Technol. B, in press.

H.-S. Jeong and R. C. White, "Low Energy Ion Beam Interactions with Electronic Polymer Surfaces," J. Vac. Sci. Technol. A, in press.

M. Xi and B.E. Bent, "Reaction of Deuterium Atoms with Cyclohexane on Cu(111): *Hydrogen Abstraction Reactions by Eley-Rideal Mechanisms," submitted to* J. Phys. Chem.

E. N. Schulman and R. C. White, "Observation of Nanometer Ordering in Multilayer Films of PMDA-ODA Using the Scanning Tunneling Microscope and Ultra High Vacuum," submitted to J. Vac. Sci. Technol.

S. Zolgharnain and R. C. White, "In-vacuum Synthesis and Characterization of Thin Aromatic Polyimide Films Prepared by a Chemical Vapor Deposition Process," submitted to J. Vac. Sci. Technol.

SIGNIFICANT ACCOMPLISHMENTS

We have shown that the channel capacity of a photon-counting optical receiver can sometimes be improved by making an initially Poisson photon stream sub-Poisson. It has been demonstrated that the photon-number distribution at the output of a cascade of erbium-doped fiber amplifiers, with coherent light at the input, maintains a noncentral-negative-binomial form even in the preseance of intervening loss.

A fractal renewal process that provides a framework for understanding charge transport in amorphous semiconductors has been constructed. Tensile strain was suggested as a new approach for enhancing exciton absorption and increasing the saturation limit in quantum wells. It has been shown that improved temperature performance can be expected from long-wavelength quantum-box lasers but not from quantum-wire lasers.

We have explicitly shown that the tuning of biaxial strain in ZnSe epilayers can be achieved by applying hydrostatic pressure.

Raman scattering has been used as an **in situ** diagnostic of temperature during the processing of GeSi alloys.

We have developed the first simple model for phonon frequencies throughout the Brillouin zone for strained layers at ambient elevated pressures. This model gives simple analytic predictions at the critical points.

We have developed a method to form a stoichiometric SiGe oxide using electron cyclotron resonance (ECR). To our knowledge, this is the first time ever that a device-quality SiGe oxide has been produced in this way. Using an ECR source, the AlGeAs/GaAs heterojunction surface was passivated with hydrogen and nitrogen plasmas. The surface leakage current was reduced by a factor of more than 200 in a heterojunction bipolar transistor and the current gain at low current was increased by two orders of magnitude. In addition we have shown that an electron-cyclotron-resonance hydrogen source can be used for oxide removal and surface passivation of single-crystal GaSb surfaces at low temperatures.

We have demonstrated that nanosecond laser pulses can be used to measure photoemission from femtosecond lifetime surface levels on metal surfaces. A second new optical technique for measuring the spatial variation of work functions on metal surfaces has also been developed. This approach relies on measuring the high energy cutoff for broad energy resonances on surfaces. This same photoemission study provides useful information on the initial stages of multiphoton discharge formation on metal surfaces. This phenomena is of interest because of its importance in plasma switches for sensor protection in U.S. Army applications.

We have discovered and characterized a novel mechanism for cooling the internal states of very hot molecules. This mechanism appears to be quite universal and may be important in determining gain or loss in laser systems as well as the reactivity of molecules on surfaces.

STM facilities at Columbia for the study of surface adsorbates and the development of optical/STM techniques have been improved. A second STM device has been added to our facility which is capable of operating in both the STM and AFM (atomic force microscopy) modes.

STM images of long chain molecules on graphite surfaces have been recorded. These molecules form epitaxial layers on the graphite which are sensitive to the underlying structure of the carbon surface. The fact that these images can be recorded under wet conditions provides an opportunity to investigate the kinetics of surface adsorption and to study the dynamic equilibrium between dissolved and surface adsorbed molecules.

We have fabricated ultra thin polyimide films (50 - 1000 Å) for microelectronics packaging on metal, silicon, and graphite substrates by spin coating and dip coating. Scanning tunneling microscopy shows that all films order into granular metallic regions varying in size from 20 - 50 Å laterally. Scanning tunneling spectroscopy reveals electronic structure varying at the same spatial resolution from metallic to low density trap states in a quasi-insulator band gap. Negative differential resistance is also observed.

Fourier transform infrared spectroscopy studies suggest that this unusual combination of electronic structure may be related to regions of oriented molecular chains in these ultra-thin films. Additionally, ultra thin films have been fabricated on metal, metal oxide, and semiconductor surfaces by chemical vapor deposition. XPS shows good chemical purity, and these CVD films passivate all surfaces except Cr, which is further oxidized during polymerization. Model polymer films have also been investigated, and a novel method for preparing monolayers of hydrocarbon chains on copper surfaces from molecular precursors and a hydrogen atom source has been developed.

COLLABORATIONS/TECHNOLOGY TRANSITIONS

Professor Osgood's work on via-hole drilling for densely-packed microwave circuits fostered a joint program with Hughes Aircraft to apply this technique to InP-based circuits. The approach was successful, has actually been applied to working integrated circuits, and has now been transitioned to Hughes, where they have rebuilt our system in their labs. Professor Osgood's group also collaborated with a small company, Litel, to demonstrate a new technique for ultrahigh-rate laser etching of polyimides.

Professor Teich delivered an Invited Lecture, "Fractal Random Processes," at the Workshop on Stochastic Resonance, organized by the Office of Naval Research and NATO, in San Diego, California, in March , 1992. He also presented a series of lectures in April, 1992, at the Navy's Coastal Systems Station in Panama City, Florida. The lectures comprised the topics of Photon Optics, Photons and Atoms, Laser Amplifiers, Laser Resonators, and Lasers. The lectures were a portion of an intensive course entitled "Lasers and Optical Engineering."

Professor Teich collaborated with J. R. Meyer of the Naval Research Laboratory, and several Columbia University researchers (Professor W. I. Wang and graduate student Y. Jiang), on a project involving HgCdTe quantum wires and quantum boxes. This

collaboration led to a joint publication: Y. Jiang, M. C. Teich, W. I. Wang and J. R. Meyer, "Auger Recombination in HgCdTe Quantum Wires and Quantum Boxes," J. Appl. Phys. **71**, 3394 (1992).

Prof. Herman has spoken on his JSEP research at Hughes Research Laboratory, and visited Philips Research Laboratory to discuss his work with Jim Gaines and D. Olego. He has continued his JSEP collaboration on light emitting semiconductor heterostructures with Drs. Joze Bevk and Robert Feldman at AT&T Bell Laboratories, and has begun a collaboration with Dr. James Tsang at the IBM T.J. Watson Research Center. Prof. Herman has spoken with Dr. O. Glembocki of the Naval Research Laboratory about starting a collaboration on ordered semiconductors. His group has also collaborated on a study with Dr. D. Lowndes at the Oak Ridge National Laboratory to determine the purity of ZnS and ZnSe films grown by laser ablation at Oak Ridge.

Prof. Herman's student Dr. Ari Tuchman, who was supported by JSEP and who graduated this year, spoke on his JSEP work at the Army research laboratory, the Harry Diamond Laboratory, and the Naval Research Laboratory. Also, Dr. Tuchman has accepted a National Research Council Postdoctoral Fellowship at the Naval Research Laboratory.

Collaboration efforts have been developed by Professor Yang with Trey Smith, Subu Iyer, K.N. Tu, and V. P. Kesan (IBM Research, Yorktown Heights) on SiGe devices and contacts, and with Y. K. Chen and A. Y. Cho (Bell Labs, Murray Hill) on MBE growth heterostructure transistors.

Prof. White has renewed a joint study contract with Samath Purushathamon (IBM Research Laboratory, Yorktown Heights, NY) for invesitgation of ion beam and plasma processing of polymers and metal/polymer interfaces. This collaboration has been fruitful in surface and interphase characterization as well as in nanometer scale adhesion measurements. Two Columbia PhD students work part time at the T. J. Watson Research Center as part of this program. An informal instrumentation proposal is currently pending

with the manager of this group (John Ritsko) to obtain a complete time-of-flight (TOF) mass spec./low energy ion beam system valued at $1M. This system would allow for the study of fundamental ion processing mechanisms in organic thin films used for packaging. Joint funding for this work is currently being sought through the Army Research Office (ARO) and the Office of Naval Research (ONR).

A KRATOS XSAM 800 photoemission/Auger system equipped with electron and ion beam capabilities has been donated to Prof. White's laboratory by AT&T Bell Laboratories (Murray Hill) as part of a collaboration with AT&T scientists, Reddy Raju, B.J. Han, and Robert Opilla. On-going collaborative research includes investigation by STM/STS of thin polyimide films as well as diazo compounds used in the AT&T POLYHIC technology. Joint research at Brookhaven National Laboratory using the UV and x-ray rings is planned for the immediate future on both of these materials systems, specifically to investigate molecular ordering in the bulk and near surface regions via secondary or Auger electron yields and fluorescence yields using the grasshopper monochromator.

Several projects are underway between Prof. White's group and John Emerson (Sandia National Laboratory, Albuquerque, NM) including packaging of tactile sensors for robotic applications, and polyimide surface and interphase modifications for optical waveguides, modulators, and rail taps which employ non-linear optical polymer materials.

Prof. Bent has initiated a collaborative effort with Francisco Zaera (University of California, Riverside, CA) to study the structure, bonding, and orientation of hydrocarbon chains bound to metal surfaces using Fourier transform infrared spectroscopy. As part of this project, one PhD student spent three months at UCR over the past year taking infrared spectra of alkyl chains on copper surfaces.

Prof. Bent has also collaborated with Paul Stevens (Exxon Research and Engineering, Annandale, NJ) in a study focussed on the use of near edge x-ray absorption fine structure at the carbon 1s edge to study the orientation of aromatic molecules on metal

surfaces. These studies are being carried out at the National Synchrotron Light Source at Brookhaven National Laboratory.

Dan Fischer (NIST, Brookhaven National Laboratory), John Gland (University of Michigan), and Simon Bare (Dow Chemical Co., Midland, MI) have collaborated with Professors White and Bent on a study of the kinetics of surface processes using fluorescence yield detection of carbon near edge x-ray absorption fine structure at Brookhaven National Laboratory. The first measurements on the orientation of carbon-halogen bonds were made in November 1992.

The techniques for probing molecules with infrared diode lasers, developed in Professor Flynn's laboratory under JSEP sponsorship over the past 5 years, are being used as diagnostic methods for the study of plasmas and plasma etching environments by Dr. James O'Neill at the IBM East Fishkill research and development plant. We are presently working in collaboration with Dr. O'Neill to develop a sensitive, reliable diode laser probing technique for following energetic argon ions. This work is aimed at the control of manufacturing processes in the production of silicon wafers and their subsequent etching to produce integrated circuits.

Two new collaborations have been developed by Professor Flynn which are bringing very novel, new infrared diagnostic capabilities to the study of molecules and their interactions. The first collaboration is with Professor Arlan Mantz at Franklin and Marshall College and involves the development of advanced techniques for stabilizing infrared diode lasers such as those being used at the IBM East Fishkill facility to probe plasma properties. The second project, being pursued in collaboration with Professor Daniel Willey of Allegheny College, makes use of a "collisional cooling cell" to study the spectroscopy and dynamics of molecules in the gas phase at 10 K. This novel cooling method is of potential interest in both quantum electronics and the study of gas-surface chemistry for materials science applications.

Professor Flynn has collaborated with Dr. Ralph Weston, Senior Chemist at Brookhaven National Laboratories, on a number of projects in chemical and collision dynamics. This work is designed to elucidate the fundamental mechanisms by which molecules exchange energy and undergo chemical reactions during collisions.

PERSONNEL

Columbia University Principal Investigators

Bent, B. E.
Flynn, G. W.
Herman, I. P.
Osgood. R. M., Jr.
Teich, M. C.
Yang, E. S.
White, R. C.

Post-Doctoral Research Fellows and Research Scientists

Breen, J.
Levy, M.
Mullin, A.
Scarmozzino, R.
Yang, Q.
Jo, S.
Lowen, S.
Park, J.
Venkataraman, B.
Yuan, H.

Graduate Students

Birchfield, B.
Burke, H. H.
Chiang, C.-M.
Eldada, L.
Freiler, M.
Heneghan, C.
Jiang, Y.
Kim, S.
Lee, Y.-S.
Li, T.
Liou, H. K.
Lu, Z.
Quiniou, B.
Schulman, E.
Stevens, A.
Tuchman, J. A.
Wang, Y.
Yang, X.
Zhu, L.
Bulovic, V.
Campos, R. A.
Chou, J.
Fang, J. M.
Furhang, E.
Jeong, H.-S.
Keilson, S.
Larchuk, T. S.
Li, P. W.
Lin, J.-L.
Longenbach, K.
Ni, C.-K.
Schowen, S.
Singer, F.
Sui, Z.
Wang, Q.
Xi, M.
Zheng, L.
Zolgharnain, S.

Undergraduate Students

Denmark, A.
New, J.
Roman, E.
Tolman, S.
Greenberg, S.
Ogwo, D.
Stewart, A.
Wang, Y.

Collaborators

Bare, S.	Dow Chemical Co., Midland, MI
Bevk, J.	AT&T Bell Laboratories
Chen, Y. K.	AT&T Bell Labs, Murray Hill, NJ
Cho, A. Y.	AT&T Bell Labs, Murray Hill, NJ
Diament, P.	Columbia University
Emerson, J.	Sandia National Laboratory, Albuquerque, NM
Feldman, R.	AT&T Bell Laboratories
Fischer, D.	NIST, Brookhaven National Laboratory
Gaines, J.	Philips Research Laboratory
Gennser, U.	MIT Bitter Magnet Lab
Gland, J.	University of Michigan, Ann Arbor, MI
Gunshor, R.	Purdue University
Han, B. J.	AT&T Bell Laboratories, Murray Hill, NJ
Hargis, M. C.	IBM, Yorktown Heights, NY
Hooper, B.	Hughes Research Lab
Humpal, F.	IBM Watson Labs
Iyer, S. S.	IBM, Yorktown Heights, NY
Jakeman, E.	Defence Research Agency, Great Malvern, England
Jones, K.	Fort Monmouth
Kesan, V. P.	IBM, Yorktown Heights, NY
Lin, P.	Bellcore
Lowndes, D.	Oak Ridge National Laboratories
Mantz A.	Physicist/Professor Franklin and Marshall College
McLain, G.	Fort Monmouth
Meyer, J. R.	Naval Research Laboratory, Washington D.C.
O'Neill, J.	Staff Scientist, IBM Fishkill Laboratories
Opilla, R.	AT&T Bell Laboratories, Murray Hill, NJ
Potasek, M. J.	Columbia University
Prucnal, P. R.	Princeton University
Purushathamon, S.	IBM Research Center, Yorktown Heights, NY
Raju, R.	AT&T Bell Laboratories, Murray Hill, NJ
Rarity, J. G.	Defence Research Agency, Great Malvern, England
Saleh, B.	University of Wisconsin
Smith III, T. P.	IBM, Yorktown Heights, NY
Smith, N.	AT&T
Stevens, P.	Exxon Research and Engineering, Annandale, NJ
Syphers, D. A.	Bowdoin College, Brunswick, ME
Tapster, P. R.	Defence Research Agency, Great Malvern, England
Tiwari, S.	IBM, Yorktown Heights, NY
Tu, K. N.	IBM, Yorktown Heights, NY
Wang, W. I.	Columbia University
Weston, R.	Senior Chemist, Brookhaven National Labs
Willey, D.	Physicist/Professor, Allegheny College
Zuera, F.	Univerisity of California, Riverside, CA